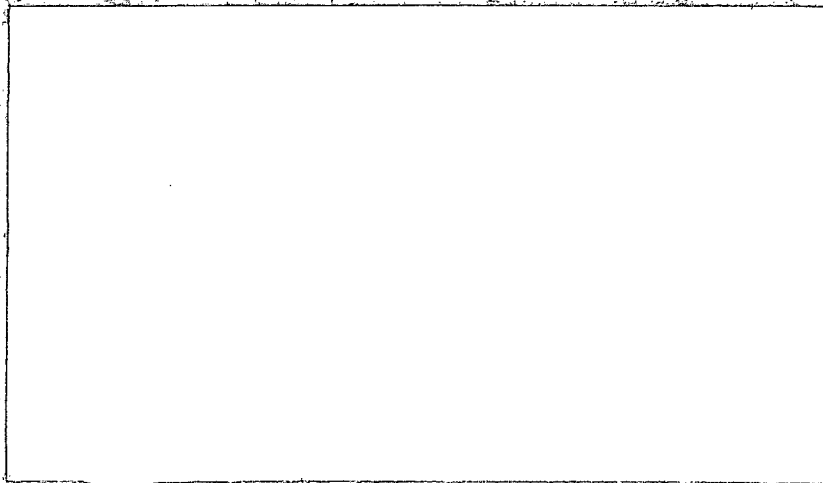
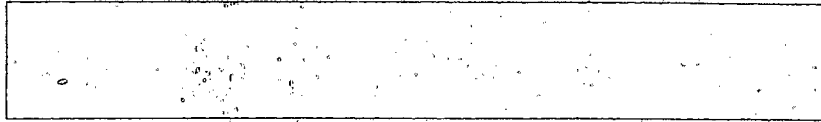


BNR 100

NO ME

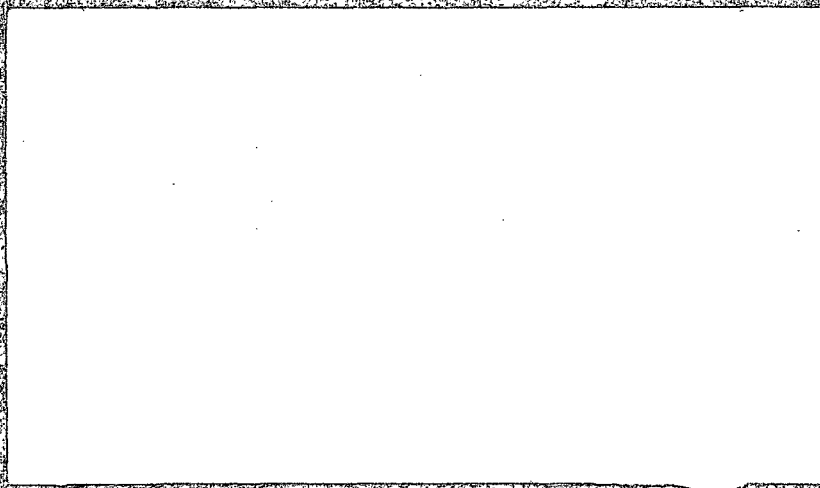


RESEARCH REPORT





BNRC77741D



RESEARCH AND DEVELOPMENT CAPABILITIES

Air & Water Pollution
 Alloy Development
 Analytical Chemistry
 Applied Mathematics
 Aquatic Biology
 Atmospheric Sciences
 Biomedical Science & Technology
 Biophysics
 Catalysis—Surface Chemistry
 Cellular & Molecular Biology
 Ceramics & Cermets
 Chemical Development & Processes
 Comparative Pathology & Physiology
 Composite Materials

Computer Simulation & Systems Analysis
 Computer Technology
 Corrosion Technology
 Ecology—Radioecology
 Electrochemistry
 Electrochemical Devices & Systems
 Electronic Devices, Circuits & Systems
 Energy Conversion Processes
 Environmental Sciences
 Fluid Mechanics
 Food Technology
 Geosciences
 Graphite Technology
 Heat Transfer

Hydraulics
 Hydrology
 Industrial & Applied Chemistry
 Industrial Economics
 Inhalation Toxicology
 Inorganic Chemistry
 Instrumentation
 Laser Technology
 Marine Science & Technology
 Materials Fabrication
 Materials Separation & Purification
 Mechanical Components & Devices
 Microscopy: X-Ray, Optical & Electron
 Mineralogy

Nondestructive Testing
 Nuclear Economics
 Nuclear Fuels Development, Processing & Separations
 Nuclear Instrumentation
 Nuclear Physics
 Nuclear Reactor Technology
 Nuclear Reactor Materials
 Nuclear Safeguards Evaluation
 Operations Research
 Optics
 Organic Chemistry
 Process & Physical Metallurgy
 Physical Chemistry

Plant Nutrition
 Process Development
 Radiation Biology
 Radiation/Irradiation Effects on Materials
 Radiation Shielding & Protection
 Radioactive Wastes Processing & Disposal
 Radio & Radiation Chemistry
 Radiobiology
 Radioisotope Technology & Applications
 Radiological Science & Technology
 Regional Economics
 Seismology
 Semiconductors—Solid State Devices

Solid State Physics
 Spectroscopy
 Statistics
 Systems Development & Analysis
 Theoretical & Applied Mechanics
 Theoretical & Mathematical Physics
 Thermodynamics
 Toxicology
 Ultraprecise Measurement Methods
 Ultrasonics
 Water Treatment, Use & Recovery
 Welding—Joining Technology

As a research and development organization, the services Battelle offers its sponsors are those beyond the normal scope of the consulting engineering organization. Similarly, Battelle does not contract to perform routine testing of the type offered by commercial testing laboratories. The Battelle concept of research and development is based on its ability to provide the varied scientific and technical skills necessary for the successful solution of a broad array of problems. In addition, Battelle retains a number of consultants to supplement its in-house abilities.

IODINE REMOVAL FROM CONTAINMENT
ATMOSPHERES BY BORIC ACID SPRAY

Principal Contributors:

A. K. Postma
L. F. Coleman
R. K. Hilliard

July, 1970

Work performed under contract No. 212B00233 REV 1 with
Consumers Power Company, Jackson, Michigan.

BATTELLE MEMORIAL INSTITUTE
PACIFIC NORTHWEST LABORATORIES
RICHLAND, WASHINGTON 99352

Battelle is not engaged in research for advertising, sales promotion, or
publicity, and this report may not be reproduced in full or in part
for such purposes.

*Pub. Info; Cons. Power 11/1/70
does not restrict or alter*

CONTENTS

	<u>Page</u>
ABSTRACT -----	i
LIST OF FIGURES -----	ii
LIST OF TABLES -----	iv
I. INTRODUCTION -----	1
II. SUMMARY AND CONCLUSIONS -----	2
III. IODINE REMOVAL THEORY -----	5
A. Material Balance Equations -----	5
B. Absorption of Elemental Iodine by Drops -----	7
1. Absorption by Fresh Spray -----	7
2. Absorption by Recirculated Spray -----	10
C. Absorption of Elemental Iodine by Wall Surfaces -----	16
D. Methyl Iodide Absorption -----	18
1. Drop Absorption -----	18
2. Wall Film Absorption of Methyl Iodide -----	19
E. Overall Equation for Total Iodine Removal -----	21
IV. MEASUREMENTS OF IODINE PARTITION COEFFICIENTS FOR BORIC ACID SPRAY SOLUTIONS -----	22
A. Purpose of Partition Coefficient Measurements -----	22
B. Experimental Equipment and Procedures -----	22
1. Experimental Equipment -----	22
2. Experimental Procedures -----	24
C. Test Conditions -----	28
D. Results of Partition Coefficient Measurements -----	28
1. Iodine Concentrations in the Gas and Liquid Phases -	28
2. Partition Coefficient Applicable to Spray Absorption	32
3. Effect of Physical Parameters on the Partition Coefficient -----	35
a. Iodine Concentration -----	35
b. Boron Concentration -----	38
c. Temperature -----	38
d. Solution pH -----	40
e. Solution Impurities -----	41

	<u>Page</u>
E. Comparison of Measured Partition Coefficients with Previous Data -----	42
F. Conclusions From Partition Coefficient Measurements -----	44
V. LARGE-SCALE EXPERIMENT OF IODINE REMOVAL BY BORIC ACID SPRAY -----	46
A. Purpose of Large-Scale Experiment -----	46
B. Experimental Conditions and Procedure -----	46
1. Description of Large-Scale Facility -----	46
a. Containment Vessel Arrangement -----	47
b. Fission Product Simulant Generation -----	49
c. Sampling Procedures -----	51
d. Spray System -----	56
2. Spray Solution Makeup and Analysis -----	58
3. Spray Flow Parameters -----	58
a. Spray Distribution -----	58
b. Drop Fall Distance -----	61
c. Drop Size Distribution -----	61
4. Sequence of Events for Run C-1 -----	61
5. Characterization of the Atmosphere in the Containment Vessel -----	63
a. Visual Observations -----	63
b. Temperature and Pressure History -----	64
C. Results of Large-Scale Spray Experiment -----	67
1. Iodine Removal from Gas Phase -----	67
a. Concentration of Iodine in the Gas Phase -----	67
b. Concentration of Iodine in Collected Drops -----	70
c. Iodine Concentration in Vessel Sumps -----	70
2. Retention of Iodine by Spray Liquid -----	74
a. Venting Effects -----	74
b. Retention of Iodine During Sample Evaporation -----	76

	<u>Page</u>
3. Aerosol Particle Washout -----	76
a. Cesium Concentration in the Gas Phase -----	76
b. Concentration of Cesium in Spray Drops -----	80
c. Concentration of Cesium in Sump Liquid -----	80
4. Comparison of Iodine Washout with CSE Run A-7 -----	84
a. Comparison of Spray Conditions for Runs A-7 and C-1 -----	84
1. Temperature of Atmosphere and Spray Liquid--	84
2. Iodine Concentration -----	85
3. Cesium Concentration -----	85
4. Spray Flow Rate and Drop Size -----	86
5. Spray Solution Composition -----	86
b. Comparison of Spray Effectiveness for Runs A-7 and C-1 -----	87
1. Elemental Iodine -----	87
2. Methyl Iodide -----	88
c. Conclusions Regarding Comparisons of Spray Effectiveness in Runs C-1 and A-7 -----	92
VI. COMPARISON OF LARGE-SCALE TEST RESULTS WITH PREDICTIONS BASED ON SMALL-SCALE PARTITION COEFFICIENT MEASUREMENTS ----	93
A. Initial Washout Rate for Elemental Iodine -----	93
B. Recirculation Period -----	95
VII. APPLICATION OF RESULTS TO A LARGE PWR -----	97
A. Scope -----	97
B. Physical Parameters and Assumptions -----	98
C. Predicted 2 Hr Dose Reduction Factor -----	99
1. Direct Application of Large Scale Test Results ---	99
2. Application of Small Scale Test Data -----	100
3. Comparison with Caustic -----	102
VIII. REFERENCES -----	103
IX. ACKNOWLEDGEMENTS -----	106
APPENDIX A - Figures of Iodine Concentration - Time Relation for Partition Experiments -----	107
APPENDIX B - Tables of Maypack Sample Data -----	120

IODINE REMOVAL FROM CONTAINMENT
ATMOSPHERES BY BORIC ACID SPRAY

Principal Contributors:

A. K. Postma
L. F. Coleman
R. K. Hilliard

ABSTRACT

The absorption of airborne iodine by boric acid sprays was measured in a large scale demonstration test, and in pilot scale partition coefficient experiments. Results showed that boric acid sprays have an appreciable capability to absorb and retain iodine under accident conditions postulated for PWR nuclear plants. The iodine absorption rate was initially lower than for a caustic spray (borated water at pH of 9.5). For the low iodine concentrations expected in PWR containment systems, trace level impurities played an important role in converting dissolved iodine to a non-volatile form.

LIST OF FIGURES

<u>Figure No.</u>	<u>Title</u>	<u>Page</u>
1	Comparison of Drop Absorption for Stagnant and Well Mixed Drops -----	11
2	Schematic Diagram of Recirculating Spray Washout -----	15
3	Concentration Profiles in Wall Film Model for Elemental Iodine Absorption -----	17
4	Schematic of Small Scale Test Equipment -----	23
5	Illustration of Iodine Preparation Technique -----	27
6	Iodine Behavior in Experiment CRA -----	31
7	H Versus Time, Boric Acid - Iodine Equilibrium Tests -	34
8	Effect of Iodine Concentration on Instantaneous Partition Coefficients in Boric Acid Solutions -----	36
9	Partition Coefficients for Inorganic Iodine in Boric Acid as a Function of Gas Phase Concentration -----	37
10	Effect of Boric Acid Concentration on Instantaneous Iodine Partition Coefficient -----	39
11	Partition Coefficients in Weakly Acid Solutions -----	43
12	Schematic Representation of Containment Vessel Arrangement -----	48
13	Schematic Diagram of a CSE Maypack -----	54
14	Response of Maypack Sampler to Sequential Release of Methyl Iodide and Elemental Iodine -----	55
15	Flowsheet of CSE Spray System for Run C-1 -----	57
16	Temperature and Pressure For the First Hour in Run C-1 -----	65
17	Temperature-Pressure History for Run C-1 -----	66
18	Airborne Iodine Early in Run C-1 -----	68
19	Airborne Iodine During Continued Spray Operation in Run C-1 -----	69
20	Iodine Concentration in Spray Drops in Run C-1 -----	71
21	Iodine Concentration in Liquid Pools in Run C-1 -----	72
22	Spray Liquid Volume in Run C-1 -----	73
23	Airborne Cesium Early in Run C-1 -----	79

<u>Figure No.</u>	<u>Title</u>	<u>Page</u>
24	Airborne Cesium During Continued Spray Operation in Run C-1 -----	81
25	Cesium Concentration in Spray Drops in Run C-1 -----	82
26	Cesium Concentration in Liquid Pools -----	83
27	Comparison of Spray Drop Effectiveness for Two Boric Acid Spray Tests -----	89
28	Partitioning of Elemental Iodine By Recirculated Sprays -----	90
29	Methyl Iodide Removal by Caustic and Boric Acid Sprays	91
30	Comparison of Iodine Washout in Run C-1 with Washout Predicted from Partition Coefficient Measurements -----	96
31	Predicted Concentration of Inorganic Iodine in the Gas Space of a PWR Using Boric Acid Spray -----	101
A-1	Iodine Behavior -- Expt CRB -----	108
A-2	Iodine Behavior -- Expt CRC -----	109
A-3	Iodine Behavior -- Expt CRD -----	110
A-4	Iodine Behavior -- Expt CRE -----	111
A-5	Iodine Behavior -- Expt CRG -----	112
A-6	Iodine Behavior -- Expt CRH -----	113
A-7	Iodine Behavior -- Expt CRJ -----	114
A-8	Iodine Behavior -- Expt CRK -----	115
A-9	Iodine Gas Phase Behavior -- Expt CRI -----	116
A-10	Iodine Behavior -- Expt C09 -----	117
A-11	Iodine Behavior -- Expt C10 -----	118
A-12	Iodine Behavior -- Expt C12 -----	119

LIST OF TABLES

<u>Table No.</u>	<u>Title</u>	<u>Page</u>
1	Physical Conditions in Proposed Partition Coefficient Experiments -----	29
2	Physical Conditions in Partition Coefficient Experiments Carried Out -----	30
3	Results of Partition Coefficient Measurements -----	33
4	Test Conditions For Run C-1 -----	50
5	Overall Material Balances for Run C-1 -----	52
6	Analysis of Granular Boric Acid -----	59
7	Spray Distribution in Containment Vessel -----	60
8	Effective Drop Flow Rate and Fall Distance -----	61
9	Airborne Iodine Concentration Decrease During Purging of the Containment Vessel -----	75
10	Iodine Loss By Evaporation of Liquid Samples -----	77
11	Cesium Loss By Evaporation of Liquid Samples -----	78
12	Comparison of Containment Temperatures For Two Boric Acid Spray Tests -----	84
13	Comparison of Iodine Concentration in Two Boric Acid Spray Tests -----	85
14	Comparison of Cesium in Two Boric Acid Spray Runs ----	86
15	Comparison of Spray Characteristics For Runs C-1 and A-7 -----	87
16	Physical Parameters Assumed For A Large PWR -----	98
17	2 Hr DRF In A PWR Predicted From Partition Coefficient Experiments -----	102
B-1	Concentrations in Main Vapor Space From Cluster Samples - Run C-1-----	121
B-2	Concentrations in Main Vapor Space From "Thief" Samples - Run C-1 -----	122
B-3	Concentrations in Main Vapor Space From "Thief" Samples - Run C-1 -----	123
B-4	Concentrations in Main Vapor Space From "Thief" Samples - Run C-1 -----	124
B-5	Concentrations in Middle Vapor Space - Run C-1 -----	125
B-6	Concentrations in Lower Vapor Space - Run C-1 -----	126

I. INTRODUCTION

Most current and proposed PWR nuclear power plants are equipped with a containment building spray system. Some systems incorporate a chemical blending system to add sodium hydroxide⁽¹⁾ or sodium thiosulfate⁽²⁾ to the dilute boric acid solution from the refueling water storage tanks which is used as the source for the fresh spray. The purpose of the caustic or sodium thiosulfate additives is to improve the system's capability for removing fission product iodine from the containment vessel atmosphere in the unlikely event of an accident in which iodine is released from the primary system. The ability of caustic sprays to rapidly remove and retain iodine has been adequately demonstrated at several laboratories, as reported recently in a special ANS session on Containment Spray Technology.⁽³⁾

Some PWR plants do not propose to add caustic to their spray solution and have not, at the present, claimed any credit for iodine removal by the acidic boric acid spray. Experiments at Battelle-Northwest⁽⁴⁾ and at Oak Ridge National Laboratory⁽⁵⁾ have shown that good removal of iodine by boric acid spray is possible. Hence, caustic addition may not be necessary to insure efficient iodine washout.

The use of boric acid without caustic has several advantages. Boric acid is a safer material from a plant personnel standpoint. Much less damage would be caused to plant equipment by accidental activation of the sprays. In addition, use of acidic borate would eliminate the caustic-aluminum reaction, and thereby eliminate a potential source of hydrogen.

The present research was undertaken to provide confirmatory information on iodine removal by boric acid sprays. A cursory examination of iodine chemistry lead to the conclusion that boric acid sprays would not be highly effective in removing iodine, a conclusion which is in contradiction with reported experiments.^(4,5) Very little basic data was available on iodine partitioning in spray solutions. Hence a series of pilot scale experiments was carried out to determine the partition coefficient of iodine in boric acid solutions for a range of concentrations and temperatures. The second part of this work was performance of a large-scale demonstration experiment under conditions closely simulating a loss-of-coolant accident. The combination of basic studies and the large-scale test was designed to provide information necessary for confident assessment of iodine removal by boric acid sprays in PWR containment vessels.

II. SUMMARY AND CONCLUSIONS

The potential capability of acidic boric acid spray for removing iodine from containment building atmospheres was investigated experimentally by performing one large-scale demonstration spray test and 13 small-scale equilibrium experiments. The demonstration experiment was performed in the 26,500 ft³ Containment Systems Experiment (CSE) vessel under conditions simulating those expected following a loss-of-coolant accident in PWR plants. The iodine gas-liquid partition experiments were conducted in a 32 ft³ stainless steel vessel under a range of conditions pertinent to scrubbing of iodine from containment atmospheres by boric acid spray systems. A simplified mathematical model was developed to a point where hand

calculations can be made to estimate iodine washout by boric acid sprays under diverse conditions.

The experimental and theoretical research supports the following conclusions:

1. Elemental iodine dissolves in boric acid solution by a 4-step process: physical absorption, a rapid hydrolysis with equilibrium attained in fractions of a second, a chemical reaction (influenced by trace impurities) which attains equilibrium in tens of minutes, and a slow, irreversible reaction which continues for many hours.
2. The physical absorption and rapid hydrolysis are effective mechanisms for removing airborne iodine by falling spray drops. The continuing chemical reactions remove dissolved elemental iodine in the liquid residing in the sump. Upon recirculation, this liquid absorbs iodine at a rate close to that of a fresh spray.
3. The magnitude of the instantaneous iodine partition coefficient, H_0 , depends on iodine concentration and the amount of impurities in the system. Values of H_0 measured in stainless steel laboratory apparatus ranged from 25 at the highest iodine concentration expected for a PWR core meltdown accident, to > 5000 for low iodine concentrations. Small amounts of impurities increased the magnitude of H_0 appreciably.

4. In the large-scale demonstration test, the inorganic iodine concentration was reduced by a factor of 25 during the 16-minute fresh spray period, by a factor of 100 in 60 minutes, and by a factor of 3700 after 6 days. A factor of 10 reduction for the fresh spray was predicted, based on H_0 values determined in the small-scale partition experiments.
5. Methyl iodide was removed slowly throughout the 6-day duration of the large-scale test. Its concentration decreased by a factor of 5 during the first two days, and by a factor of 40 during the 6-day period.
6. Particulate iodine was removed very rapidly and could be considered as part of the inorganic iodine total.
7. Cesium and uranium particle washout was similar to previous experiments with caustic sprays. Airborne particle concentration was reduced by a factor of 25 during the fresh spray and by 10^4 after one day.
8. The magnitude of H_0 was found to be independent of boron concentration in the aqueous phase.
9. H_0 is not expected to vary greatly with temperature. This conclusion is based on hydrolysis theory and an experimental measurement made as part of this study.
10. Inorganic iodine was not removed from the containment atmosphere as rapidly in the present work as in a previous experiment (CSE Run A-7). The results of the two experiments are consistent when differences in initial iodine concentration and impurity level of the boric acid solution are considered.

III. IODINE REMOVAL THEORY

The design of iodine removal experiments should be based on understanding of the mechanisms which govern absorption of iodine by aqueous sprays. The theory presented in this chapter outlines the thinking used in designing the experiments reported in this document.

Application of experimental data on iodine spray removal to full scale containment vessels is best done through mathematical models which account for size effects. Although detailed numerical evaluation of a washout model for specific cases of application was beyond the scope of the present work, the theory presented in this chapter forms the basis for application of the experimental results to reactor containment systems.

A. Material Balance Equations

A material balance written for a single airborne species in the main gas volume of a containment system may be expressed as

$$V \frac{dC_g}{dt} = G + (C_{g2} - C_g) B_{12} - \sum_j [k_g (C_g - C_{gi}) A]_j - R_G \quad (1)$$

in which

V = volume of main containment space,

C_g = gas phase concentration of solute in main containment volume,

t = time,

G = generation rate of solute within the main containment volume,

C_{g2} = gas phase concentration of solute in connected volumes,

B_{12} = exchange coefficient for interroom transport,

k_g = mass transfer coefficient at a deposition surface,

- C_{gi} = gas phase concentration of solute at a deposition surface,
A = surface area available for deposition,
 R_G = rate of gas phase chemical reaction of a species in
the main containment volume.

The left member of Equation (1) is the accumulation rate of solute which occurs as a result of generation and depletion. The first term on the right side is the generation rate, or addition rate of solute to the gas phase. The second term is transport from connected rooms. The third term of the right hand member of Equation (1) represents deposition of a specie onto j surfaces within the main room. The last term on the right accounts for disappearance of a specie by a homogenous gas phase reaction.

Equation (1) is only one of the set of simultaneous material balance equations which are needed to describe the gas phase concentrations. Equations similar to Equation (1) are needed for each of the connected volumes. A second set of equations are also needed to account for phase equilibria. Fortunately, for many cases of practical interest, the material balance equations may be greatly simplified. For the spray experiments described in this report, the generation rate, G , and gas phase reaction rate, R_G , may be neglected. Also, absorption surfaces are either falling drops or wetted walls. Interroom transport may be neglected for much of the spray time. The material balance equation resulting from these simplifying assumptions is

$$V \frac{dC_g}{dt} = \left[k_g (C_g - C_{gi}) A \right]_{\text{drops}} + \left[k_g (C_g - C_{gi}) A \right]_{\text{wall}} \quad (2)$$

Evaluation of the mass transfer rates to drops and wall film will now be considered.

B. Absorption of Elemental Iodine by Drops

1. Absorption by Fresh Spray

The absorption rate of a spray may be calculated as the sum of the absorption rates for the individual spray drops. For a single drop, the absorption rate depends on the solute concentration in the gas phase, the exposure time, the drop size, the overall mass transfer coefficient, and the equilibrium solubility of the solute gas within the drop.

Elemental iodine undergoes rapid hydrolysis reactions in water solution which influence the partition coefficient. An overall partition coefficient may be defined in terms of the total amount of iodine in solution as

$$H = \frac{[I_2(aq)] + [I_2(reacted)]}{[I_2(g)]} = H_u (1 + K_1) \quad (3)$$

where H = overall partition coefficient for spray absorption,

$[I_2(aq)]$ = concentration of unreacted iodine in aqueous phase,

$[I_2(reacted)]$ = concentration of iodine in reacted forms in solution,

H_u = partition coefficient for unreacted iodine,

K_1 = equilibrium constant for fast hydrolysis reaction.

The partition coefficient, H , defined by Equation (3) thus includes the effect of chemical reactions which attain equilibrium in time periods which are short compared to the few second drop exposure times. For slower chemical reactions the reaction kinetics must be considered. Hence, slow chemical reactions cannot be included in determining the effective H

as defined by Equation (3). The extent of fast hydrolysis reactions will be influenced by the iodine concentration in the liquid. Since the iodine concentrations of interest in containment vessels are dilute, impurities in the spray solution would be expected to influence the rate and extent of solution chemical reactions. The magnitude of the overall partition coefficient (Eq. (3)) would not remain constant at low concentration due to the variable influence of chemical reactions. Only H_u , the partition coefficient for unreacted iodine, would be expected to obey Henry's Law, which states that the partition coefficient is independent of concentration for dilute solutions.

Realistic models of drop absorption must account for the degree of mixing which occurs in the liquid phase. Fortunately, for drop sizes and exposure times applicable to containment sprays, upper and lower limits of absorption predicted from stagnant and well-mixed models do not differ greatly. Models based on these limiting assumptions will be briefly discussed.

The drop absorption rate, expressed in Equation (2) as

$[k_g (C_g - C_{gi})A]_{\text{drops}}$ may be written as

$$\text{spray absorption rate} = H C_g \sum_d F_d E_d \quad (4)$$

where H = equilibrium partition coefficient,

C_g = solute concentration in gas phase,

F_d = spray flow rate for drops of diameter, d ,

E_d = fractional saturation attained by
drops of diameter, d .

Equation (4) is written as a summation over drop size to account for the change in E with drop size. Use of a proper mean size to represent the drop size distribution gives

$$\text{spray absorption rate} = H C_g F E \quad (4a)$$

where E is the average fraction saturation for the entire spray.

For well mixed drops, the fractional saturation may be obtained from solution of a differential equation based on a material balance on the drop liquid. At the gas-liquid interface, surface saturation, the boundary condition ordinarily used, is applied. The resulting equation is

$$E = 1 - \exp \left(- \frac{6 k_g t_e}{H d} \right) \quad (5)$$

- where k_g = gas phase mass transfer coefficient,
 t_e = drop exposure time,
 H = equilibrium partition coefficient,
 d = drop diameter.

Equation (5) gives the upper limit to drop absorption because liquid phase mass transfer resistance has been neglected.

A lower limit to drop absorption may be predicted from a stagnant drop model presented by Danckwerts. (6)

$$E = \frac{6 h^2}{a} \sum_{n=1}^{\infty} \frac{1 - \exp(-Dt \alpha_n^2)}{\alpha_n^2 \left[a \alpha_n^2 + h (ah-1) \right]} \quad (6)$$

- where $h = \frac{k_g}{HD}$,
 D = diffusivity in liquid phase,
 a = drop radius,
 α_n = nth root of $(a\alpha) \cot(a\alpha) + ah - 1 = 0$.

The well-mixed drop model, Equation (5), is easy to evaluate by hand. The stagnant drop model, Equation (6), involves an infinite sum and hence requires use of a computer. These two models have been evaluated for a range of conditions of practical interest. The results, presented in terms of the ratio of absorption of stagnant to well-mixed drops, are shown in Figure 1. For drop fall heights applicable to CSE (34 ft) and PWR containment vessels, the maximum difference between stagnant and well-mixed drops is about 30%. This maximum discrepancy occurs at an H of about 10^3 . For lower or higher values of H, the effect of mixing would cause differences in absorption of less than 30%. It is worth noting here that the numerical value of the partition coefficient, H, is often known less precisely than $\pm 30\%$. Hence the potential error associated with drop mixing is not expected to be highly significant in applying theory to containment spray systems.

2. Absorption by Recirculated Spray

Recirculation of spray liquid through the nozzles causes mixing within the two phases and mass transfer between the gas and liquid phases, so that equilibrium between well-mixed spray liquid and well-mixed gas will eventually occur.

The absorption or desorption which occurs for a given spray drop falling through the containment atmosphere may be calculated using equations (5) or (6) if a dimensionless concentration difference is used. For drops entering with non-zero solute concentrations, the concentration change is given by

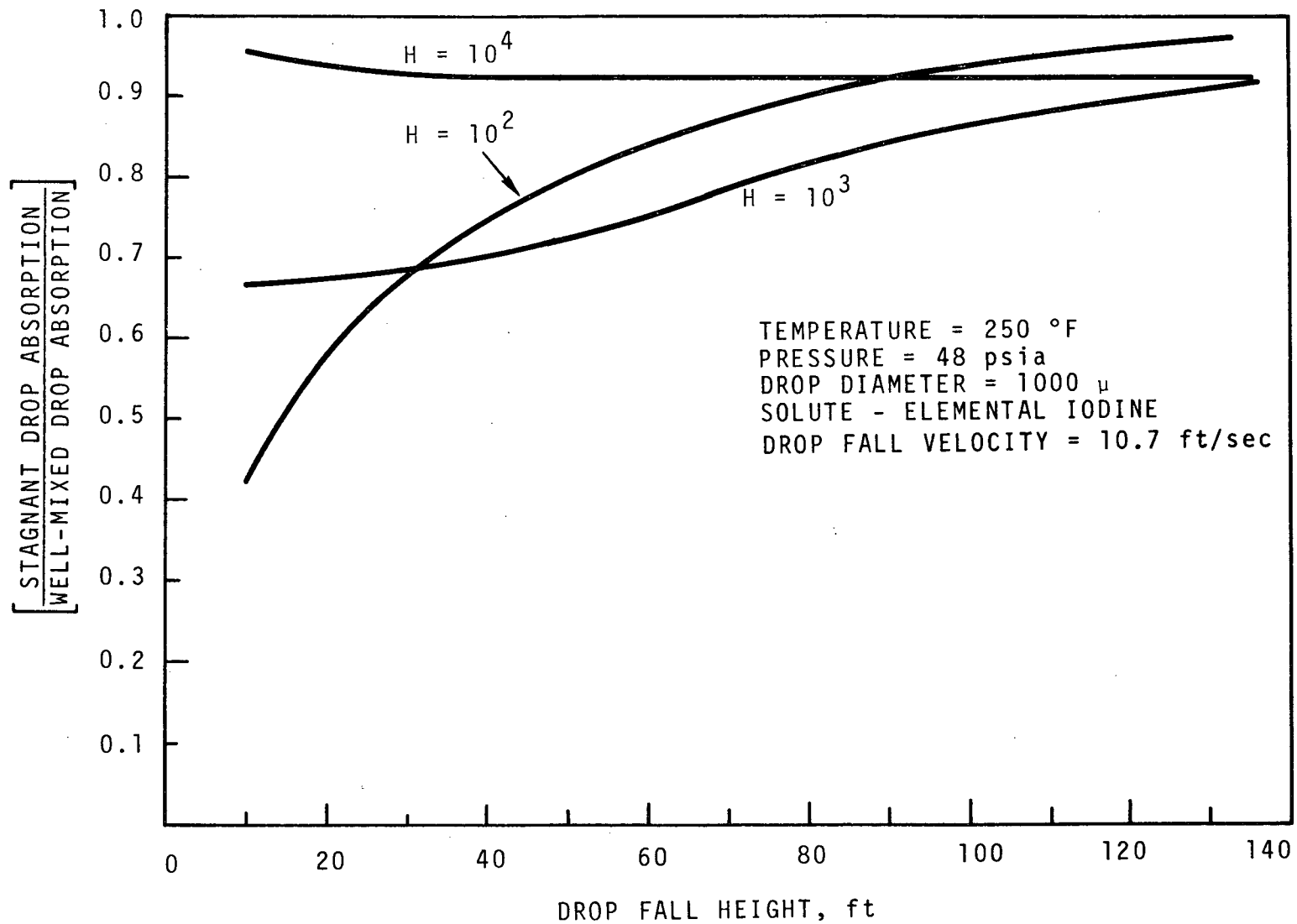


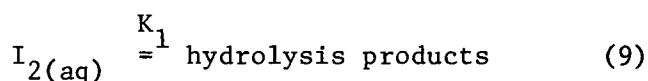
FIGURE 1. COMPARISON OF DROP ABSORPTION FOR STAGNANT AND WELL MIXED DROPS

$$\frac{C_l - C_{l1}}{HC_g - C_{l1}} = E \quad (7)$$

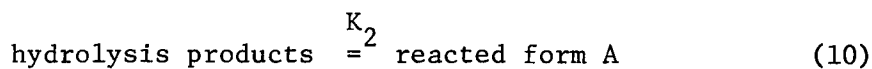
- where C_l = solute concentration in drop at end of fall,
 C_{l1} = solute concentration in entering drop,
 C_g = solute concentration in gas phase,
 H = instantaneous partition coefficient,
 E = mass transfer efficiency, defined in Eqs. (5) and (6).

The concentration of iodine in the entering spray depends on the amount of iodine absorbed by the fresh spray, on the mixing which has occurred in the sump, and on the degree to which chemical reaction alters the form of the dissolved iodine. The amount of iodine dissolved in the sump may be predicted from the initial gas phase concentration and the absorption efficiency, E . The mixing which occurs within a sump depends on its geometric design and the liquid flow rates. For reactor containment spray systems it appears reasonable to assume that mixing is complete within each phase. In the outline of theory discussed here, it has been assumed that the sump liquid is well mixed during recirculation. The remaining factor which is important in determining the concentration of iodine in entering drops is the rate and extent of chemical reactions in the sump, and these will be discussed in the following paragraphs.

Experiments and theory of iodine absorption (discussed in more detail in Chapter IV of this report) have shown that dissolved iodine reacts in solution according to the following reactions.



fast
equilibrium



slow
equilibrium



irreversible, first order

The dissolution reaction, Eq. (8), has an equilibrium constant, H_u , equal to the equilibrium partition coefficient for unreacted iodine. For this specie, Henry's Law applies, hence H_u would be independent of concentration.

Fast hydrolysis reactions which occur when iodine dissolves are all included in Equation (9). Additional discussion of these reactions is given in Chapter IV of this report. The numerical value of the equilibrium constant, K_1 , would be expected to vary with both the gas phase iodine concentration and the composition of the solution.

The hydrolysis products formed by the fast equilibrium undergo reaction as shown by Equation (10). This reaction is too slow to enhance absorption during a single drop fall time (a few seconds exposure time) but will cause appreciable disproportionation in the sump, where many minutes are available for reaction.

Finally, the reacted forms undergo irreversible chemical reaction as indicated by Equation (11). Based on these reactions, one would expect the equilibrium gas phase concentration to decrease slowly over an extended time period.

An iodine washout model for the recirculating spray period may be based on Equation (7), accounting for the chemical reactions represented by Equations (8) through (11). A schematic diagram for the washout model is shown in Figure 2. A material balance on the gas phase of the sprayed volume gives

$$0 = F(C_{\ell 2} - C_{\ell 1}) + V_g \frac{dC_g}{dt} \quad (12)$$

A material balance on the sump liquid gives

$$F C_{\ell 2} = F C_{\ell 1} + R + V_\ell \frac{dC_{\ell 1}}{dt} \quad (13)$$

where R = rate of reaction of iodine and products of fast equilibrium.

Simultaneous solution of Equations (12) and (13), using Equations (7) through (11) leads to the following expression for the gas phase concentration during recirculation.

$$C_g = C_1 e^{-\frac{FHE}{V_g} t} + C_2 e^{-\alpha_1 t} + C_3 e^{-\alpha_2 t} \quad (14)$$

In Equation (14) C_1 , C_2 , C_3 , α_1 , and α_2 are constants whose value depend on system parameters. Equation (14), when corrected to account for wall deposition, may be used in applying CSE test results to other containment vessels.

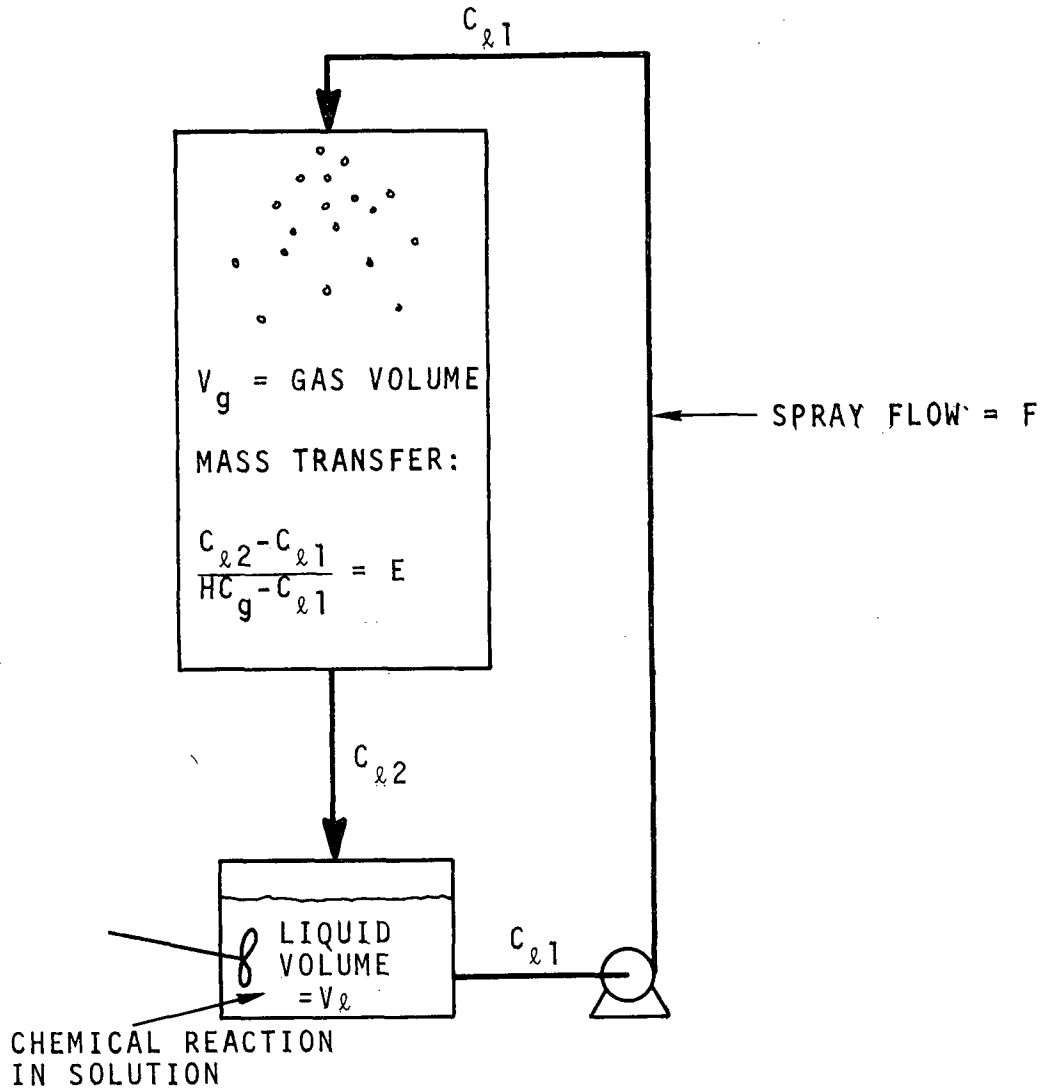


FIGURE 2. SCHEMATIC DIAGRAM OF RECIRCULATING SPRAY WASHOUT

C. Absorption of Elemental Iodine by Wall Surfaces

Wall surface areas in PWR containment vessels may be larger than the surface area exposed by spray drops, hence wall absorption needs to be evaluated. From Eq. (2) the wall deposition rate may be written as

$$\text{absorption rate} = k_g (C_g - C_{gi}) A \quad (15)$$

Earlier CSE tests⁽⁴⁾ have shown that, for caustic sprays and pure steam condensate films early in the spray period, C_{gi} could be taken as zero. For boric acid sprays, the instantaneous partition coefficient is expected to be lower than for basic solutions, hence the assumption of zero back pressure at the gas-liquid interface may not be met. Concentration profiles for wall deposition in a spray chamber are portrayed in Figure 3. The deposition rate must be obtained from simultaneous solution of the transport equations in the three phases. Although this model cannot be solved directly, simplifying assumptions may be introduced to permit easy evaluation of the absorption rate. For boric acid sprays one would expect that the wall film would become saturated after a few feet of exposure. Additional absorption would be caused only by paint absorption. Hence for this simplified model, the absorption rate is given by

$$\text{absorption rate} = k_1 H C_g A_w + F_w H C_g \quad (16)$$

where k_1 = deposition velocity for dissolved iodine,

A_w = surface area exposed by wall film,

F_w = wall film flow rate.

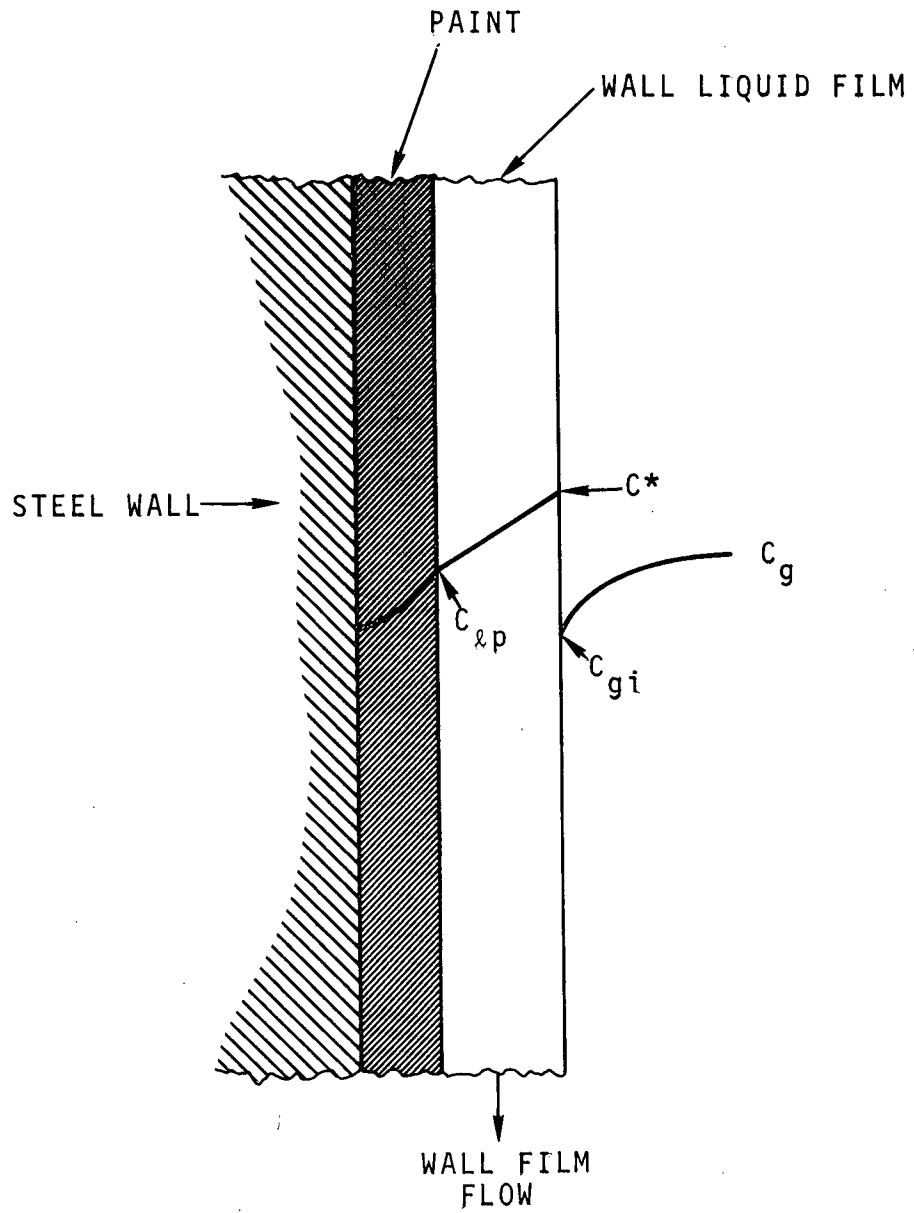


FIGURE 3. CONCENTRATION PROFILES IN WALL FILM MODEL FOR ELEMENTAL IODINE ABSORPTION

The iodine deposition velocities for various paints used in containment vessels have been measured by Rosenberg, et al. (7) For large vessels, wall deposition will be small compared to spray absorption and may be neglected. Neglect of wall film absorption for elemental iodine introduces a factor of conservatism in calculated dose reduction factors.

D. Methyl Iodide Absorption

1. Drop Absorption

For falling drops, the methyl iodide absorption rate may be bracketed by models based on stagnant and well-mixed drops. The fractional saturation achieved by a stagnant drop falling through a containment vessel is given by the Danckwerts (6) Equation,

$$\frac{C_l}{H C_g} = 6 \beta \sum_{n=1}^{\infty} \frac{\alpha + \left(\frac{\beta n^2 \Pi^2}{\alpha + \beta n^2 \Pi^2} \right) \left[1 - \exp - (\alpha + \beta n^2 \Pi^2) \right]}{\alpha + \beta n^2 \Pi^2} \quad (17)$$

where C_l = methyl iodide conc. in drop at end of fall,

C_g = methyl iodide conc. in gas phase,

H = equilibrium partition coefficient for methyl iodide,

β = Fourier No. = $\frac{Dt}{a^2}$,

α = kt ,

k = first order reaction rate constant in drop,

t = drop exposure time,

a = drop radius,

D = diffusivity of methyl iodide in spray liquid.

A numerical evaluation of Equation (17) for ranges of α and β applicable to reactor containment vessels has been presented by Postma. (8)

For well-mixed drops, the fractional saturation is simply

$$\frac{C_l}{H C_g} = 1 + \alpha \quad (18)$$

Water sprays which contain only boric acid or sodium hydroxide as additive are nominally unreactive toward methyl iodide. For such solutions, the product kt is small compared to unity, hence the reaction has little influence on absorption by drops during their fall through a containment vessel. Both Equation (17) and Equation (18) predict for these unreactive sprays,

$$\frac{C_l}{H C_g} \approx 1.0 \quad (19)$$

Equation (19) applies for drop absorption for fresh spray. It also applies for recirculated spray if the sump liquid remains above about 200 °F. For temperatures above this level, hydrolysis of methyl iodide effectively destroys it, and the spray entering the nozzle is virtually free of unreacted methyl iodide. If the sump liquid should remain at lower temperatures, reaction of methyl iodide would be incomplete, and the more general expression for the fractional saturation, Equation (7), would have to be employed in Equations (18) and (19) to predict washout by recirculated spray.

2. Wall Film Absorption of Methyl Iodide

Wall film absorption of methyl iodide is in principle similar to wall film absorption of elemental iodine. Due to the much lower partition

coefficient of methyl iodide, gas film mass transfer resistance is entirely negligible. For a stagnant wall film with negligible adsorption at the paint surface, the absorption rate per unit area is⁽⁴⁾

$$q = C^* \sqrt{kD} \tanh\left(\sqrt{\frac{k}{D}} \delta\right) \quad (20)$$

where $C^* = H C_g$,

k = first order reaction velocity in liquid,

D = diffusivity in liquid film,

δ = thickness of film.

In deriving Eq. (20) it has been assumed that the concentration gradient at the liquid film-paint interface was zero. If the paint adsorbs methyl iodide with a deposition velocity, K , the absorption rate is

$$q = \frac{-\sqrt{Dk} C^* \left[K \cosh\left(\sqrt{\frac{k}{D}} \delta\right) - \sqrt{Dk} \sinh\left(\sqrt{\frac{k}{D}} \delta\right) \right]}{K \sinh\left(\sqrt{\frac{k}{D}} \delta\right) + \sqrt{Dk} \cosh\left(\sqrt{\frac{k}{D}} \delta\right)} \quad (21)$$

where K = deposition velocity of methyl iodide from film onto paint.

The use of a deposition velocity implies that all methyl iodide adsorbed by the paint is retained irreversibly by the paint. The correctness of this assumption depends on the thickness of the paint and its reactivity toward methyl iodide. More complex models are required if methyl iodide adsorption by the paint is reversible.

Adding wall film absorption to drop absorption gives for methyl iodide,

$$\frac{C_g}{C_{go}} = \exp - \left[\frac{F \left(\frac{C_l}{C_g} \right)}{V} + \frac{qA}{V} \right] t \quad (22)$$

where $\left(\frac{C_l}{C_g} \right)$ = drop enrichment at end of fall,

C_{go} = methyl iodide concentration at time zero,

F = flow rate of drops,

q = methyl iodide absorption rate per unit area of wall surface,

A = wall surface area,

V = volume of gas space,

t = time after beginning of spray operation.

E. Overall Equation for Total Iodine Removal

The total concentration of iodine is the sum of the concentrations of all chemical forms which are present. In CSE tests, and in power reactor containment vessels the predominant forms considered are elemental iodine and methyl iodide. Thus the total concentration is simply

$$C_{\text{Total}} = C_{\text{I}_2} + C_{\text{CH}_3\text{I}} \quad (23)$$

Particulate associated iodine is a third form of iodine considered in accident analysis calculations. However, all CSE experiments have shown that particulate associated iodine is removed as fast as elemental iodine by sprays. For this reason iodine associated with airborne particles will be considered a part of the elemental iodine fraction.

IV. MEASUREMENTS OF IODINE PARTITION
COEFFICIENTS FOR BORIC ACID SPRAY SOLUTIONS

A. Purpose of Partition Coefficient Measurements

The purpose of the pilot scale partition coefficient study was to provide experimental data for a wider range of conditions than could be considered in large scale tests. These results are necessary input in mathematical models used to apply the large scale test results to a diversity of accident cases.

B. Experimental Equipment and Procedures

1. Experimental Equipment

Figure 4 illustrates the 900 liter, insulated, stainless steel vessel used in the pilot scale tests. Gas-liquid contacting was accomplished using a wetted wall and a spray. A circumferential spray header near the vessel top, made by perforating a 1/2" stainless tube, served to wet the outer wall of the vessel with spray solution. A Spraying Systems Co.* 1/4 G-3 spray nozzle, centered at mid elevation and directed upward, provided spray contact. A liquid recirculation loop allowed liquid to be pumped from the pool through a rotometer to the individual spray systems or returned directly to the liquid pool. Returned liquid entered the pool tangentially to induce mixing.

Fifteen thermocouples were positioned throughout the gas and liquid phases to monitor the temperature: Indicated temperature varied by less than 1/2 °C after equilibrium conditions were established. Temperature was maintained within ± 1 °C during the tests.

*Spraying Systems Co., Bellwood, Ill.

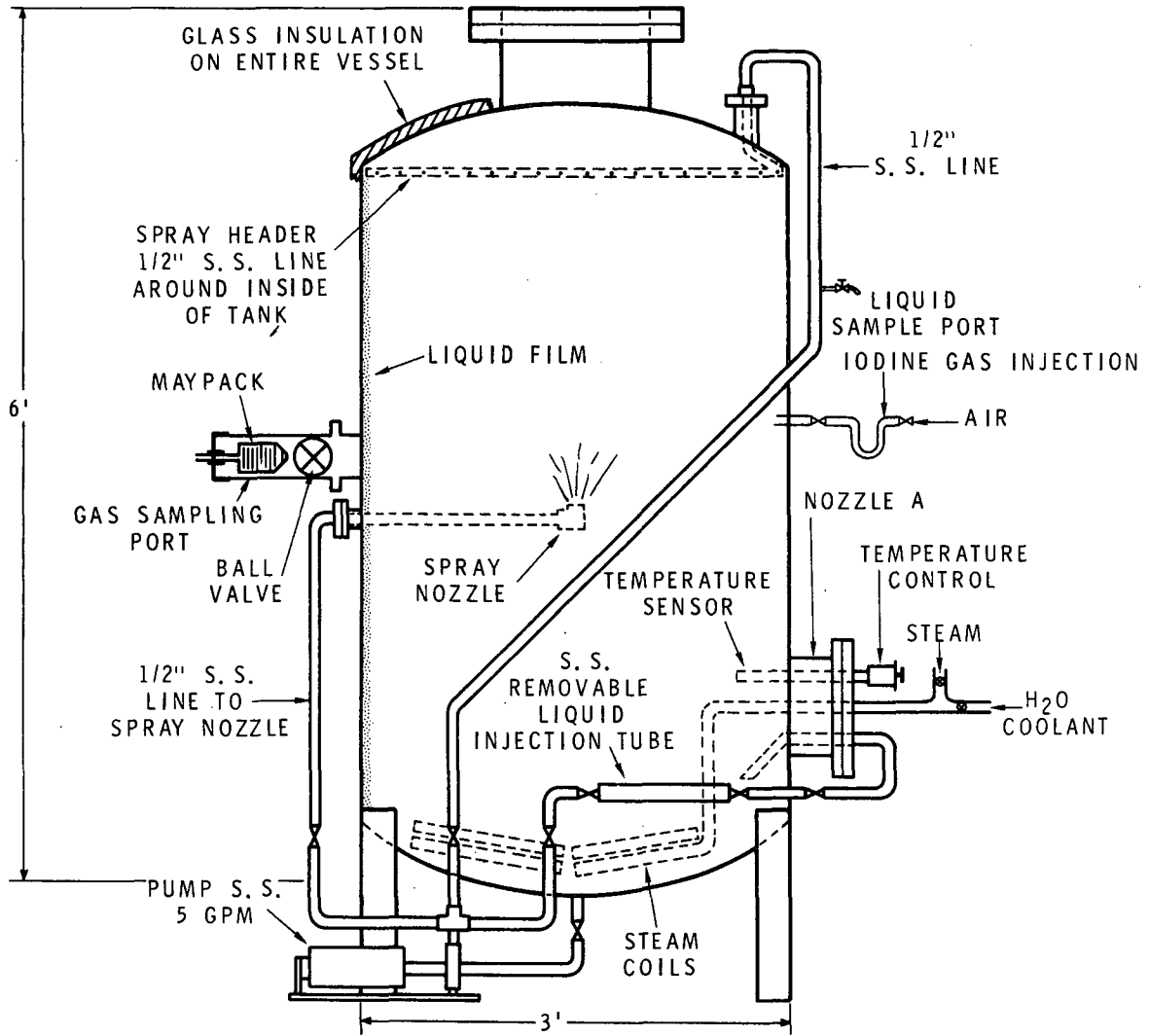


FIGURE 4. SCHEMATIC OF SMALL SCALE TEST EQUIPMENT

A steam heating coil submerged in the liquid phase furnished heat to the system to make up for heat losses. Process water could be passed through the heating coil when it was desired to cool the system. Also, demineralized water or process water could be metered directly to the spray nozzles to cool and decontaminate the system after test completion.

Iodine concentrations were determined by Maypack gas samplers and liquid samples taken from the spray recirculation loop.

A temperature controller was used to control steam feed to the system. Pressure within the vessel was kept constant by adding compressed air. This was done automatically.

Iodine could be injected into the gas phase or liquid phase. The release was accomplished by crushing a glass ampoule positioned within a thin stainless steel tube. Fluid flow through the tube containing the crushed ampoule, carried the iodine into either the gas phase or liquid phase of the vessel.

The vessel and piping were insulated with a glass fiber mat.

2. Experimental Procedures

Prior to each test, the vessel was decontaminated by steaming at 120 °C, 50 psia with steam generated from demineralized water in the liquid pool. The vessel was vented, drained, and flushed at least three times prior to a new test. Resistivity of the final recirculated cleansing liquid was greater than 250,000 ohm cm.

Water was metered into the vessel to give 100 liters of solution phase. The liquid phase was brought to 80 °C to facilitate rapid dissolution of the added boric acid. The vessel was then sealed and brought to operating conditions by proper adjustment of the temperature and pressure regulatory systems. A total liquid flow rate of 20 liters per minute was maintained during the entire test.

Once equilibrium conditions were established, iodine was introduced into the system, times recorded, and sampling commenced.

Iodine preparation and addition to the system deserves additional comment. Stable iodine was tagged with I-131 for analytical purposes. In experiment CRA, the lowest iodine concentration test, the labelled iodine was prepared by oxidizing dry tracer (NaI) plus stable iodide with molten potassium dichromate and sweeping the volatilized iodine with helium into an ampoule cooled to -77 °C. In all other cases, the labelled iodine was prepared by first evaporating carrier-free NaI^{131} to dryness in a double "U" tube glass ampoule. A weighed quantity of stable elemental iodine was then added, the ampoule evacuated and sealed, and then equilibrated at 150° overnight with the iodine in the liquid phase. Iodine was then transferred from the residue by positioning one leg of the "U" tube in a liquid nitrogen bath positioned in the 150 °C oven. The straight section of the glass ampoule was then sealed, positioned within a section of stainless steel tubing in the liquid or gas phase release loop. For release into the gas phase, electrical resistance heaters brought the flowing transport gas to 150 °C. The ampoule was crushed by collapsing the stainless

steel tube in a number of places with a dulled bolt cutter. Liquid phase release was similar. Liquid was recirculated past the glass ampoule for 5 to 10 minutes to preheat the ampoule and then the ampoule was crushed. Figure 5 illustrates the iodine preparation sequence. The exchange reaction between I-131 present as iodide and I-127 present as liquid has a half-life less than 10 minutes if the solubility of iodide in the liquid iodine is not exceeded.⁽⁹⁾ About 5 mCi I-131 was used in each individual test.

Gas samples were taken at pre-established time intervals with frequent sampling at early times when the gas concentration was changing rapidly. All samples were for 2 minute duration at an air flow rate of 5 liters per minute (STP). Maypack samplers containing particulate filters, silver screens, a charcoal impregnated paper and a charcoal bed were used to characterize the iodine. A discussion of these samplers has been reported by McCormack.⁽¹⁰⁾ The Maypack sampler was heated to the vessel temperature in an oven, and inserted into the gas phase of the vessel through an air lock. A metal shield positioned over the Maypack inlet prevented falling drops from entering the Maypack.

All gas analyses reported are for concentrations in mass per geometric volume of containment space. After passing through the Maypack, the gas stream passed through a water cooled condenser and then through glass bead and charcoal traps cooled to -77 °C. The stream was then warmed to room temperature before reaching the flow measuring rotometer. The metered volume of dry air was converted to a geometric containment volume by correcting for temperature, pressure, and steam-air ratios at vessel conditions.

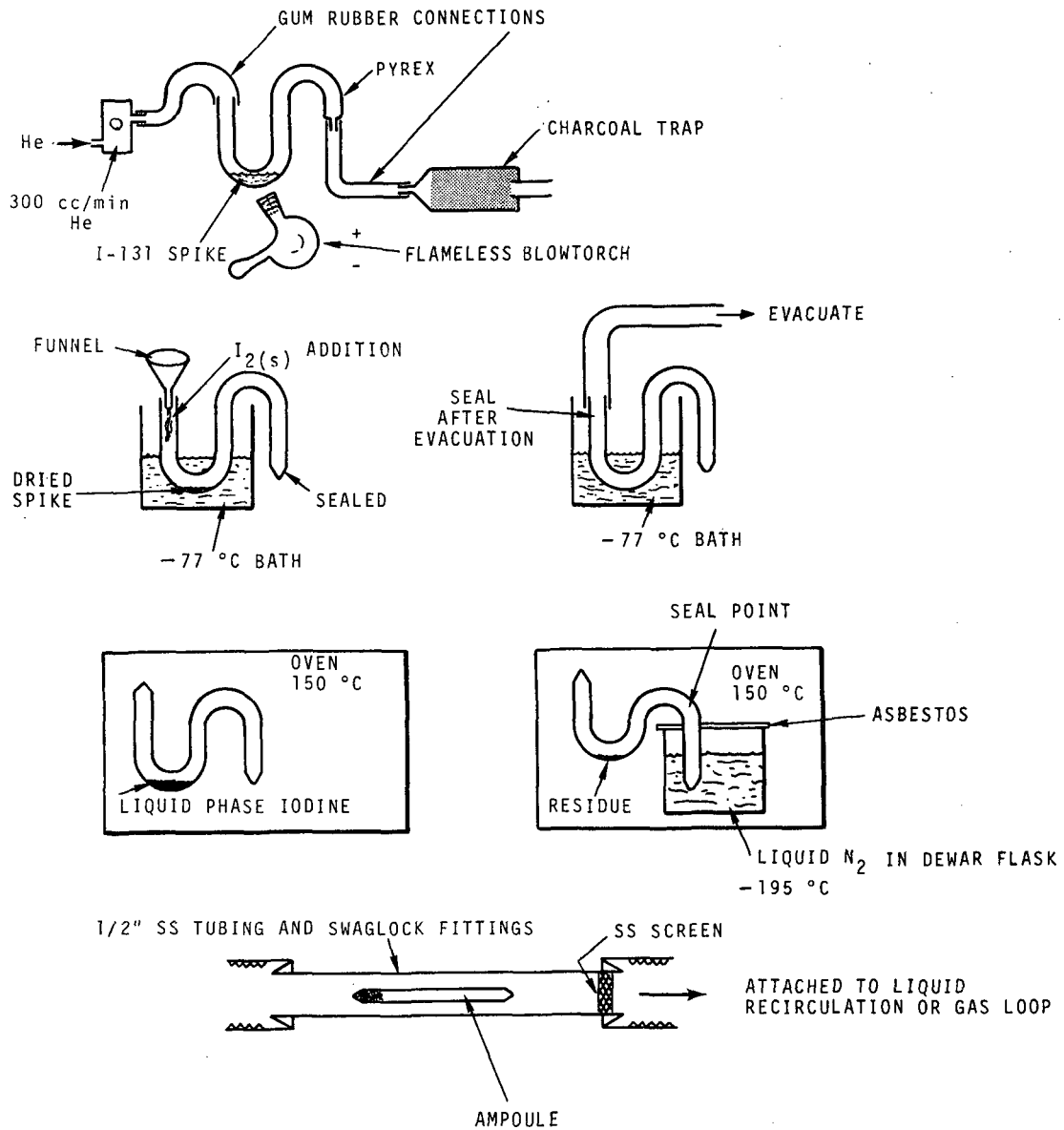


FIGURE 5. ILLUSTRATION OF IODINE PREPARATION TECHNIQUE

Liquid samples were withdrawn from the spray header loop each time a gas sample was taken. Twenty-five ml of solution were first withdrawn to purge the 1/8" sample tubing, and then 50 ml samples were taken. The pH of the solution was measured as soon as possible. The temperature of the liquid in the pH meter was typically 70 to 80 °C and the temperature compensating pH electrode system was adjusted accordingly.

C. Test Conditions

Experimental parameters for the 8 small scale tests initially proposed are presented in Table 1. Table 2 lists the conditions for the experiments actually performed. The main variables considered were iodine concentration, boric acid concentration and temperature. Secondary consideration was given to the release method (gas phase versus liquid phase) and spray solution make-up. More tests were performed than listed in the proposal. The additional tests permitted the effect of spray solution make-up to be studied.

In experiment CRK, the iodine concentration was varied by making incremental additions of iodine to the system. This was done in an attempt to map the effect of iodine concentration on the partition coefficient in a single experiment.

D. Results of Partition Coefficient Measurements

1. Iodine Concentrations in the Gas and Liquid Phases

The behavior of iodine in experiment CRA is illustrated in Figure 6 where the gas and liquid phase concentrations are plotted as functions

TABLE 1. PHYSICAL CONDITIONS IN PROPOSED

PARTITION COEFFICIENT EXPERIMENTS

<u>Experiment Identification</u>	<u>I Concentration in Liquid g/l</u>	<u>Temperature °F</u>	<u>Boric Acid Concentration ppm B</u>
A	5×10^{-5}	250	1500
B	2×10^{-3}	250	3000
C	2×10^{-3}	100	1500
D	2×10^{-3}	250	1500
E	2×10^{-3}	250	500
F	8×10^{-2}	250	1500
G*	2×10^{-3}	250	1500
J**	6.2×10^{-3}	250	3000

*Gas Phase release of iodine. All other tests employed release into liquid phase.

**Experiment J to use spray solution from large scale spray test.

TABLE 2. PHYSICAL CONDITIONS IN PARTITION
COEFFICIENT EXPERIMENTS CARRIED OUT

<u>Experiment Identification</u>	<u>I Concentration in Liquid g/l</u>	<u>Temperature °C</u>	<u>Boric Acid Concentration ppm B</u>	<u>Total Pressure psia</u>	<u>pH of Liquid</u>
CRA	5×10^{-5}	120	1500	49	5.2
CRB	2×10^{-3}	120	3000	49	5.0
CRC	2×10^{-3}	31	1500	14.4	4.6
CRD	2×10^{-3}	120	1500	49	5.5
CRE	2×10^{-3}	120	500	49	4.0
CRG ^(a)	2×10^{-3}	120	1500	49	5.3
CRH	2.5×10^{-2}	120	1500	49	4.7
CRI ^(b)	2×10^{-3}	120	1500	49	5.8
CRJ ^(c)	6.2×10^{-3}	120	3000	49	5.4
CRK ^(b)	5×10^{-4} and varied	120	1500	49	5.2
CR 9	5×10^{-4}	120	3000	49	4.8
CR 10	2.5×10^{-2}	120	3000	49	4.4
CR 12	2.5×10^{-2}	120	3000	49	4.8

(a) Release was to gas phase. In all other experiments release was to liquid phase.

(b) Liquid phase was steam condensate.

(c) Liquid phase was spray solution from large scale spray test.

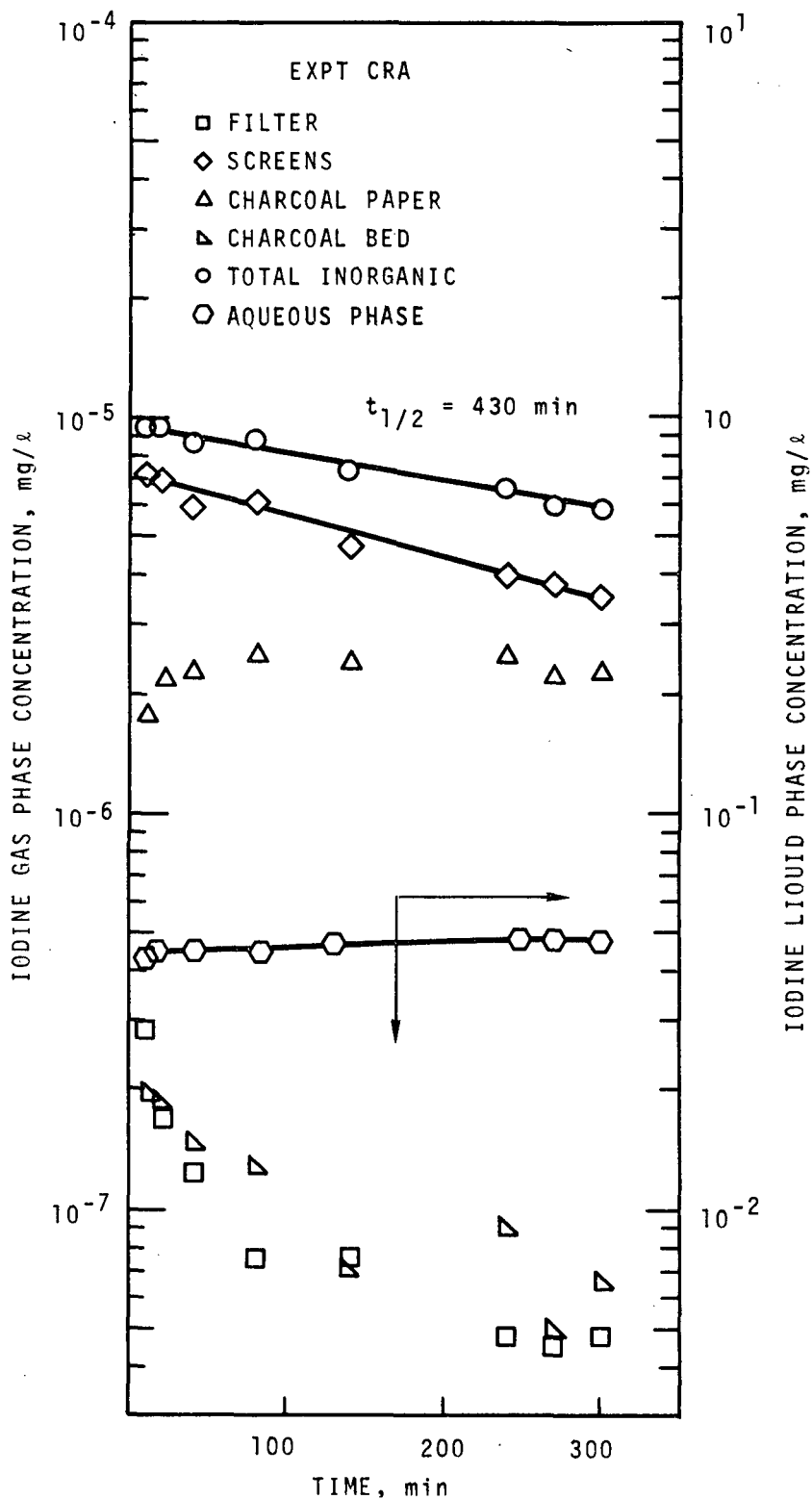


FIGURE 6. IODINE BEHAVIOR IN EXPERIMENT CRA

of time. Similar plots for the remaining 12 small scale experiments are presented in Appendix A.

With the exception of the 31 °C experiment, CRC, the concentration of total inorganic iodine in the gas phase continued to decrease with time for all small scale experiments. Analyses of the Maypack components showed that the bulk of the iodine was deposited on the silver screens, indicative of elemental iodine. Little activity was observed on the charcoal bed component early in the experiments. Hence, methyl iodide was initially a minor constituent. At the lower iodine concentrations and after long times after iodine injection, methyl iodide makes up a larger percentage of the total airborne iodine because elemental iodine is effectively tied up by solution phase chemical reactions.

Values for the partition coefficient at specific times are listed in Table 3. The partition coefficients are for inorganic iodine. The gas phase concentration of inorganic iodine was computed as the total minus methyl iodide (charcoal bed deposit). The liquid phase concentration of inorganic iodine was taken equal to the total iodine in solution.

2. Partition Coefficient Applicable to Spray Absorption

The iodine partitioning behavior is illustrated in Figure 7 where the partition coefficient (C_L/C_g) is plotted as a function of time. To apply these data to spray absorption models, values for the "instantaneous" partition coefficient and the rate of slower reactions are needed. The "instantaneous" partition coefficient was obtained by extrapolating the measured partition coefficients to time zero. These numbers would be

TABLE 3. RESULTS OF PARTITION COEFFICIENT MEASUREMENTS

Experiment Identification	I Concentration in Liquid g/l	Temperature °C	Partition Coefficient at Listed Times			
			Time Zero	100 Min	350 Min	1000 Min
CRA	5×10^{-5}	120	5.2×10^3	6.2×10^3	9.3×10^3	
CRB	2×10^{-3}	120	30-50	2×10^2	3×10^3	$\sim 9 \times 10^3$
CRC	2×10^{-3}	31	1×10^2	1.3×10^2	1.2×10^2	
CRD	2×10^{-3}	120	50	5.0×10^2	3.7×10^3	
CRE	2×10^{-3}	120	20-50	6.0×10^2	3.0×10^3	
CRG	2×10^{-3}	120	50	6.7×10^2	3.7×10^3	
CRH	2.5×10^{-2}	120	10-20	20	60	
CRI	2×10^{-3}	120	1.3×10^3	1.7×10^3	3.1×10^3	
CRJ	6.2×10^{-3}	120	60	2×10^3	3.5×10^3	1.1×10^4
CRK	5×10^{-4}	120	5.0×10^3	6.0×10^3		
CR 9	5×10^{-4}	120	3.3×10^3	4.3×10^3	8.1×10^3	
CR 10	2.5×10^{-2}	120	10-20	15	50	
CR 12	2.5×10^{-2}	120	10-20	20	70	$\sim 1 \times 10^3$

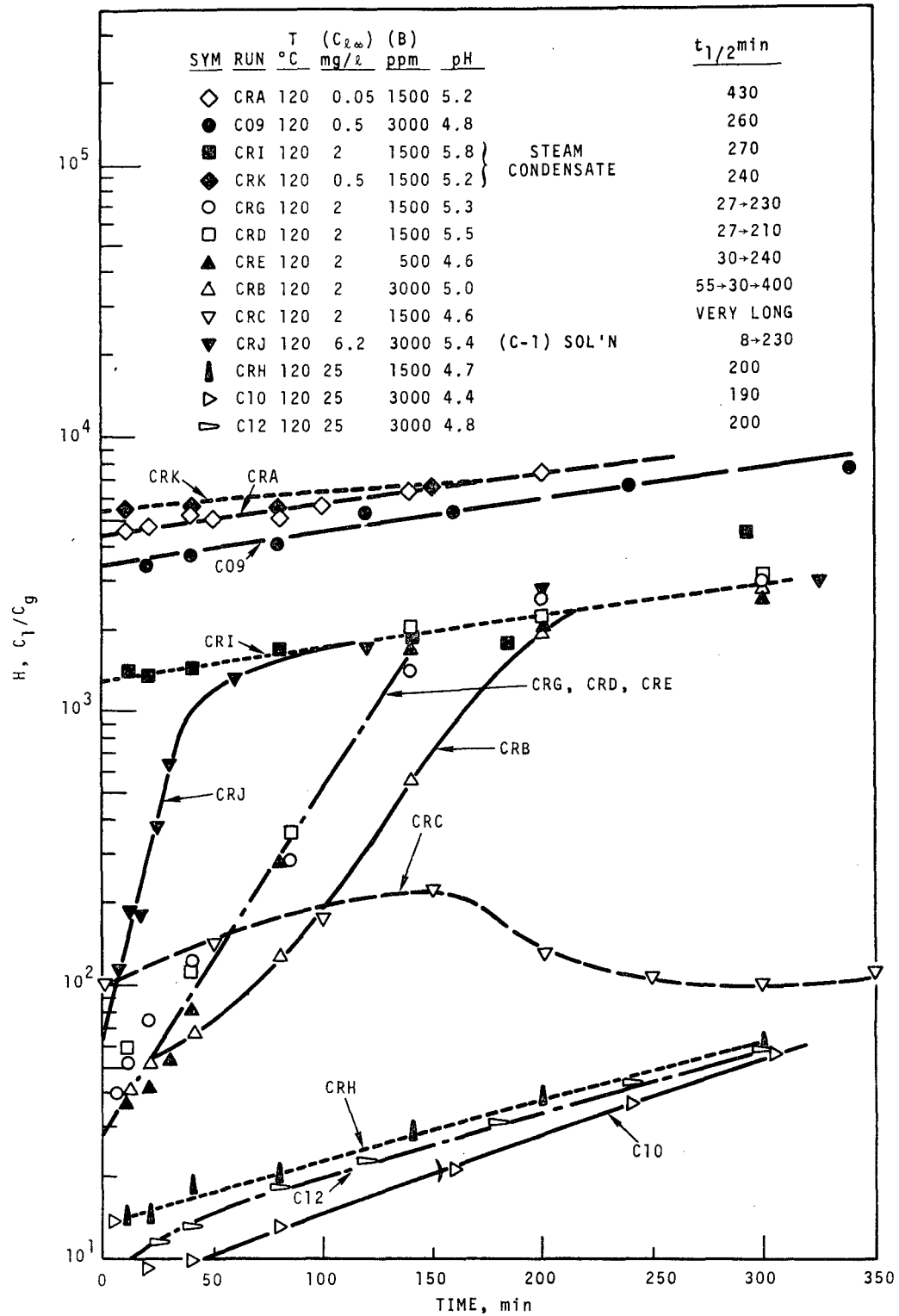


FIGURE 7. H VERSUS TIME, BORIC ACID-IODINE EQUILIBRIUM TESTS

applicable to drop washout where residence times are of the order of a few seconds. The time zero partition coefficient, H_0 , is influenced by hydrolysis reactions which are rapid. Slower solution phase reactions (reaction completion half-times of the order of minutes) are of importance for recirculated sprays where the holdup in the liquid pool may be long enough to react much of the volatile iodine.

The final slow change (gas phase depletion half-time of hours) has little influence on short term (a few hours) washout. However, slow reactions are important in determining the airborne concentration many hours after an accident.

3. Effect of Physical Parameters on the Partition Coefficient

a. Iodine Concentration

Iodine concentration was found to be an important variable relative to the boric acid-iodine system. Figure 8 is a plot of time zero partition coefficients as a function of iodine concentration in the liquid phase. Figure 9 is a plot of the same data as a function of the gas phase concentration.

In one experiment, CRK, incremental additions of iodine were made to study the concentration effect in a single experiment. The general trend was the same as observed in other experiments but the data are displaced toward higher partition values. A small part of this displacement is attributed to solution reaction time between iodine addition. The reaction rate-time effect was minimized by making large iodine additions relative

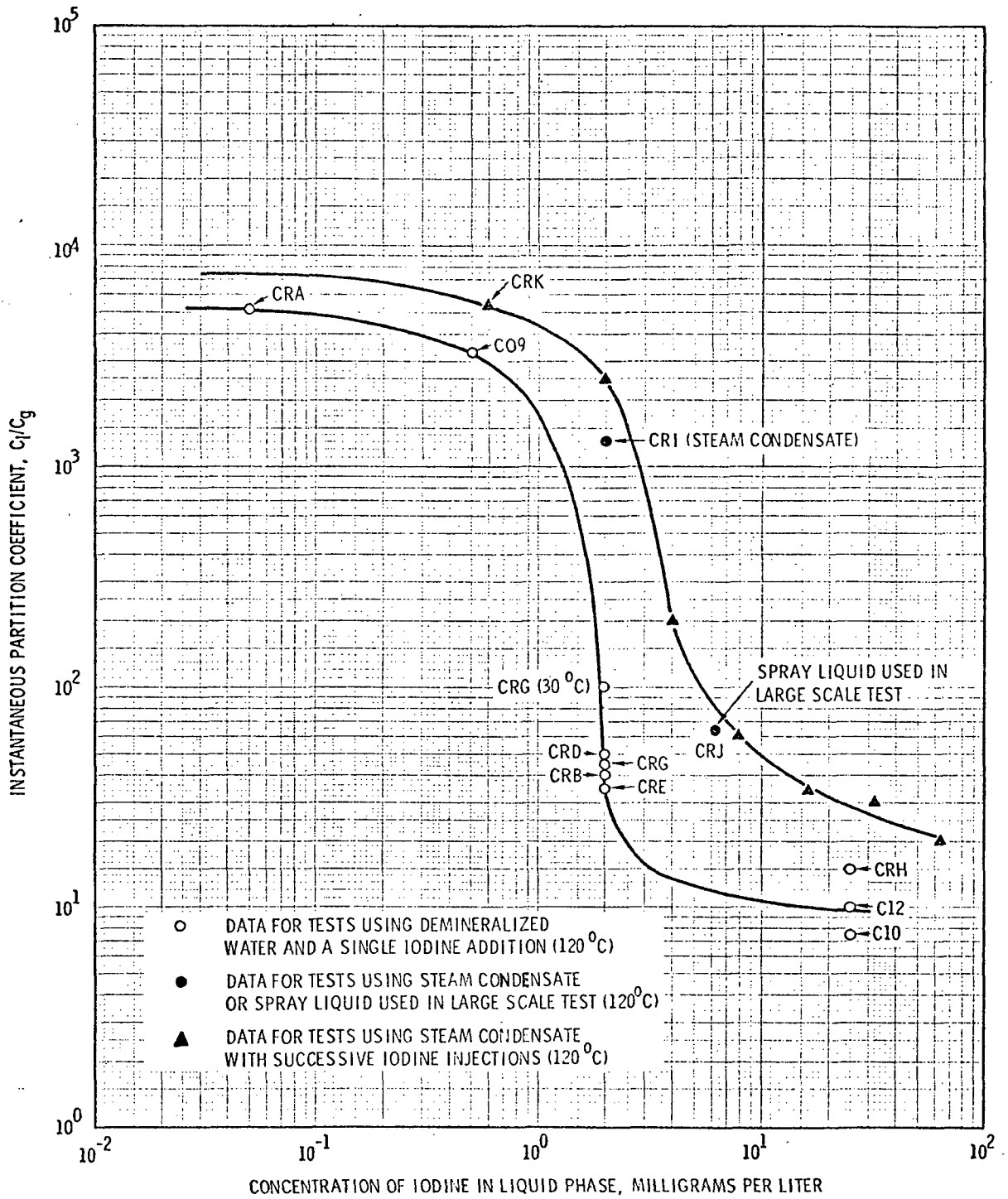


FIGURE 8. EFFECT OF IODINE CONCENTRATION ON INSTANTANEOUS PARTITION COEFFICIENTS IN BORIC ACID SOLUTIONS

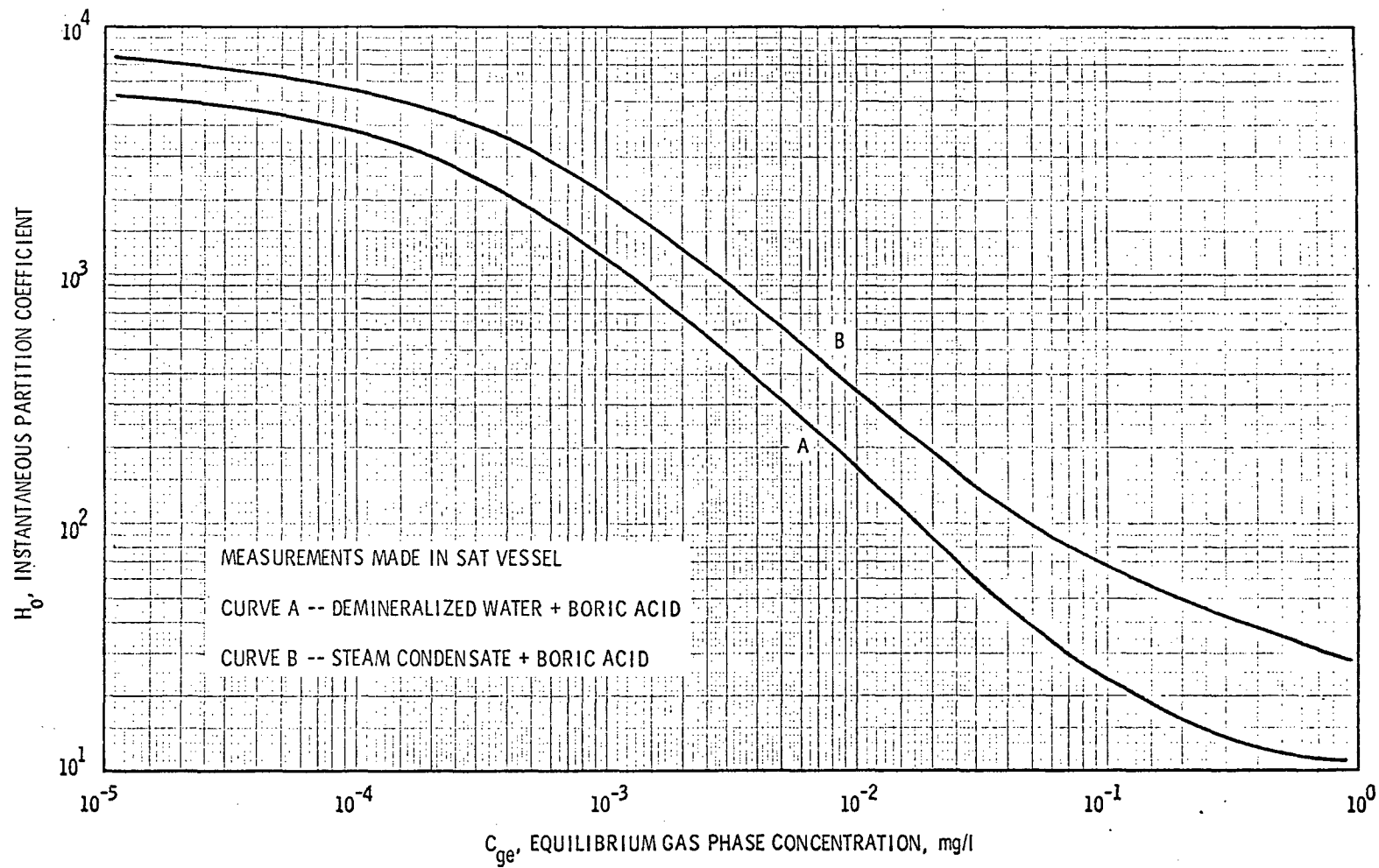


FIGURE 9. PARTITION COEFFICIENTS FOR INORGANIC IODINE IN BORIC ACID AS A FUNCTION OF GAS PHASE CONCENTRATION

to the starting mass. The aqueous phase in this experiment was steam condensate which contains impurities which react with iodine in solution. Agreement of the results for tests CRK, CRI, and CRJ implies that impurities caused the larger partition coefficient. The data for test CRK are shown in Figure A8 in Appendix A. The concentrations shown in Figure A8 are relative concentrations. They are proportional to the concentrations expressed as disintegrations of I-131 per unit volume. The mass concentrations may be obtained from the masses of iodine added at each increment. The incremental masses added are also listed in Figure A-8.

b. Boron Concentration

The limited variation of boron concentration (500 to 3000 ppm B as boric acid) showed a little affect on the initial partition coefficient. This is shown in Figure 10 where data from experiments CRD, CRG, CRE, and CRB are shown. These experiments, all at 2 mg/l iodine concentration, gave essentially the same results for boron concentration from 500 to 3000 ppm. Similar results were evident for experiments CRJ and CRK at 10 mg/l iodine and CRH, C10 and C12 at 25 mg/l iodine concentration. Analyzed Reagent Grade boric acid (Baker Lot 0084) was used in all but the CRJ test where Special Quality Grade (U. S. Borax Co.) boric acid was used, and C10 where technical grade material was used. The analysis of the Special Quality Grade boric acid is given in Chapter 5 of this report.

c. Temperature

Of the 13 partition coefficient experiments performed, 12 were carried out at 120 °C and one at 31 °C. The partition coefficient at time

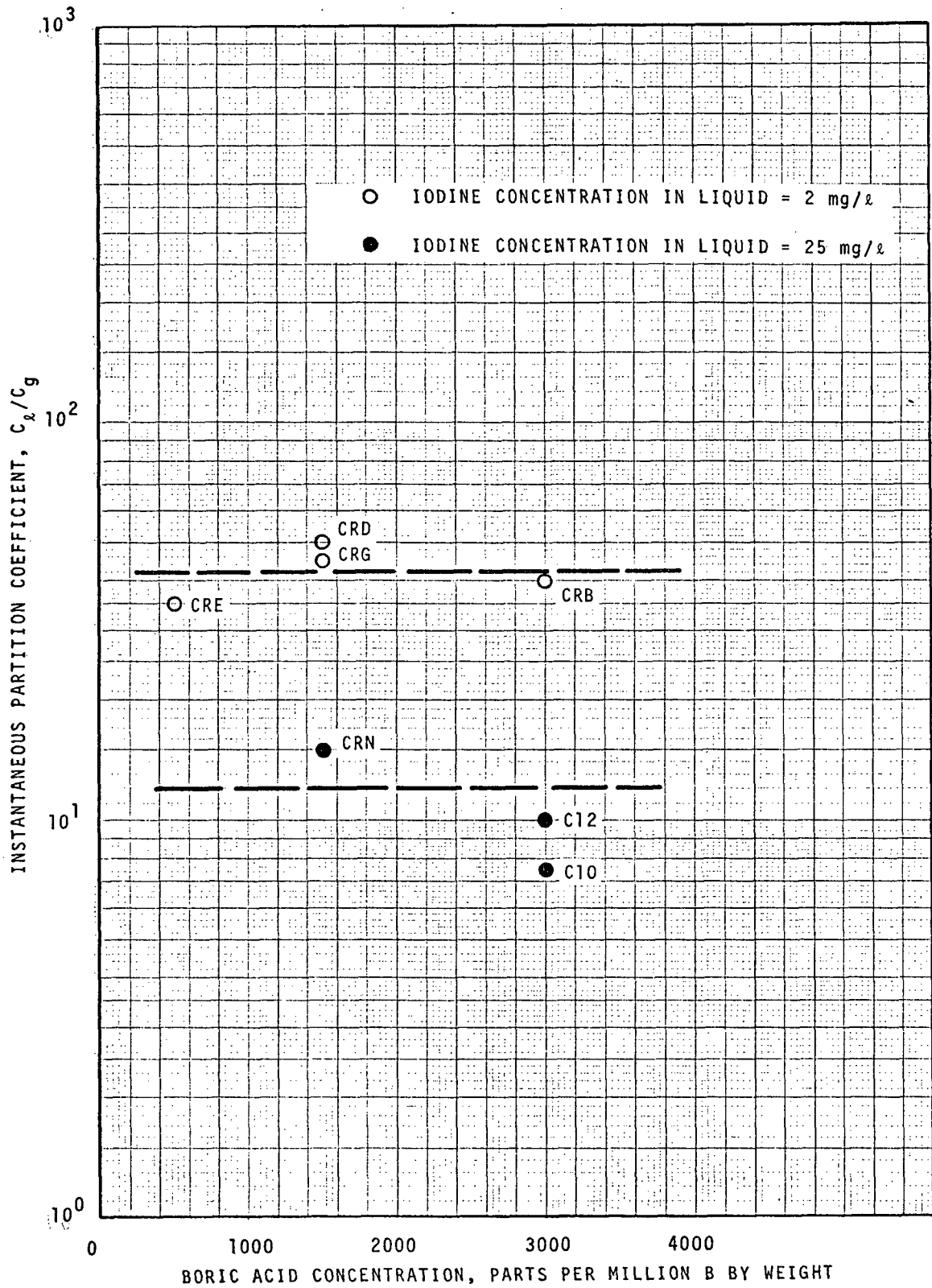


FIGURE 10. EFFECT OF BORIC ACID CONCENTRATION ON INSTANTANEOUS IODINE PARTITION COEFFICIENT

zero for the 31 °C test falls above the curve for tests obtained at 120 °C as shown in Figure 8. At longer times, the partition coefficient for the higher temperature experiments is greater than that at 31 °C. This is shown in Figure 7. These results indicate that H_0 would be larger for lower temperatures, where the Henry's Law constant is greater. For longer times, chemical reactions cause the partition coefficient to increase with temperature. Very little data were obtained in this study on the effect of temperature, and hence the generalizations made above must be considered tentative. Since the temperatures of interest in containment vessels are close to 120 °C, lack of data at lower temperatures is not a substantial practical limitation.

d. Solution pH

The pH of the boric acid solutions varied from pH 4.4 to 5.8 and no gross effects on the partition coefficient were observed. Over the boron concentration range studied, the pH was expected to vary about 1/2 pH unit at 120 °C. Byrnes⁽¹¹⁾ and subsequent computational results of Meek⁽¹²⁾ show the influence of temperature, boron concentration and added base on the pH of boric acid systems. The pH values reported in Table 2 differ slightly from the predicted values. Part of the variation is attributed to errors in the pH measurements. Data obtained in the present study indicate variations in measured pH values of less than ± 0.3 units for identical samples. At 120 °C the pH for 500, 1500 and 3000 ppm B would be predicted to be about pH 5.2, 4.9, and 4.7 respectively.

A theoretical treatment of iodine behavior in aqueous systems based on a number of equilibrium reaction equations for iodine has been presented by Eggleton.⁽¹³⁾ Eggleton's⁽¹³⁾ calculations indicate that pH would have a marked influence on iodine partitioning. The fact that only minor effects were observed in the boric acid experiments reported here may be explained in two ways. First, the pH values of all of the boric acid solutions used were close to the same value, and large changes in partition coefficient would not be expected. Second, impurities present in solution react with dissolved iodine. Such reactions are not accounted for in the simple theory outlined by Eggleton.⁽¹³⁾

e. Solution Impurities

Solution impurities may have a pronounced effect on iodine chemistry particularly at low concentration. This is demonstrated by the variation between experiments carried out using demineralized water and those which used process steam condensate. Where steam condensate was used (CRI, CRK) the time zero partition coefficient and the initial gas phase depletion rate were different than the similar case where demineralized make up water was used. This difference is attributed to reaction of dissolved iodine with impurities. Other explanations are not obvious.

Demineralized water used in these experiments had a resistivity greater than 500,000 ohm cm and a pH of 6.5 to 7. Condensed process steam condensate had a pH from 7.5 to 7.7. Spectrochemical analyses showed traces of iron in the process steam condensate. Permanganate demand was about 3 milligrams per liter. Previous steam condensate analyses have shown 0.5 to 1 ppm of octadecylamine (an organic filming agent for corrosion inhibition) to be present.

Permanganate demand for test CRJ which used spray solution from the large scale test was also about 3 milligrams/liter and spectrochemical analyses showed iron to be the major trace impurity.

Although an investigation of solution phase impurities was beyond the scope of this investigation, the limited results suggest that impurities have an influence on iodine chemistry in dilute aqueous systems.

E. Comparison of Measured Partition Coefficients with Previous Data

Available data on the partitioning of elemental iodine in weakly acid solutions are shown in Figure 11. The data from the present study are represented by the curves drawn through the data presented in Figure 8. Also shown are data obtained in Canada by Watson, et al⁽¹⁴⁾ and data obtained in Japan by Nishizawa.⁽¹⁵⁾ Calculations based on Eggleton's⁽¹³⁾ theory (not including the iodate reaction) are shown for comparison.

Several important results are evident from the comparison of results shown in Figure 11. At high iodine concentrations, all of the results merge, and experimental measurements are in agreement with simple hydrolysis theory. At concentrations below about 1 milligram per liter, the experimentally measured partition coefficients deviate grossly from the simple hydrolysis theory. The degree of enhancement of the measured partition coefficient compared to hydrolysis theory depends on the liquid iodine concentration and the purity of the water solution. For concentrations below 2 milligrams per liter, the data of Watson⁽¹⁴⁾ fall above and below the measurements made in this study. This is explainable in terms of impurities in solution which react with dissolved iodine.

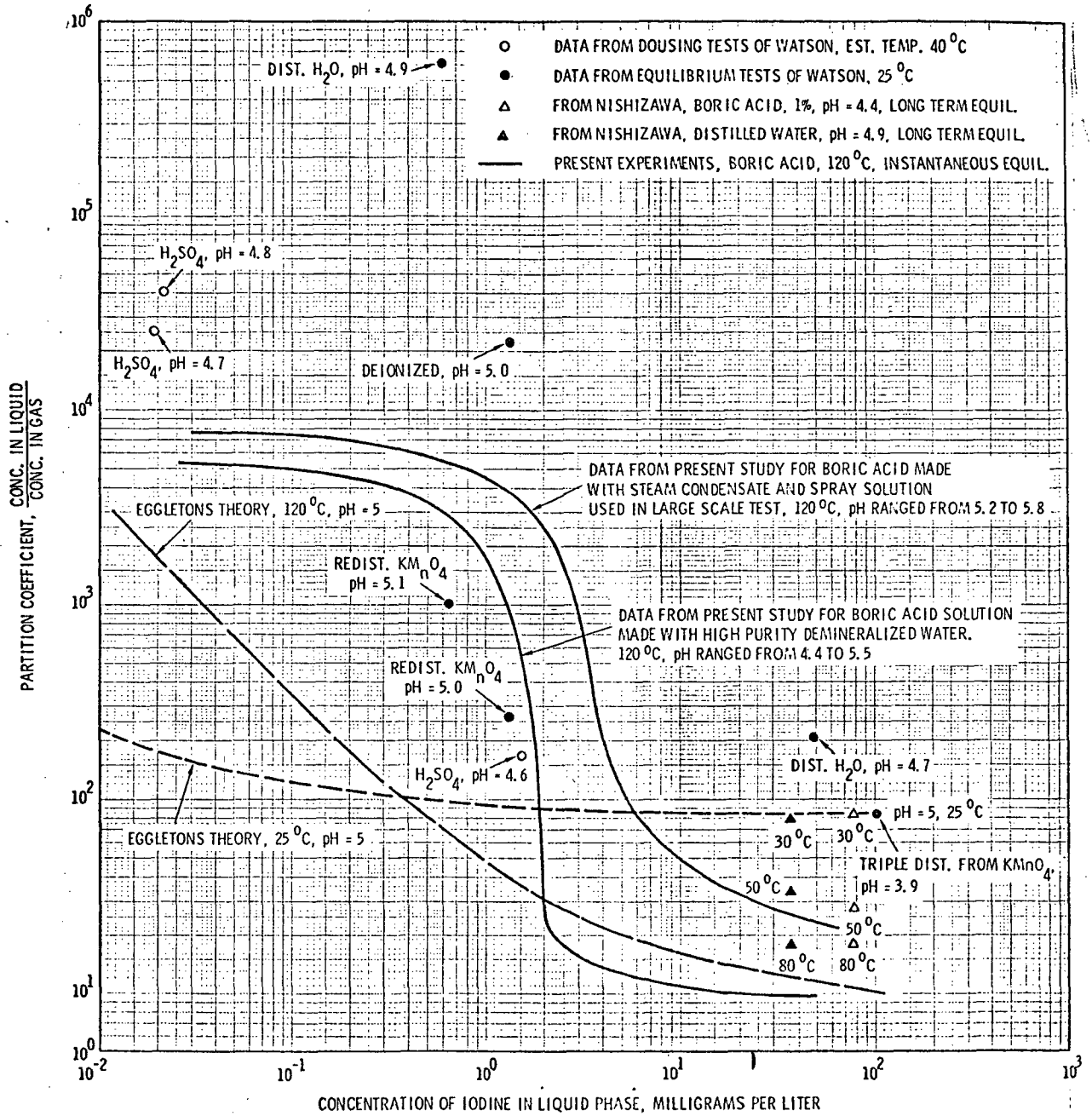


FIGURE 11. PARTITION COEFFICIENTS IN WEAKLY ACID SOLUTIONS

The experiments reported have for the most part been carried out in clean laboratory apparatus, using highly purified water and chemical reagents. Therefore, for the low concentrations range (< 10 mg/l) where impurities are important, one would anticipate that spray solutions used in reactor refueling basins would contain more impurities than the solutions used in the laboratory experiments. It follows that the iodine partition coefficient would be greater for the containment sprays than that of the laboratory experiments.

Eggleton⁽¹³⁾ pointed out the potential role of impurities in determining iodine partition coefficients at low concentrations, and suggested that solutions be characterized in terms of the redox potential. Unfortunately the redox potential was not measured in the partition coefficient experiments reported to date.

F. Conclusions From Partition Coefficient Measurements

Results of the pilot scale equilibrium partition coefficient study support the following conclusions.

1. At high liquid phase iodine concentrations (> 20 mg/l) simple hydrolysis theory predicts a partition coefficient which agrees with the measured value.
2. For iodine concentrations below 20 mg/l, measured partition coefficients are appreciably greater than predicted from simple hydrolysis theory. This enhancement is believed due to reaction of dissolved iodine with trace impurities present.
3. Boric acid concentration has little influence on the iodine partition coefficient for conditions applicable to containment

spray systems. For two test series carried out at 120 °C, changes in the boric acid concentration from 500 to 3000 ppm B caused negligible change in the iodine partition coefficient.

4. The influence of temperature on the partition coefficient depends on the iodine concentration. At high concentrations, the partition coefficient decreases with increasing temperature. At low concentrations, existing data indicate that temperature is not an important variable compared to the character of impurities in a specific solution.
5. The small scale studies indicate that spray washout of iodine in a containment vessel would be rapid for concentrations below 2 milligrams per liter. At higher concentrations, the partition coefficient appears to be too low to give washout rates approaching the perfect sink case.
6. Iodine dissolution occurs by a several step process. The first step is physical dissolution with a very rapid hydrolysis. The second step involves continued chemical reaction, the rate of which depends on impurities and temperature. The second step involves an equilibrium which is attained after tens of minutes. The third step is a slow, irreversible, reaction which progresses over hour periods. Only the first of these steps is effective in causing absorption by spray drops because of the small contact times. The second of these steps would be important during the recirculation time period in a containment spray system. The third step would reduce the airborne iodine concentration in a containment vessel to very low levels after time periods of days.

V. LARGE-SCALE EXPERIMENT OF IODINE REMOVAL BY BORIC ACID SPRAY

A. Purpose of Large-Scale Experiment

The large-scale spray experiment, designated Run C-1, represents a proof test of the ability of boric acid sprays to remove and retain iodine. As such, experimental conditions were chosen to match as closely as practical the conditions expected for postulated accidents in PWR plants. This matching permits extrapolation of results with the smallest possible change in important parameters, hence reduces potential errors in applying the results to larger containment vessels.

Large-scale tests are relatively expensive, hence must be limited in number. Thus they do not permit investigation of ranges of parameters. Other data must be used for this. The purpose of the large-scale spray test was to provide an experimental verification of the rate of removal of iodine by a boric acid spray and to demonstrate the long-term retention of the absorbed iodine by the acidic spray solution. Since extrapolation of results to larger vessels was to be required, it was necessary to perform the experiments in such a way as to provide data required as input to a mathematical model.

B. Experimental Conditions and Procedure

1. Description of Large-Scale Facility

The experimental equipment used for the large-scale demonstration test was essentially the same as had been used in previous Commission-sponsored experiments in the Containment Systems Experiment (CSE) program. The equipment is described in detail by Linderoth⁽¹⁶⁾, Hilliard, et al⁽⁴⁾, Coleman⁽⁹⁾, and McCormack⁽¹⁰⁾. A brief description is included in the present report to provide a basic understanding of the procedure used.

a. Containment Vessel Arrangement

Figure 12 is a schematic drawing of the containment vessel arrangement used in Run C-1. The containment vessel is composed of three interconnected vessels. An outer vessel, called the main containment vessel, 30,680 ft³, an inner vessel, called the drywell, 2286 ft³; and the vessel composing two-thirds of the annular space between the drywell and the main containment vessel, called the wetwell, 4207 ft³. The main containment vessel is 25 ft diameter, 66.7 ft overall height. All interior surfaces are coated with a modified phenolic paint, Phenoline 302.*

The top of the wetwell forms a solid deck which effectively separates the contained gases into what is termed the "main room" above the deck and the lower rooms below the deck. The lid of the drywell was raised so that its volume was common to the main room. The combined volume of this "main room" is 21,005 ft³. One-third of the annular space between the drywell and main containment vessel is a small access area called the "middle room", 2089 ft³ in volume. Below the middle room, drywell, and wetwell is a third space called the "lower room", 3380 ft³ in volume. The wetwell volumes were sealed off and not exposed to steam or fission product simulants in the spray experiment. Two 4 ft diameter holes in the deck connect the main room to the middle room. One 4 ft diameter opening connects the middle room to the lower room.

*Phenoline 302, manufactured by Carboline Corp., St. Louis, Mo.

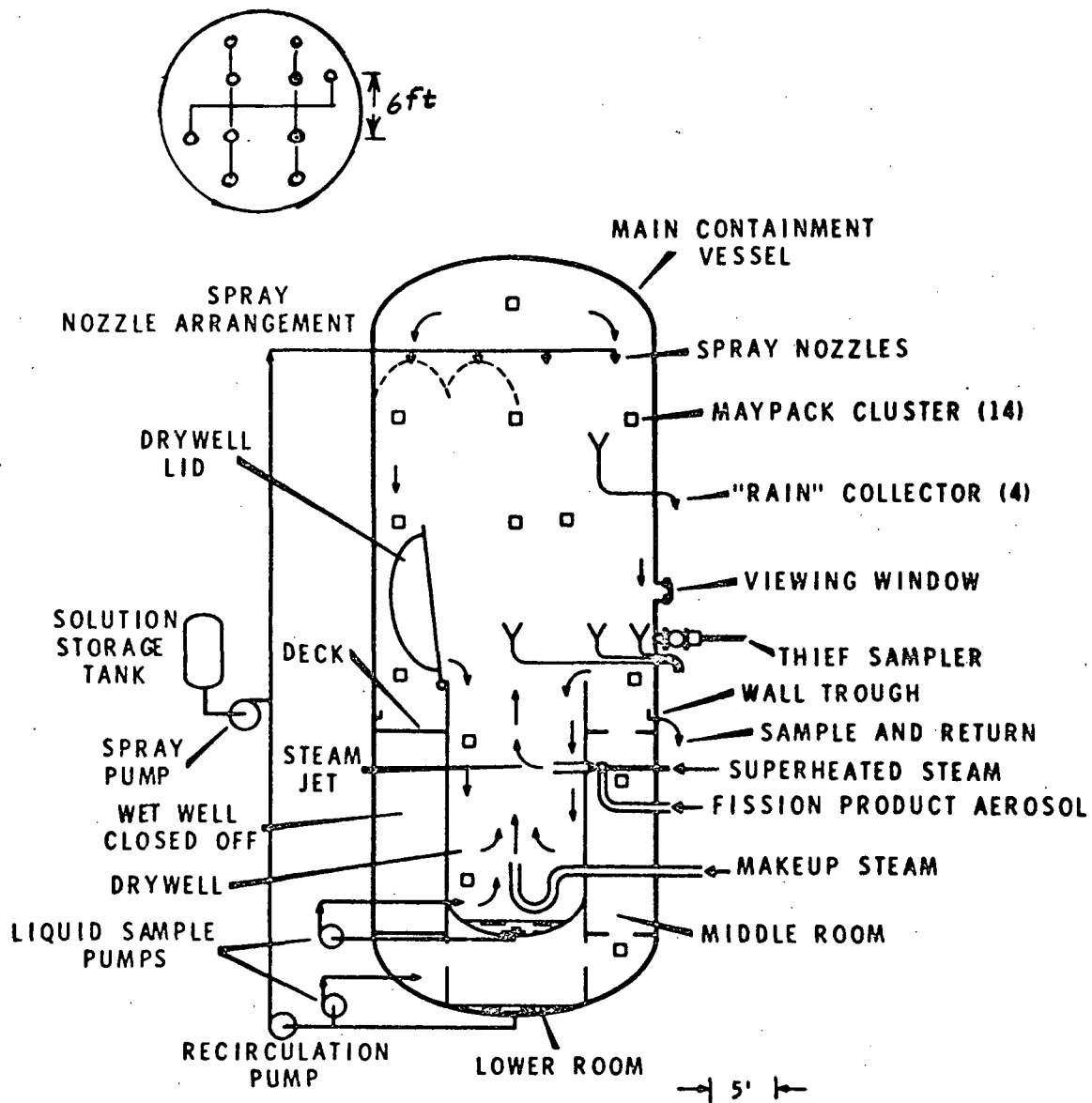


FIGURE 12. SCHEMATIC REPRESENTATION OF CONTAINMENT VESSEL ARRANGEMENT

Steam condensate and spray liquid accumulated in three locations: the drywell pool, the main vessel pool located in the lower room, and on the flat deck of the main room. The first two were stirred, sampled frequently, and the liquid volume monitored. The liquid on the deck was not monitored. It drained into the main pool and together with the main room wall trough was the source of the main vessel pool.

A pipe from the plant steam boiler, terminated near the bottom of the drywell, provided steam input to heat the vessel and its atmosphere. A steam flow meter was provided. Table 4 lists the volumes and surface areas of the various rooms within the containment vessel.

b. Fission Product Simulant Generation

Four materials were released to permit mass transfer measurements: elemental iodine, methyl iodide, cesium, and particles formed by melting unirradiated Zircaloy-clad UO_2 . Coleman⁽⁹⁾ has described the method of generating the fission product simulant in detail, but a brief description follows. About 100 g of stable elemental iodine was equilibrated with about one curie of ^{131}I , which served as a tracer for analytical purposes. When release was desired, the flask was heated electrically and air carried the elemental iodine through the hot zone of the UO_2 melting furnace. Some particulate-associated iodine and organic iodides were produced.

About five grams of iodine in the form of reagent grade methyl iodide was equilibrated with ^{131}I in a stainless steel U-tube. When release was desired, air was passed through the U-tube to sweep the methyl iodide directly into the containment vessel (bypassing the UO_2 furnace).

TABLE 4

TEST CONDITIONS FOR RUN C-1

Solution Composition	3000 ppm B as H ₃ BO ₃
pH	5.0
Nozzle type	Spraco 1713
Spraying pressure, psid	40 ± 2
Drop mass median diam., microns	1100
Drop geometric std. dev.	1.5
Number of nozzles	10
Total spray flow rate, gpm	160 ± 5
Wall flow rate, gpm	2.1
Duration of fresh spray period, min	16.3
Total fresh spray addition, gal	2610 ± 30
Initial vapor temperature, °F	249
Initial pressure, psia	47.0
Vapor temp. at end of fresh spray, °F	192
Pressure at end of fresh spray, psia	31.1
Volume of main room, ft ³	21,005
Surface area of main room, ft ²	6,140
Volume of middle room, ft ³	2,089
Surface area of middle room, ft ²	1,363
Volume of bottom room, ft ³	3,384
Surface area of bottom room, ft ²	2,057
Total volume, ft ³	26,477
Total surface area, ft ²	9,560
Iodine and cesium release duration, min	6
Mass of elemental iodine released, g	95.5
Mass of methyl iodide released, g	5
Mass of cesium released, g	3.2
Mass of uranium released, g	~ 2

About 12 g of stable cesium as cesium oxalate was equilibrated with about one curie of ^{137}Cs in a nickel boat and calcined to oxide at $< 400^\circ\text{C}$. When release was desired, the nickel boat was heated inductively to $\sim 1200^\circ\text{C}$ and an air stream carried the volatilized cesium and cesium oxides through the UO_2 furnace into the containment vessel.

The unirradiated Zircaloy-clad UO_2 was melted 10 minutes before the start of iodine and cesium release and cooled rapidly at the time that iodine and cesium release was finished. A steam jet at the drywell acted as a compressor for injecting the volatilized simulants into the pressurized vessel.

Table 5 gives the overall material balance for iodine and cesium. The top half of the table relates to generation and release to containment, based on the known mass of starting material. The lower half of Table 5 is based on the mass calculated to have been delivered to the containment vessel. Values listed in the table are believed to be accurate to $\pm 10\%$.

The suitability of the fission product simulant generated by these methods as tracers to represent actual fission products in containment atmospheres was demonstrated by small-scale tests in the Aerosol Development Facility (ADF)⁽¹⁷⁾ and at Oak Ridge National Laboratory.⁽¹⁸⁾

c. Sampling Procedures

The main gas sampling system consisted of 14 Maypack clusters located throughout the vapor space. This remotely operated system is described by McCormack.⁽¹⁰⁾ Supplementary gas samples, known as "thief" Maypack samples, were taken at three locations near the outer vessel walls by manually inserting Maypacks through airlocks into the

TABLE 5

OVERALL MATERIAL BALANCES FOR RUN C-1

<u>Location</u>	<u>Iodine</u>		<u>Cesium</u>	
	<u>Grams</u>	<u>%^(a)</u>	<u>Grams</u>	<u>%^(a)</u>
<u>Aerosol Generation</u>				
Starting Material	104.85	100.00	11.16	100.00
Generation Apparatus	3.98	3.79	7.26	65.08
Injection Line	0.48	0.46	0.66	5.92
Accounted For	4.46	4.25	7.92	71.00
Delivered to Containment (By Difference)	100.39	95.75	3.24	29.00
<u>Containment</u>	<u>Grams</u>	<u>%^(b)</u>	<u>Grams</u>	<u>%^(b)</u>
Delivered to CV	100.39	100.00	3.24	100.00
In Liquid Pools at t = 146 hr ^(c)	31.55	31.43	2.08	64.42
Samples	0.30	0.29	0.007	0.21
Purge to Stack	0.00004	~ 0	nil	nil
Decontamination	4.77	4.75	0.13	3.96
Accounted For	36.62	36.47	2.22	68.52
On Surfaces (By Difference)	63.78	63.53	1.02	31.48

(a) Percent of starting mass.

(b) Percent of delivered mass.

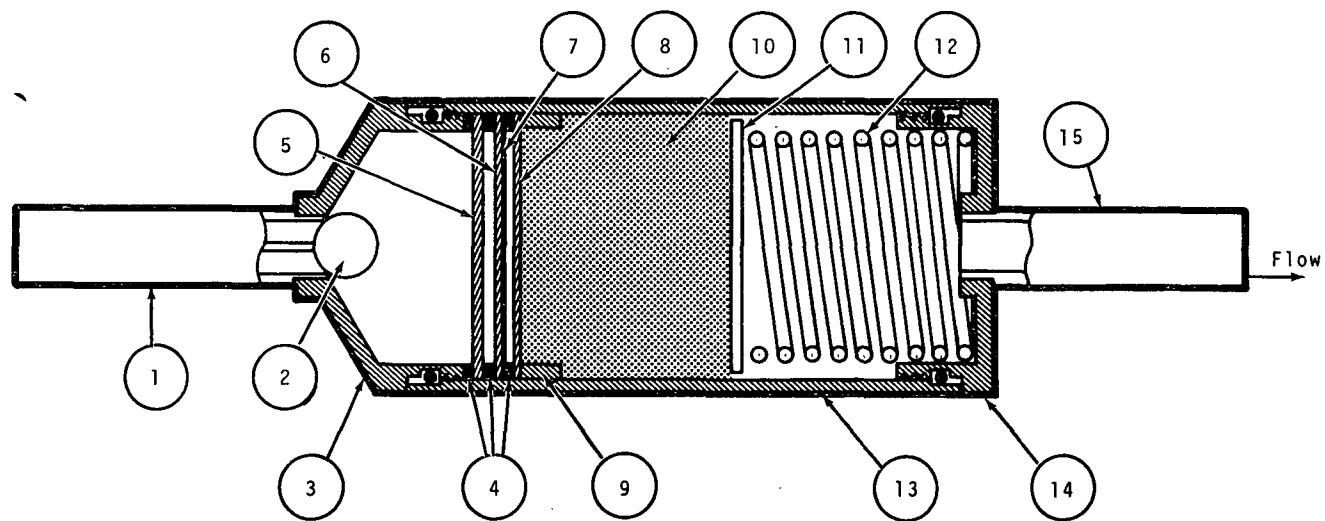
(c) Includes spray solution and steam condensate.

containment atmosphere and immediately withdrawing them for analysis. Flow through all Maypacks was controlled at $0.5 \text{ ft}^3/\text{min}$ (STP) dry air for 3 min duration. Sampling error was determined to be $\leq 10\%$ at the 68% confidence level.

Figure 13 shows a sectional view of the Maypack used in the Maypack clusters. Twelve Maypacks were hung in a vertical orientation in each cluster, permitting a maximum of twelve different sampling times. In Run C-1 the 12th Maypack was not operated and served as a blank for background information. Each Maypack had its own solenoid valve at the outlet nipple for on-off flow control. Five samples were obtained from each Maypack:

- Inlet decontamination
- Filters (2 Gelman Type A)
- Silver surfaces (6 screens + one membrane, 5μ pore size)
- Charcoal filter paper (Gelman Type AC)
- Charcoal granules (2 in. activated coconut, 8-14 mesh)

The Maypack is not a perfect discriminator of iodine forms, but extensive calibration has shown that reliable classification of the elemental and methyl iodide forms were obtained.⁽¹⁰⁾ Iodine associated with particles and other inorganic and organic forms are less reliably identified. An example of the manner in which the several forms of iodine deposited in the Maypack is shown in Figure 14. The data shown in Figure 14 were obtained in Run C-1. Methyl iodide was released one hour before the elemental iodine was released. More than 95% of the methyl iodide was found on the charcoal bed at times previous to release of elemental iodine, with only 0.1% being found on the silver components. Immediately after 100 grams of



- | | | |
|------------------------|-----------------------------|------------|
| 1 Inlet | 6 Six Silver Plated Screens | 11 Screen |
| 2 Teflon Ball | 7 Silver Membrane Filter | 12 Spring |
| 3 Nose Cone | 8 Charcoal Loaded Filter | 13 Body |
| 4 Teflon Gasket | 9 Stop Ring | 14 End Cap |
| 5 Two Particle Filters | 10 Charcoal Bed | 15 Outlet |

FIGURE 13. SCHEMATIC DIAGRAM OF A CSE MAYPACK

RESPONSE OF MAYPACK SAMPLER TO SEQUENTIAL RELEASE OF METHYL IODIDE AND ELEMENTAL IODINE

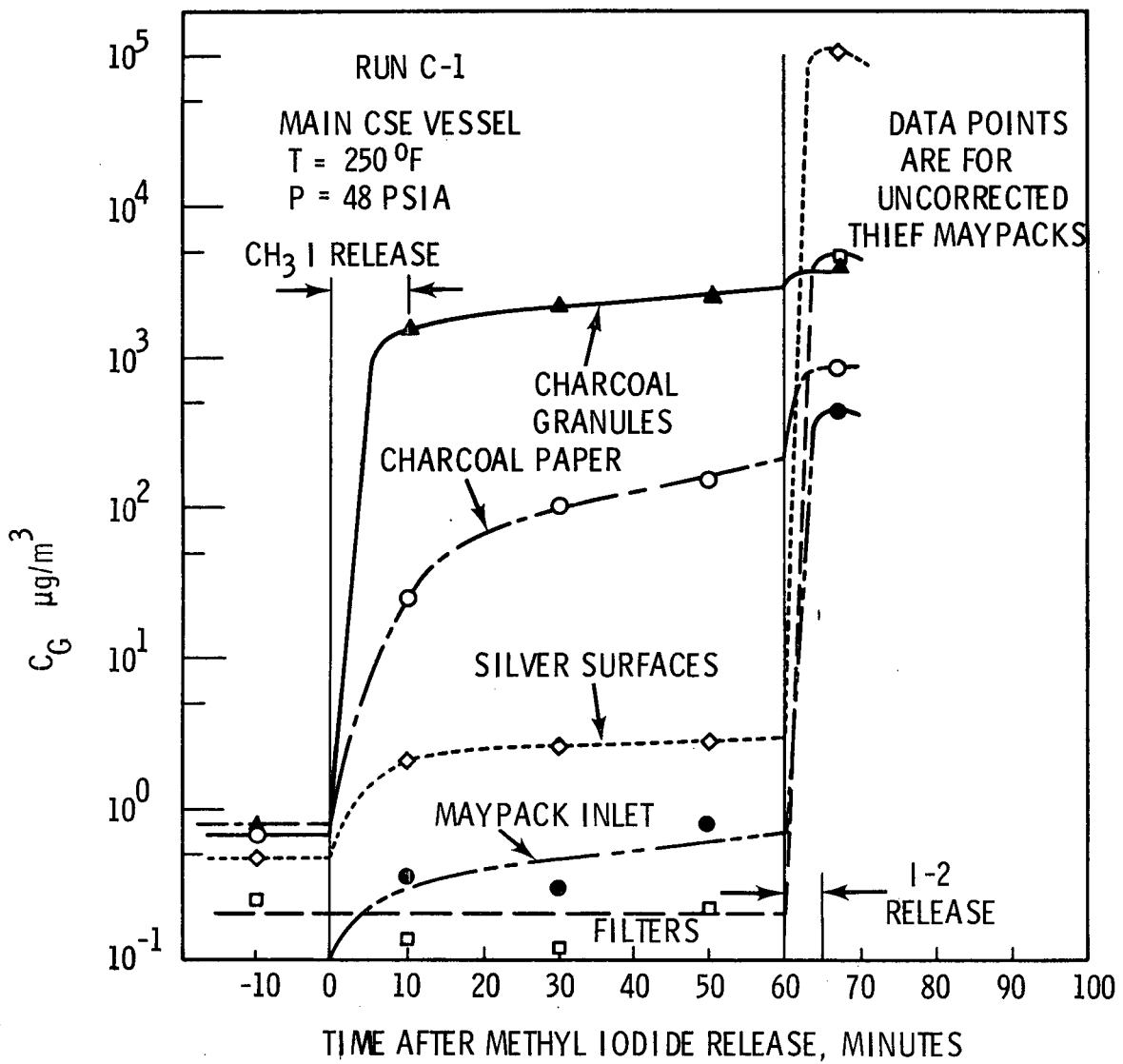


FIGURE 14. RESPONSE OF MAYPACK SAMPLER TO SEQUENTIAL RELEASE OF METHYL IODIDE AND ELEMENTAL IODINE

elemental iodine was released, 92% of the total gasborne iodine was found on the silver surfaces, while the charcoal granules showed only a slight increase. The iodine on the thin charcoal paper may be a mixture of HOI, I₂, and CH₃I.

Liquid samples were taken from four locations: The main vessel sump, the drywell sump, the 360° wall trough, and drop collector funnels. In addition, special "thief" drop samples were taken by manually inserting collectors through airlocks at two elevations.

d. Spray System

The spray system flow sheet is shown in Figure 15. Demineralized water was charged to a 3000-gal SS-304L solution makeup and storage tank. Boric acid was added directly to the tank on a weight basis, and the solution was mixed by recirculation in an all-stainless steel system for four days. The fresh solution pump did not have sufficient capacity for this high flow rate experiment, so immediately prior to the fresh spray period, the boric acid solution was pumped to an empty wetwell. A 50-gallon sample was taken from the wetwell for an iodine gas-liquid equilibrium test in the small-scale experiments (Run CRJ), and then the solution was pumped to the spray manifold and nozzles inside the containment vessel, using the large spray recirculation pump.

The spraying rate was controlled by maintaining a pressure differential of 40 ± 2 psi across the spray nozzles. 2610 gallons were sprayed during the fresh spray period which lasted 16.3 minutes, for an average flow rate of 160 gal/min. The temperature of the fresh spray entering the vessel varied from 92 °F at the start to 103 °F at the end.

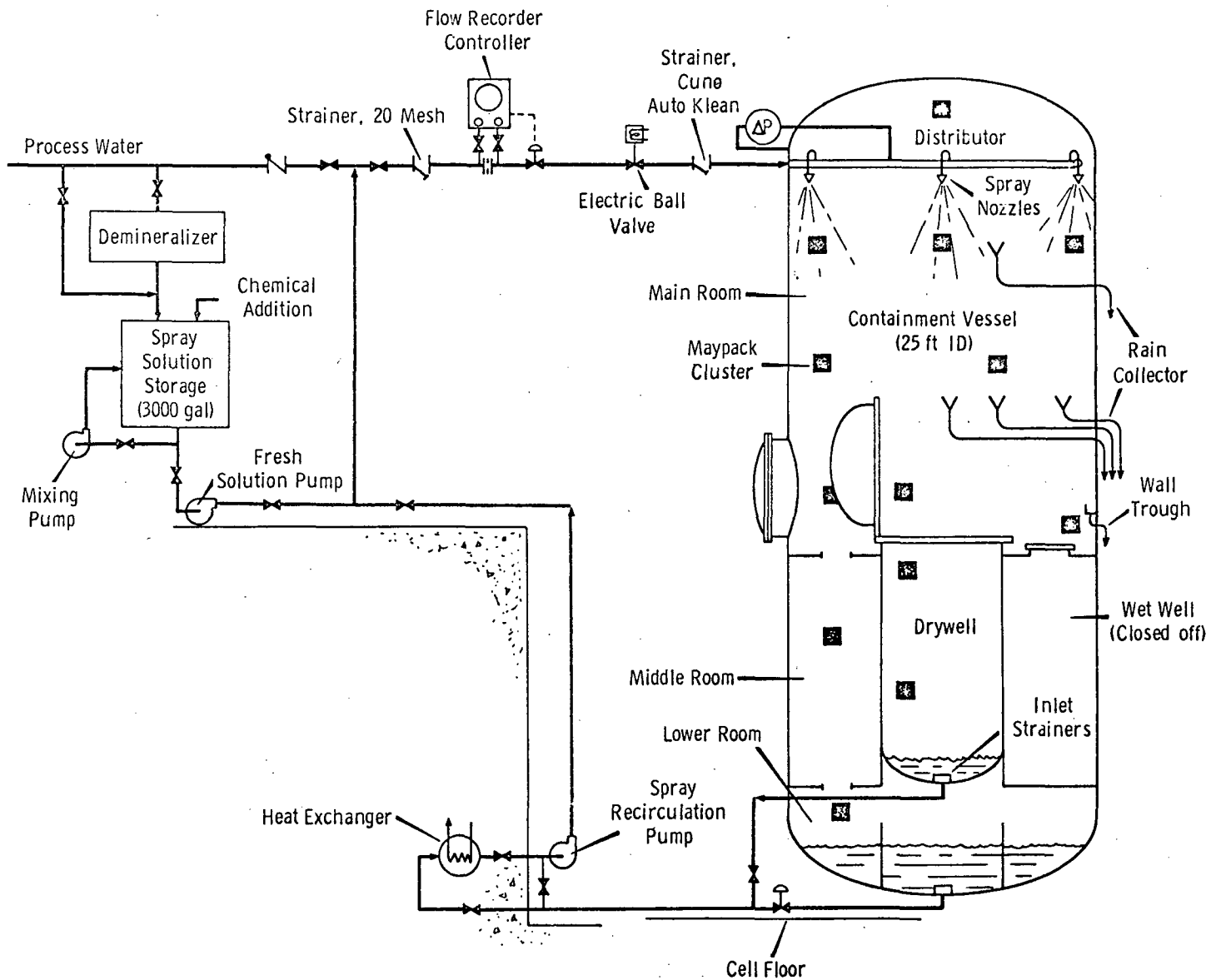


FIGURE 15. FLOWSHEET OF CSE SPRAY SYSTEM FOR RUN C-1

About 100 ft of the piping was carbon steel, with about 200 ft being SS-304. The storage tank, wetwell, and all pumps and lines and nozzles had been thoroughly flushed with several thousand gallons of demineralized water during shakedown tests. Just prior to injection of the fission product simulant the spray header was primed with solution in order to provide a prompt start time for the fresh spray.

The nozzles were Spray Engineering Co. Type 1713, constructed of stainless steel. The nozzles were obtained on loan from Bechtel Corp., San Francisco, California. Ten nozzles were used at a 6-ft rectangular spacing, as shown by the inset in Figure 12.

2. Spray Solution Makeup and Analysis

The boric acid was "Special Quality Grade" granular material, obtained from the U. S. Borax and Chemical Company, Los Angeles, California. Table 6 is a copy of the analysis provided by U. S. Borax Co.

After thoroughly flushing the makeup tank and all lines with demineralized water, the 3000 ppm B spray solution was prepared by dissolving 435 lbs of granular H_3BO_3 in 24,900 lbs of demineralized water. The resistivity of the demineralized water was > 0.15 megohm-cm, and its pH was about 6.5.

Samples of the boric acid solution from the makeup tank were analyzed and showed 2950 ppm boron and a pH of 5.0. A spectrochemical analysis showed traces ($< 0.01\%$) of Cr, Cu, Mg, Mn, Ni, and Si. Iron was present in trace-to-moderate amounts (0.01 to 0.1%). No other cations were detected.

3. Spray Flow Parameters

a. Spray Distribution

Two shakedown tests were performed with the spray system, using demineralized water and with the containment vessel pressurized to 35 psig

TABLE 6

ANALYSIS OF GRANULAR BORIC ACID



**TYPICAL ANALYSIS OF
SPECIAL QUALITY GRADE**



CHEMICAL

Boric Oxide (B ₂ O ₃)	56.4%
Water (H ₂ O)	43.6
Boric Acid (H ₃ BO ₃)	100.1

Impurities	Maximum	Typical
Sodium (Na)	0.001%	0.000%
Chloride (Cl)	0.00004	0.00002
Sulfate (SO ₄)	0.00016	0.00009
Phosphate (PO ₄)	0.001	0.000
Iron (Fe)	0.0002	0.00008
Heavy metals (as Pb)	0.0002	0.00010
Calcium (Ca)	0.005	0.000
Water-insoluble	0.005	0.000

SCREEN

U.S. Standard Sieve No.	Percent Cumulative	
	Granular	Powdered
8		
12	0.1	
16	5	
20	17	
30	33	
40	51	
50	66	
70	80	
100	90	
140	96	
200	98	1
270		2

BULK DENSITY

	Pounds per cubic foot	
	Loose Pack	Tight Pack
Granular	64	67
Powdered	30	38

CONTAINERS

Fiber drums with polyethylene or kraft liners. Granular, 325 lbs. net; Powder, 210 lbs. net.

INDUSTRIAL USES

For various purposes where the highest purity of BORIC ACID is essential; Special Quality grade is superior to either the U.S.P. grade or the so-called C.P. grade of BORIC ACID. It finds application in the manufacture of electrolytic condensers and as a reagent grade chemical, in which latter respect it exceeds standard specifications of purity.

with air. In these shakedown tests the fraction of the total spray collected in three locations was measured, as shown in Table 7. The portion collected by the 360° wall trough located near the main deck represented the drops which impinged on the vertical walls plus drops collected by the horizontal projection of the trough exposed to falling drops. The horizontal projected area of the wall trough was 2.0% of the entire vessel horizontal cross section. The wall film flow was calculated by subtracting from the total trough flow, the flow rate of drops expected for a uniform drop flux. This calculation provides a lower limit to the wall film flow rate.

By visual inspection, wall impingement occurred very close to the spray nozzles. This portion of the total spray can be assumed to have existed as drops for a negligible period of time for iodine absorption purposes, but should be effective for pressure suppression purposes.

TABLE 7
SPRAY DISTRIBUTION IN CONTAINMENT VESSEL

	Collection ^(a) Rate <u>gal/min</u>	Percent of Total	Adjusted ^(b) Percent
Wall Trough	5.0 ^(c)	3.2	1.4
Main Sump	113	70.5	71.9
Drywell Sump	<u>42</u>	<u>26.3</u>	<u>26.7</u>
Total	160	100.0	100.0

(a) Volume collected divided by spraying time.

(b) Corrected for horizontal projection of wall trough.

(c) 2.9 gpm calculated collected as drops, 2.1 gpm by wall film.

b. Drop Fall Distance

The main room in the containment vessel had an irregular floor section due to the open drywell (see Figure 12). Table 8 gives the volumetric spray rate to the main deck and to the bottom of the drywell and the associated drop fall distances. The volumetric average fall distance was 38.1 ft.

TABLE 8
EFFECTIVE DROP FLOW RATE AND FALL DISTANCE

	<u>Spray Drop Flow Rate</u>		<u>Drop Fall</u>
	<u>gal/min</u>	<u>Percent</u>	<u>Distance</u>
			<u>ft</u>
To Main Deck	115.9	73.4	33.8
To Drywell Pool	<u>42.0</u>	<u>26.6</u>	<u>50.0</u>
Total	157.9	100.0	38.1
			(Volumetric avg.)

c. Drop Size Distribution

The spray drop size distribution was not measured. Spraco 1713 nozzles were used, with 40 ± 2 psi differential pressure maintained across the nozzles. Information provided by W. D. Fletcher, Westinghouse Electric Corporation states that at 40 psid, the mass median diameter (MMD) is 1100μ and the geometric standard deviation is 1.5.

4. Sequence of Events for Run C-1

A detailed "Run Plan" was written for guidance to the Operations staff in preparing for and conducting the experiment. As in previous CSE experiments, responsible engineers participated in all phases of the experimental work. The chronological sequence of important events was as follows:

1. The equipment was prepared, calibrated, cleaned, and shakedown tests performed with the spray system. Spray solution was prepared.

2. The vessel was sealed and plant boiler steam was fed until the temperature and pressure reached 250 °F, 48 psia. The steam feed was reduced to the rate required to maintain thermal equilibrium (~ 300 lb/hr).
3. One hour before time zero, methyl iodide was released over a 10-min period. Gas samples were taken to show Maypack performance.
4. At 10 minutes before time zero, the Zircaloy-clad UO₂ was melted.
5. At time zero, t₀, elemental iodine and cesium oxide release started.
6. At t = 6 min, iodine, cesium and uranium release was terminated.
7. At t = 10 min, the fresh spray was started.
8. At t = 26.3 min, the fresh spray was stopped.
9. At t = 35 min, liquid from the main sump was started recirculating to the spray header. The heat exchanger was by-passed.
10. Gas and liquid samples were taken as per Run Plan before, during and after the fresh spray period.
11. Recirculation from the sump continued until t = 72 hours.
12. The steam feed was 300 lb/hr until the end of the fresh spray period, then it was increased to 2050 lb/hr for 2 hr, then back to ~ 300 lb/hr until t = 24 hr, then the steam feed was stopped.
13. The vessel was allowed to cool to 100 °F.

14. At $t = 8587$ min, purging started by exhausting the containment atmosphere through the stack at 2000 CFM, replacing with clean air.
15. At $t = 8647$ min, purging was stopped.
16. Sampling continued until $t = 8768$ min.
17. After the last samples were taken, the liquid in the sumps was pumped to waste.
18. The vessel was opened and the Maypack clusters were retrieved.
19. The vessel was resealed and decontaminated by alternate steaming and spraying with water for 3 days. Decontamination streams were measured and analyzed.
20. The samples were analyzed.

5. Characterization of the Atmosphere in the Containment Vessel

a. Visual Observations

Immediately prior to release of iodine and cesium the atmosphere in the vessel was clear. A fog developed as soon as iodine and cesium release commenced, with visibility estimated at 20 ft by the end of the release. A definite violet color was evident. The spray started about 5 seconds after the start signal was given. The violet color disappeared within about 1 minute. The spray drops appeared to cover the space uniformly. Considerable swirling of drops was noted. Visibility remained poor during the fresh spray period. The spray stopped abruptly at the stop signal. Small drops or mist could be seen for about 30 seconds, after which the atmosphere was very clear. The recirculation spray started promptly on signal.

b. Temperature and Pressure History

The temperature was nominally isothermal for 24 hours after release of iodine. A slow temperature decay over a several day period to ambient conditions followed termination of steam addition. Introduction of the cold fresh spray liquid caused a rapid decrease in temperature and pressure causing a transient during the nominally constant temperature period. At the beginning of the fresh spray, the atmosphere in the main gas space was 249 ± 2 °F and the pressure was 47.0 ± 0.2 psia. At the end of the 16 min fresh spray the temperature averaged 191 °F and the pressure 31.0 psia.

The steam feed was maintained at 300 lb/hr during the spray, then was increased to 2050 lb/hr immediately after the spray stopped and kept at the higher rate for 2 hr. Then it was reduced to about 300 lb/hr to maintain thermal equilibrium at 250 °F.

Figure 16 is a plot of the temperature and pressure during the first hour, which includes the fresh spray period. The temperature of the spray solution entering the vessel increased from 92 °F at the start to 103 °F at the end of the fresh spray period. The temperature in the main room was the arithmetic average of 5 shielded Chromel-Alumel thermocouple readings. Individual thermocouples differed by < 5 °F at any time. In Figure 17 the temperature and pressure are shown for the entire 145 hour test duration.

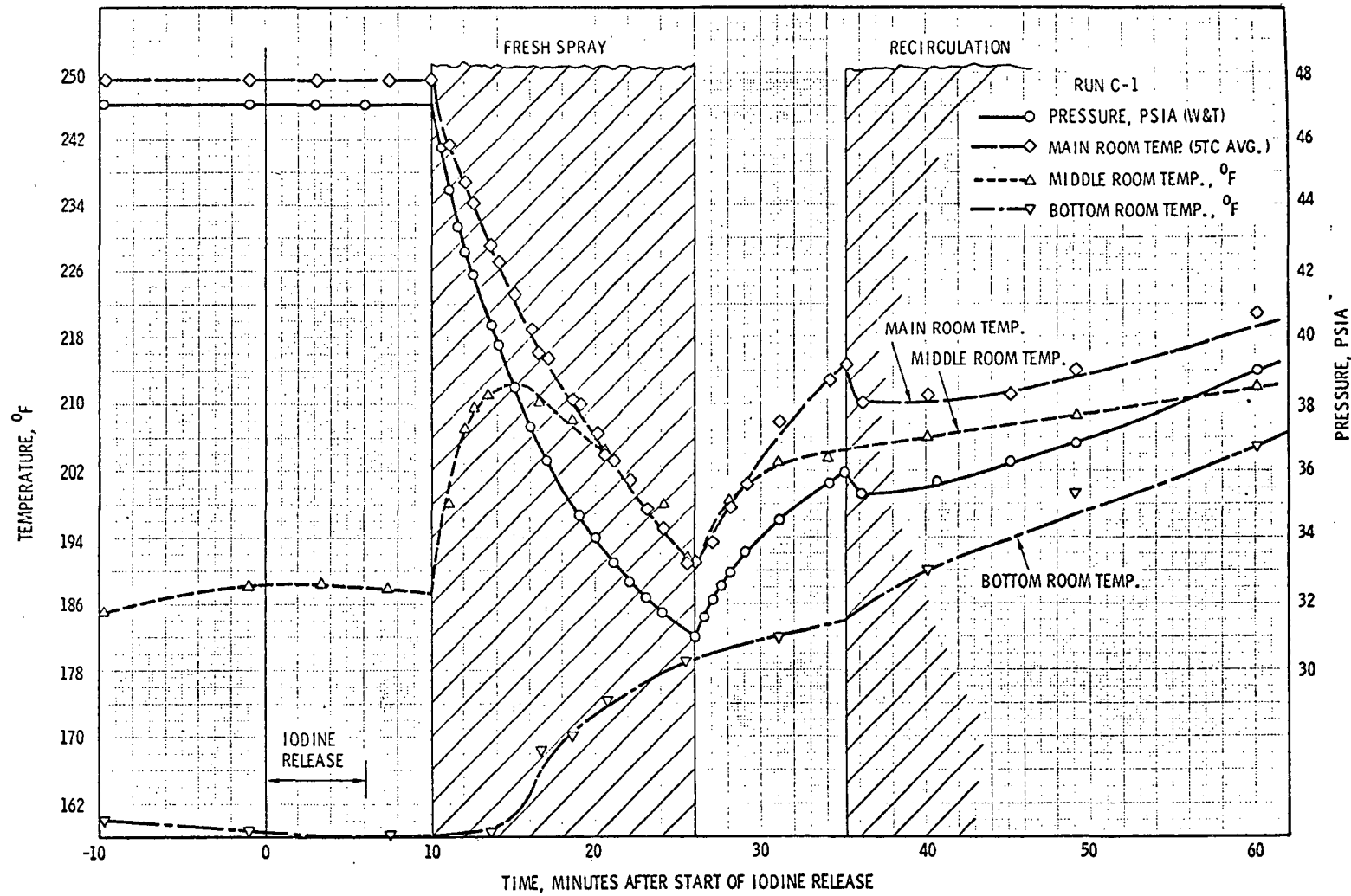


FIGURE 16. TEMPERATURE AND PRESSURE FOR THE FIRST HOUR IN RUN C-1

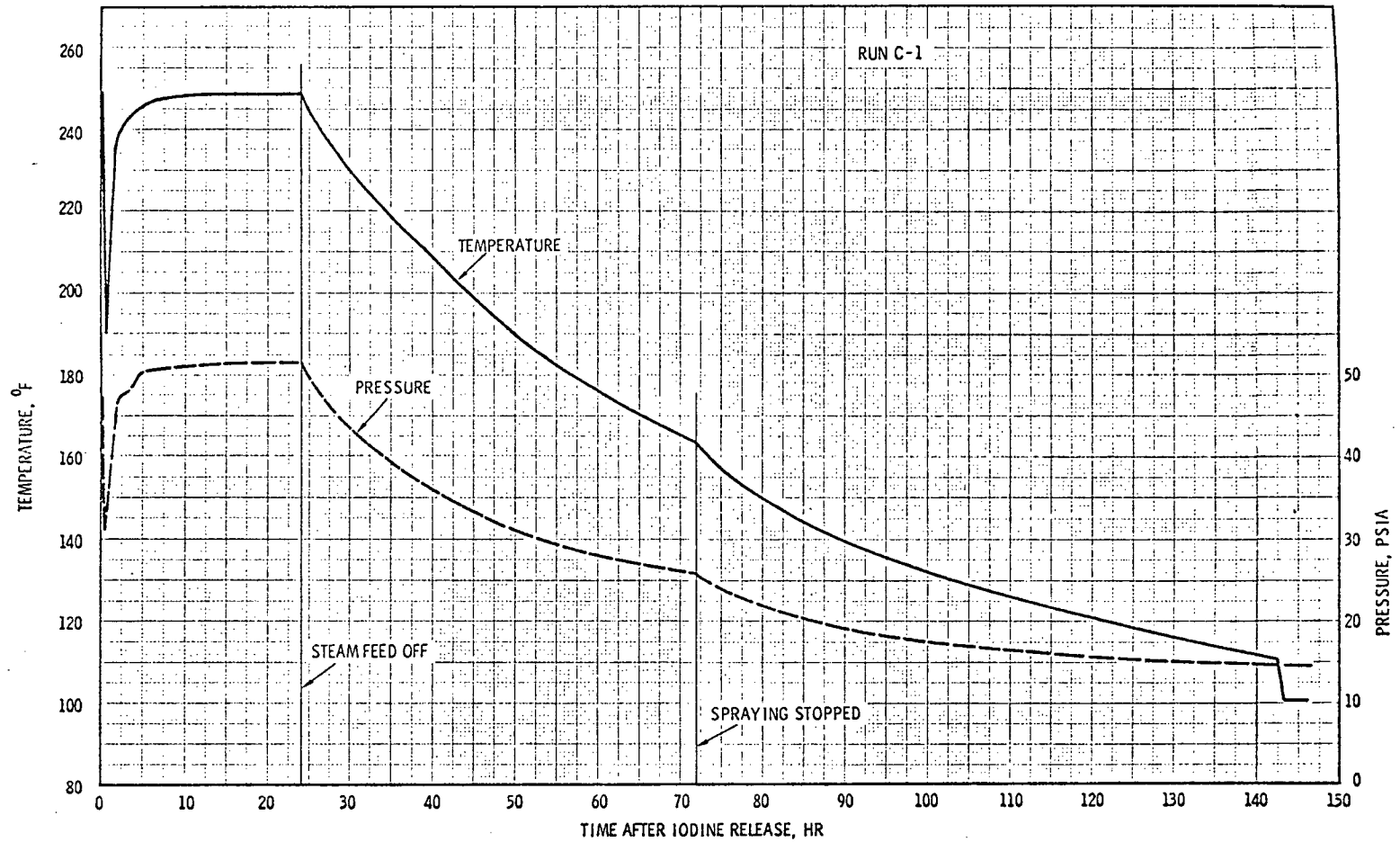


FIGURE 17. TEMPERATURE-PRESSURE HISTORY FOR RUN C-1

C. Results of Large-Scale Spray Experiment

1. Iodine Removal From Gas Phase

a. Concentration of Iodine in the Gas Phase

The airborne concentration of iodine was measured over a 6-day period following release into the containment vessel. The concentrations of airborne iodine, cesium and uranium as measured at each sampling time are tabulated in Appendix B. For clarity of presentation the time period has been divided into two intervals. The first covers the washout by fresh spray, and early during recirculation when the concentration is falling rapidly. The second time period covers the entire time span of 8500 minutes. The airborne concentrations of iodine forms during the early part of the experiment are shown in Figure 18. The iodine concentration decreases during the fresh spray with a half-life of 3.3 minutes. Additional washout occurs during recirculation before equilibrium is attained. The airborne concentration of all forms decreases slowly after 50 minutes of spraying including 35 minutes of recirculation. The inorganic iodine concentration decreased to 1% of its maximum concentration in this 50 min time period. Methyl iodide was not removed significantly by the fresh spray.

Long term behavior of iodine is shown in Figure 19. The airborne concentration continued to decrease over the remainder of the run. Methyl iodide was the dominant airborne specie for times greater than 40 minutes. It is important to note that the airborne concentration continued to decrease with continued recirculation at all temperatures.

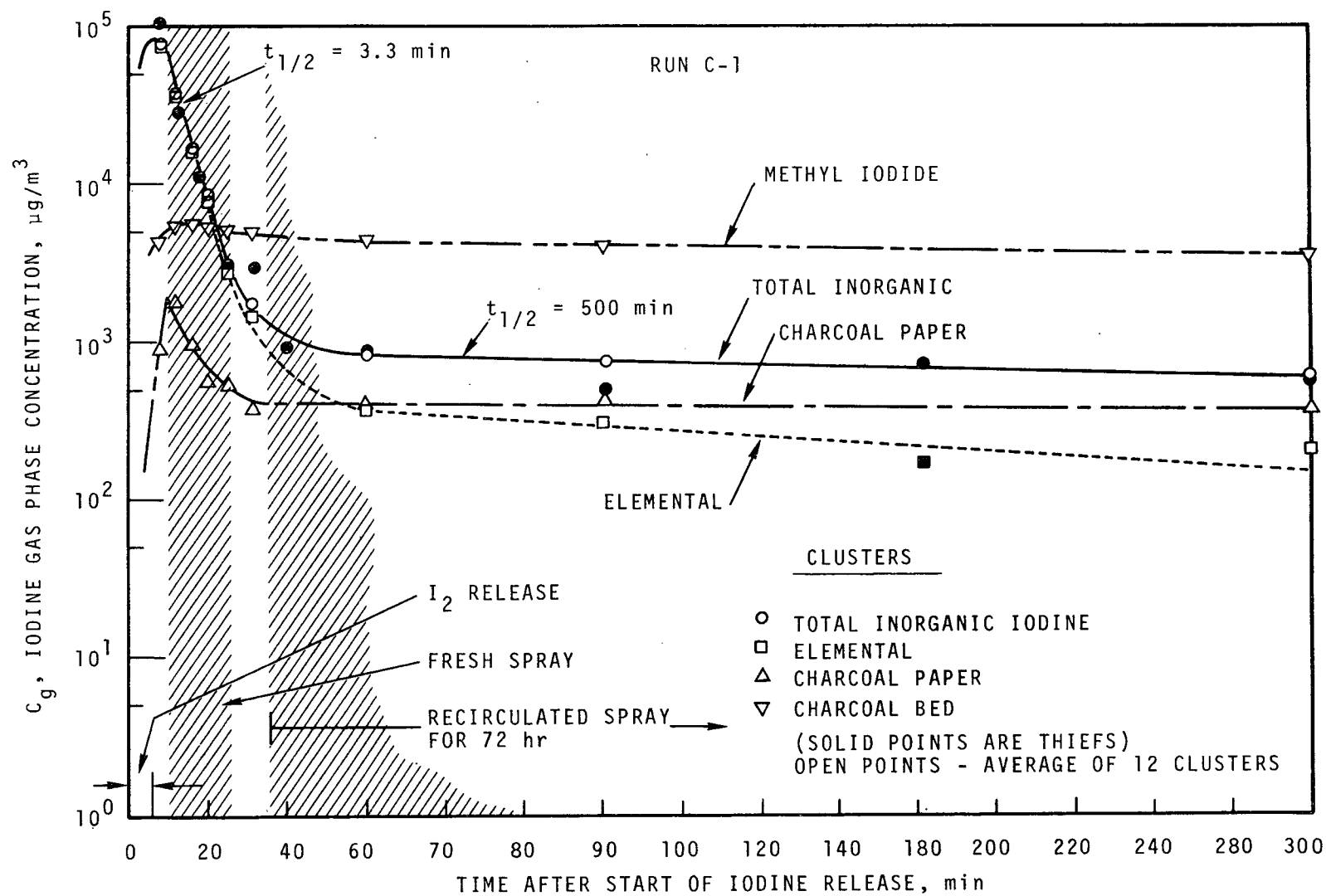


FIGURE 18. AIRBORNE IODINE EARLY IN RUN C-1

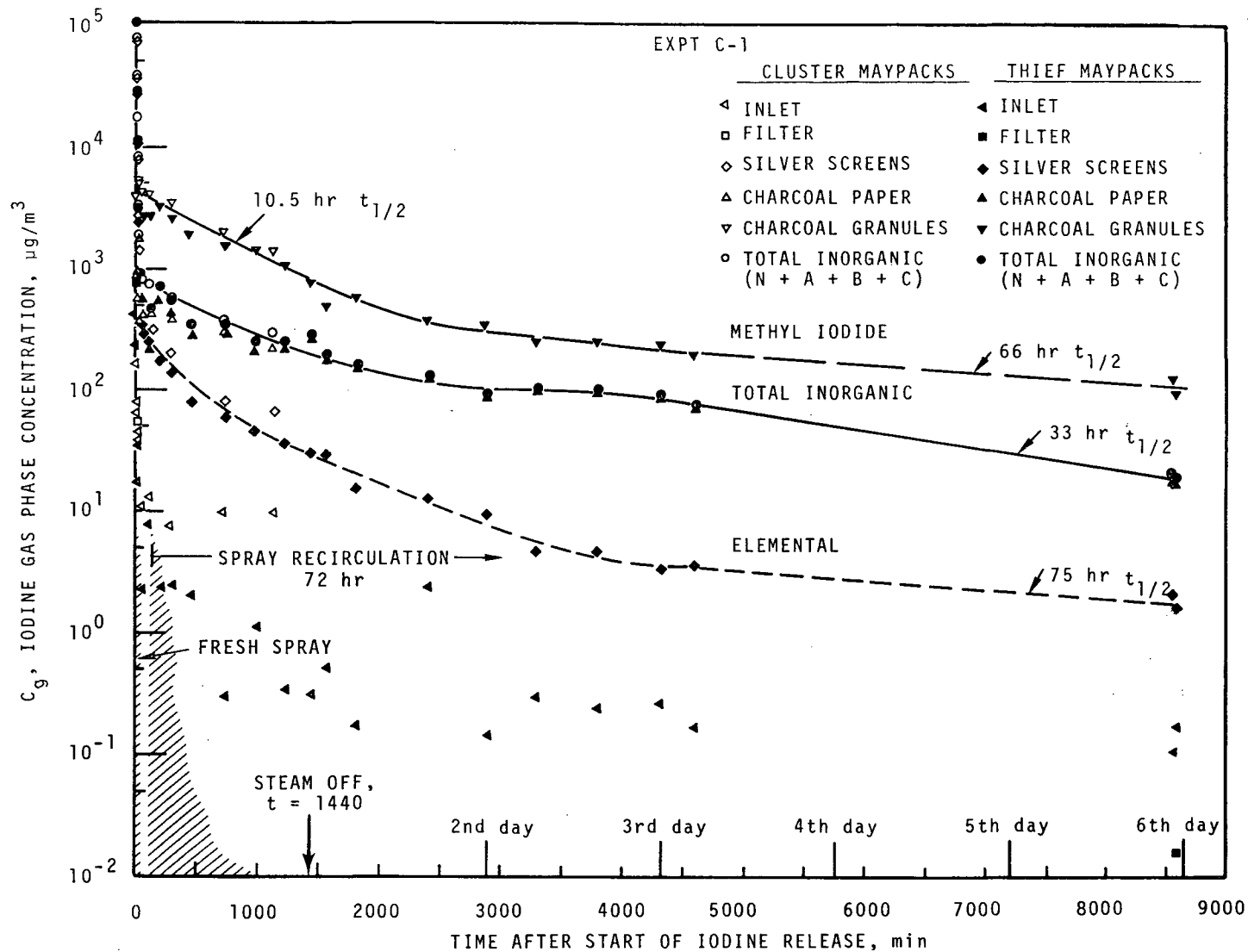


FIGURE 19. AIRBORNE IODINE DURING CONTINUED SPRAY OPERATION IN RUN C-1

b. Concentration of Iodine in Collected Drops

As noted earlier, spray drops were removed from the vessel and their fission product concentrations measured. Results of these measurements are shown in Figure 20. Measurements made by thief samplers and those made with funnel collectors are in good agreement. The liquid concentration decreased with approximately the same half-time as the gas phase. This shows that the relative effectiveness of the spray remained constant during the fresh spray period. Shortly after recirculation had begun, the liquid concentration became constant. This shows that the sumps are well mixed and that most of the easily absorbed iodine had already been removed by the spray.

c. Iodine Concentration in Vessel Sumps

The concentration of iodine in the spray liquid collected in the drywell sump and main vessel sump is shown in Figure 21. The drops falling into the drywell fell a greater distance than those falling into the main vessel sump, hence would tend to absorb more iodine than those falling onto the floor of the main room. Also, the iodine entered the containment vessel within the drywell, and experience has shown that an appreciable part of the injected iodine deposits within the drywell. The drywell iodine concentration increased faster, and reached a higher level than that of the main sump. This behavior is in agreement with expectations based on the previously noted factors. After 80 minutes, both sumps were intermixed, and the concentration was the same as measured in collected spray, as expected.

The volume of liquid spray solution increased slowly with time due to condensation of steam. The volumes of water within the drywell sump, main vessel sump, and the total liquid in the containment vessel are shown in Figure 22.

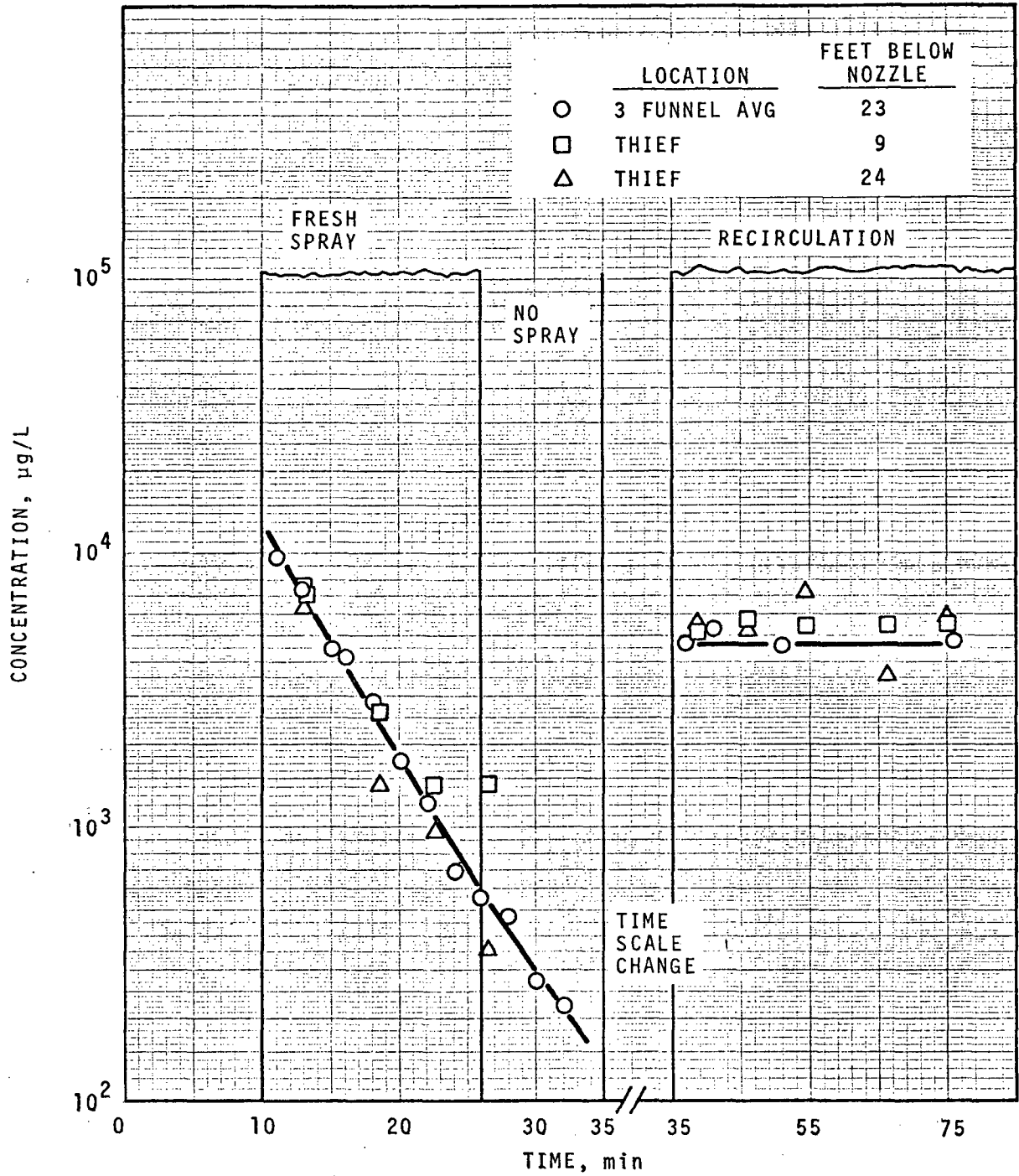


FIGURE 20. IODINE CONCENTRATION IN SPRAY DROPS IN RUN C-1

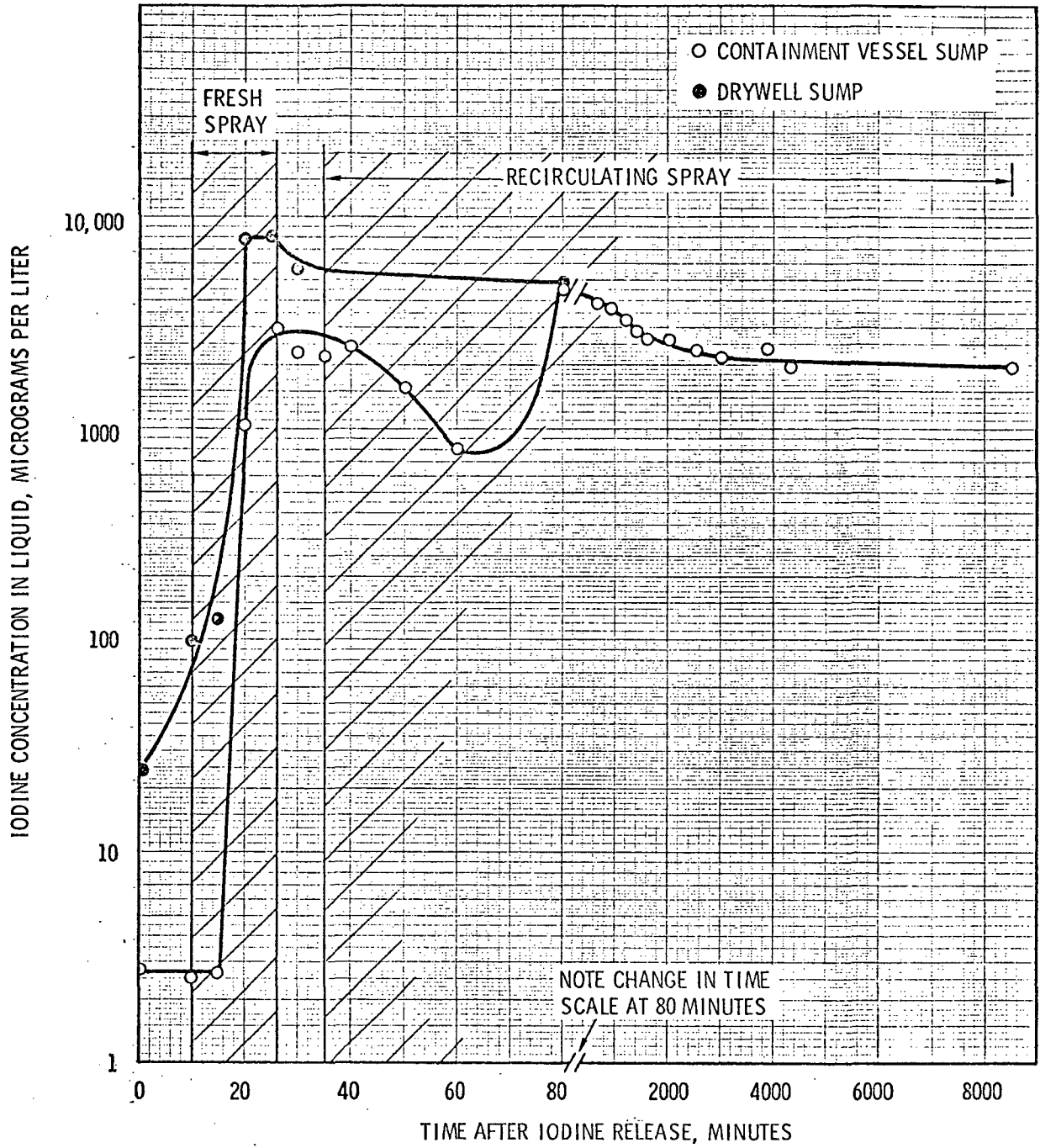


FIGURE 21. IODINE CONCENTRATION IN LIQUID POOLS IN RUN C-1

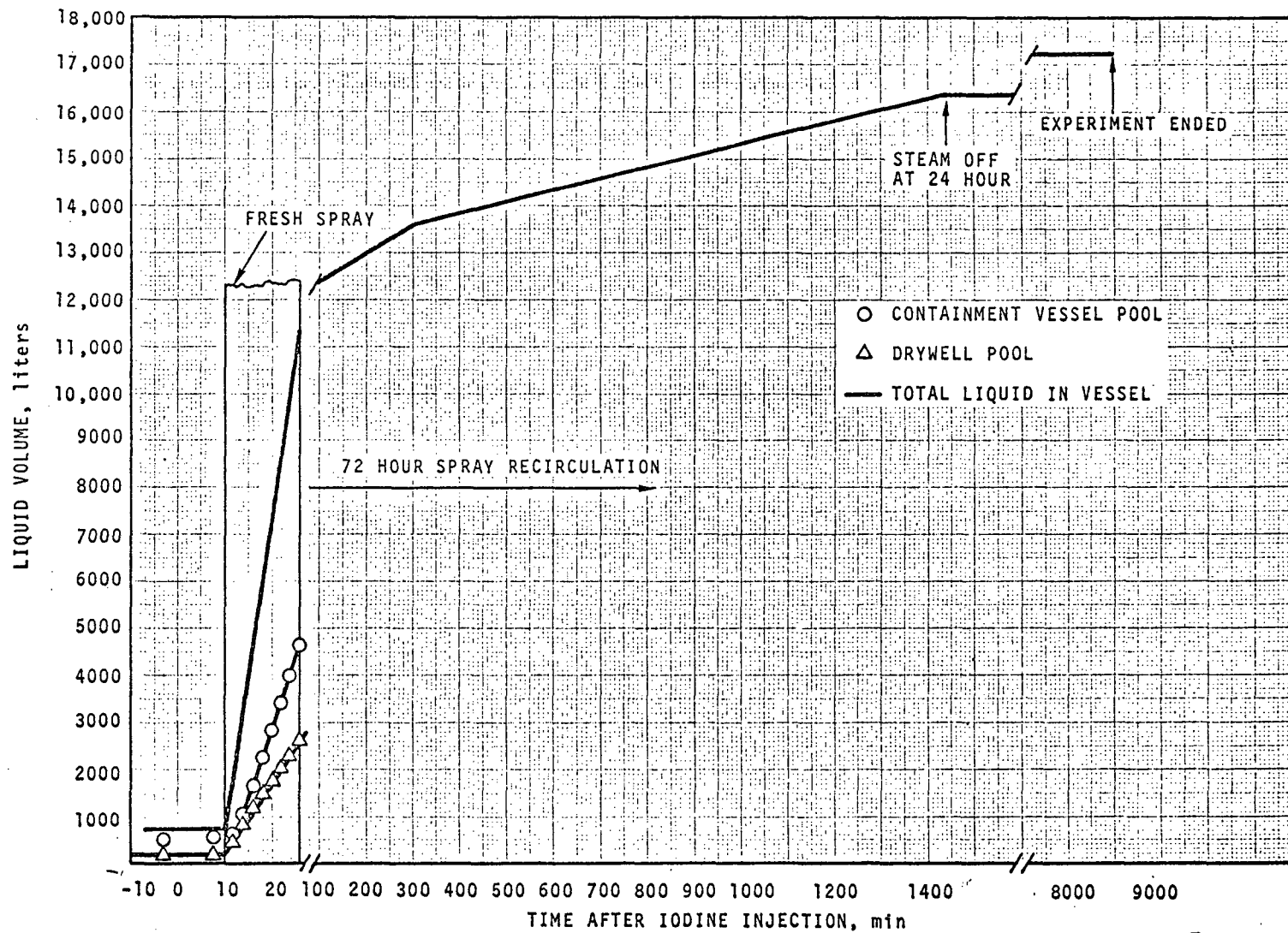


FIGURE 22. SPRAY LIQUID VOLUME IN RUN C-1

2. Retention of Iodine by Spray Liquid

a. Venting Effects

Reactor containment systems may be vented to the atmosphere several weeks after an accident to prevent the buildup of hydrogen gas concentration to the explosive level. After 6 days of sampling in Run C-1, the vessel atmosphere was purged with 2000 cfm of air for one hour (about 5 vessel volumes). The concentrations observed within the gas space (average of 3 simultaneous samples) are listed in Table 9. Purging began at 8587 minutes, and was completed prior to sample withdrawal at 8649 minutes.

As expected, the airborne concentration of all iodine forms decreased markedly during the purge. Methyl iodide concentration decreased to less than 3% of its pre-purge concentration. Total inorganic iodine decreased to about 10% of its pre-purge concentration. The maximum theoretical concentration to which the post-purge atmosphere could rise due to desorption from liquid pools depends on the fraction of a partitioning specie which resides in the liquid. For methyl iodide, the partition coefficient is of order of unity. Since the liquid volume is only about 0.01 of the gas volume, greater than 90% of the methyl iodide present in the vessel would be expected to be removed by the purge. Evolution of methyl iodide with continued purging would be minimal.

For total inorganic iodine, the concentration decrease was less than for methyl iodide, but much greater than if all iodine in solution were in equilibrium with the gas phase. This behavior is consistent with conversion of dissolved iodine to a non-volatile form by an irreversible chemical reaction, and mass transfer limitations. Thus, continued purging would reduce the gas phase concentration to lower and lower values. This

TABLE 9
AIRBORNE IODINE CONCENTRATION DECREASE
DURING PURGING OF THE CONTAINMENT VESSEL (a)

	$C_g, \mu\text{g}/\text{m}^3$				
	<u>t=8548</u>	<u>t=8578</u>	<u>t=8649</u>	<u>t=8708</u>	<u>t=8768</u>
Elemental Iodine	2.08	1.66	0.35	0.24	0.31
Particulate Iodine	0	0.02	0.11	0.37	0.13
Iodine Associated with Charcoal Paper	18.1	16.5	1.50	0.78	0.55
Iodine on Maypack Inlet	0.10	0.16	0.08	0.10	0.10
Total Inorganic Iodine	20.3	18.3	2.04	1.49	1.09
Methyl Iodide	121	93.7	2.14	0.79	0.25
Total Iodine	141	112	4.18	2.28	1.34

(a) Air purge at 2000 CFM for 60 minutes. Start at t=8587 min; stop at t=8647 min.

behavior mitigates the release of iodine which would occur during venting. The total amount released would be small compared to that estimated on the basis of a constant concentration.

The effort expended here is not definitive but demonstrates that the iodine mass released during venting will be substantially less than estimated on the basis of a constant gas phase concentration.

b. Retention of Iodine During Sample Evaporation

Samples of the spray liquid were withdrawn from the vessel at selected time intervals, and then evaporated. Evaporation was carried out about 24 hours subsequent to sample withdrawal. Samples were evaporated in a 500 ml Pyrex flask heated by an oil bath maintained at 115 °C. The water vapor was swept to a condenser with an airflow of 100 cc/min. The condenser catch flask was vented through a Maypack. After dryness, the evaporation flask was decontaminated with caustic and HF. The flask outlet tube, condenser and condensate catch flask were washed and the liquid analyzed separately. Results of the evaporation tests are tabulated in Table 10 for iodine and Table 11 for cesium. These data show that only a relatively small fraction of the iodine was in a chemical form which was in equilibrium with the gas phase. This is consistent with irreversible conversion to a non-volatile form as outlined earlier.

The fractional loss of iodine from solution evaporated to dryness may be compared with similar tests carried out in an earlier CSE test which used a caustic spray solution (Run A-9). For the caustic spray samples, an average loss of 8% was observed, accounting for loss by entrainment (based on Cs carryover). This agrees closely with the average of 9% observed for the present boric acid samples, and it is concluded that the boric acid solutions effectively bind the iodine chemically.

3. Aerosol Particle Washout

a. Cesium Concentration in the Gas Phase

The airborne concentration of cesium early in the run is shown in Figure 23. Initial washout occurs with a half-life of about 1.6 minutes. After the airborne concentration was reduced to below 10% of the maximum

TABLE 10

IODINE LOSS BY EVAPORATION OF LIQUID SAMPLES (a)

	d/m per ml					
	Sample L03C03	Sample L03C09	Sample L03C12	Sample L03C18	Sample L03C23	Sample L03C30
	<u>t=15</u>	<u>t=50</u>	<u>t=100</u>	<u>t=600</u>	<u>t=1600</u>	<u>t=8500</u>
Flask outlet tube	1.45	353	693	1140	2420	1180
Condenser	9.47	2580	5010	8710	7620	1490
Maypack filter	0.72	5	22	29	66	16
Maypack silver	0.75	4	55	29	51	16
Maypack charcoal paper	0.49	172	323	219	330	112
Maypack charcoal bed	<u>0.00</u>	<u>20</u>	<u>46</u>	<u>2</u>	<u>11</u>	<u>4</u>
Total leaving flask	12.87	3133	6150	10130	10450	2820
Total remaining in flask	<u>46.10</u>	<u>21400</u>	<u>63800</u>	<u>52500</u>	<u>32100</u>	<u>28700</u>
Total recovered	58.97	24533	69950	62630	42500	31500
Gross fraction lost	0.218	0.127	0.088	0.162	0.245	0.089
Fraction entrained ^(b)	0.031	0.089	0.033	0.089	0.072	0.050
Fraction lost by desorption	0.187	0.038	0.055	0.073	0.173	0.039

(a) Samples from main sump evaporated to dryness at 115 °C.

(b) Assumed to be same as fraction of cesium lost.

TABLE 11

CESIUM LOSS BY EVAPORATION OF LIQUID SAMPLES ^(a)

	d/m per ml					
	Sample L03C03 <u>t=15</u>	Sample L03C09 <u>t=50</u>	Sample L03C12 <u>t=100</u>	Sample L03C18 <u>t=600</u>	Sample L03C23 <u>t=1600</u>	Sample L03C30 <u>t=8500</u>
Flask outlet tube	0	0	0	0	14	763
Condenser	34.7	427	691	1910	1450	216
Maypack	<u>0.82</u>	<u>0.9</u>	<u>1.8</u>	<u>4</u>	<u>4.6</u>	<u>2</u>
Total leaving flask	35.5	428	693	1914	1470	979
Total remaining in flask	<u>1116</u>	<u>4404</u>	<u>20420</u>	<u>19680</u>	<u>18740</u>	<u>18470</u>
<u>Total recovered</u>	<u>1151</u>	<u>4832</u>	<u>21100</u>	<u>21600</u>	<u>20210</u>	<u>19450</u>
Fraction lost from flask	0.031	0.089	0.033	0.089	0.072	0.050

(a) Samples from main sump evaporated to dryness at 115 °C.

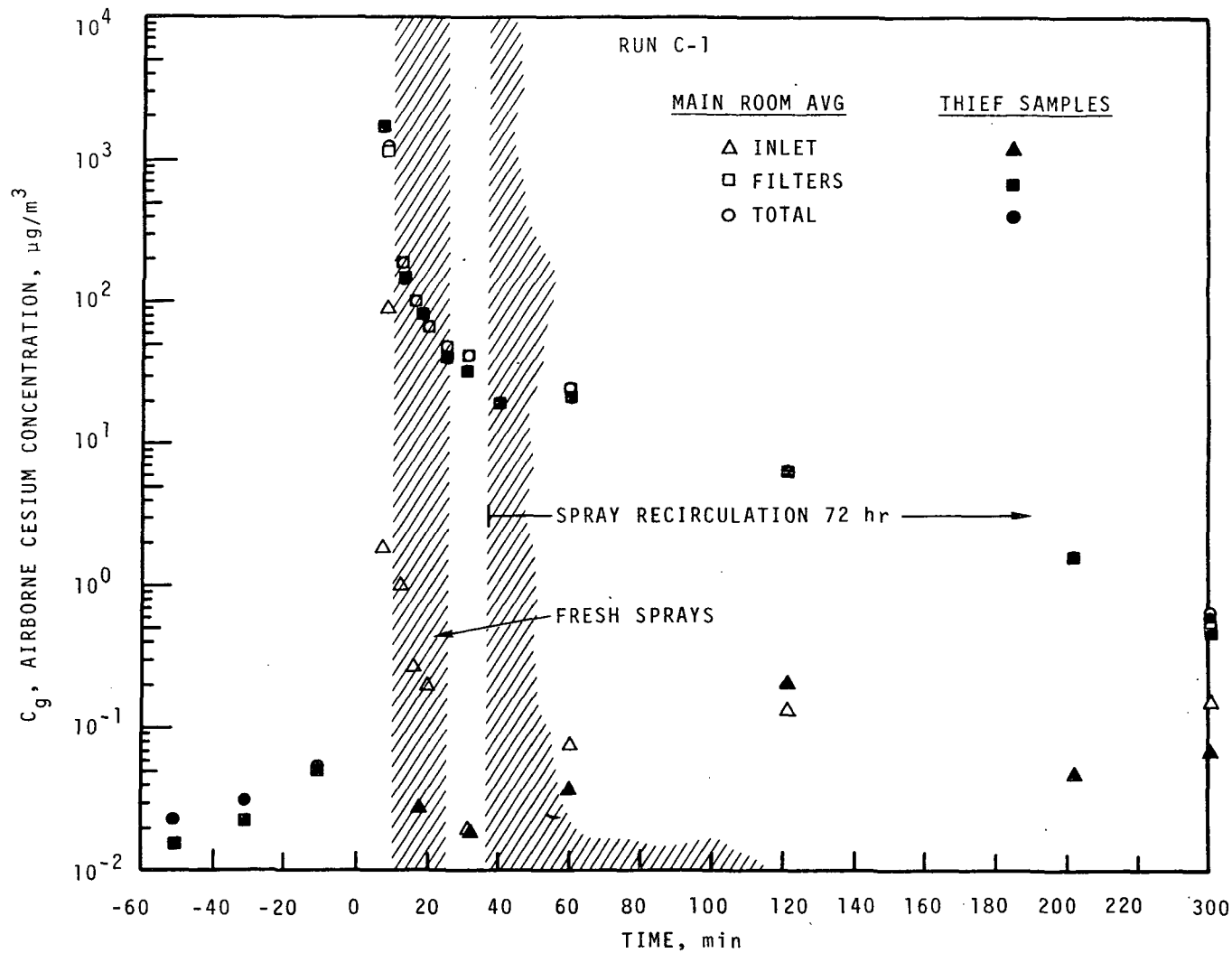


FIGURE 23. AIRBORNE CESIUM EARLY IN RUN C-1

concentration, the washout rate decreased in magnitude, but the washout continued.

The airborne concentration of cesium for the entire run is shown in Figure 24. The airborne concentration is reduced by 4 orders of magnitude after some 8 hours of spraying. The concentrations measured at longer times are near the background level of the measurement technique, hence represent upper limit concentrations.

The cesium washout rate observed here is in agreement with results obtained in previous CSE tests. Inasmuch as solution composition would be expected to have virtually no influence on particle washout, agreement between cesium washout rates measured in previous CSE tests and Run C-1 was anticipated.

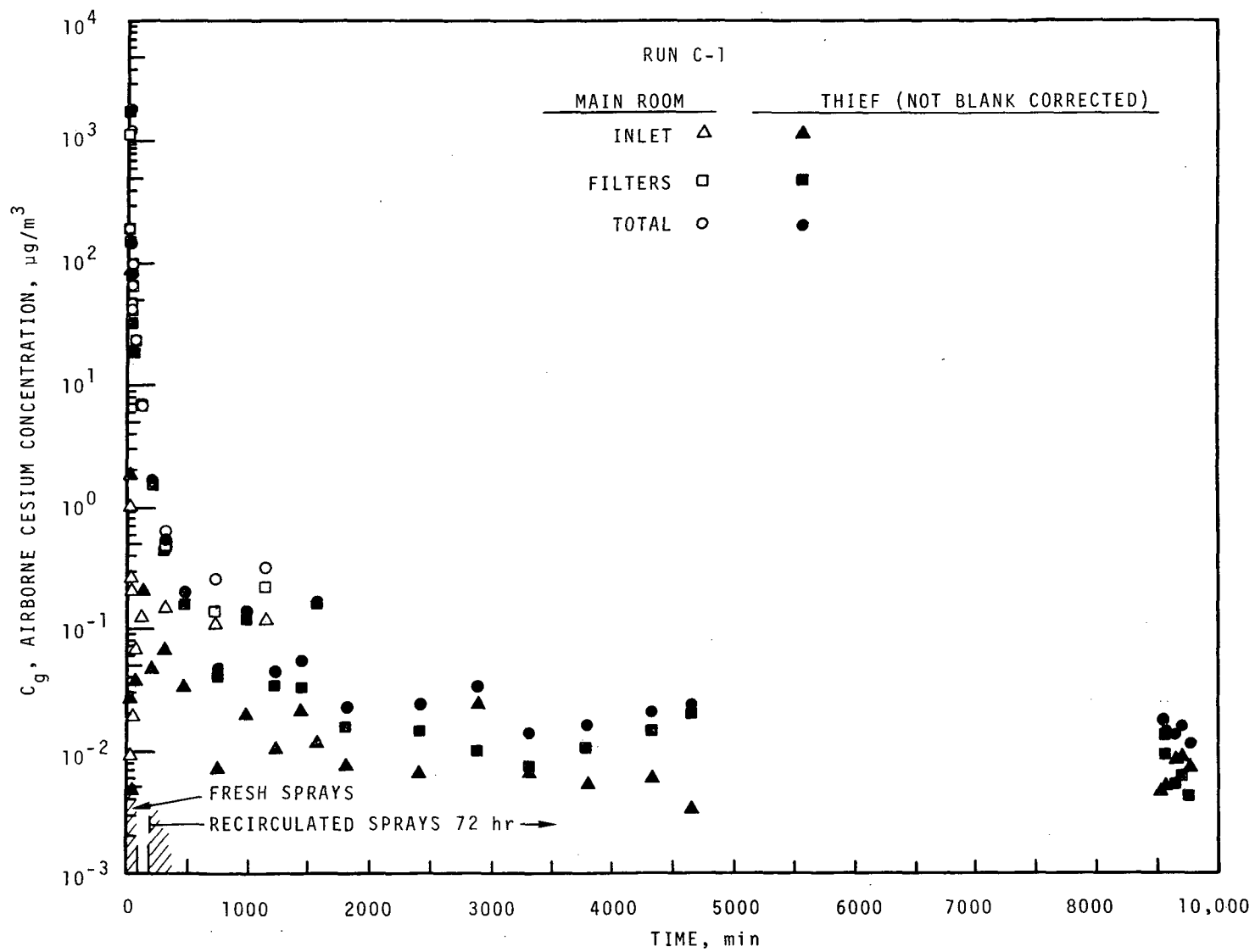
b. Concentration of Cesium in Spray Drops

Spray liquid collected by thief samples and funnel rain samplers was analyzed for cesium as well as iodine. The concentration of cesium in collected liquid is shown in Figure 25. The thief samplers indicate appreciably less cesium than the funnel samplers early in the spray period. This difference is likely due contamination of funnel surfaces with cesium prior to spray operation. Other reasons for the discrepancy are not apparent.

c. Concentration of Cesium in Sump Liquid

The concentration of cesium in the drywell and containment vessel sumps are shown in Figure 26. As in previous CSE tests, the drywell sump is more concentrated than the main vessel sump. This is due to deposition of injected cesium into the drywell and more efficient collection

FIGURE 24. AIRBORNE CESIUM DURING CONTINUED SPRAY OPERATION IN RUN C-1



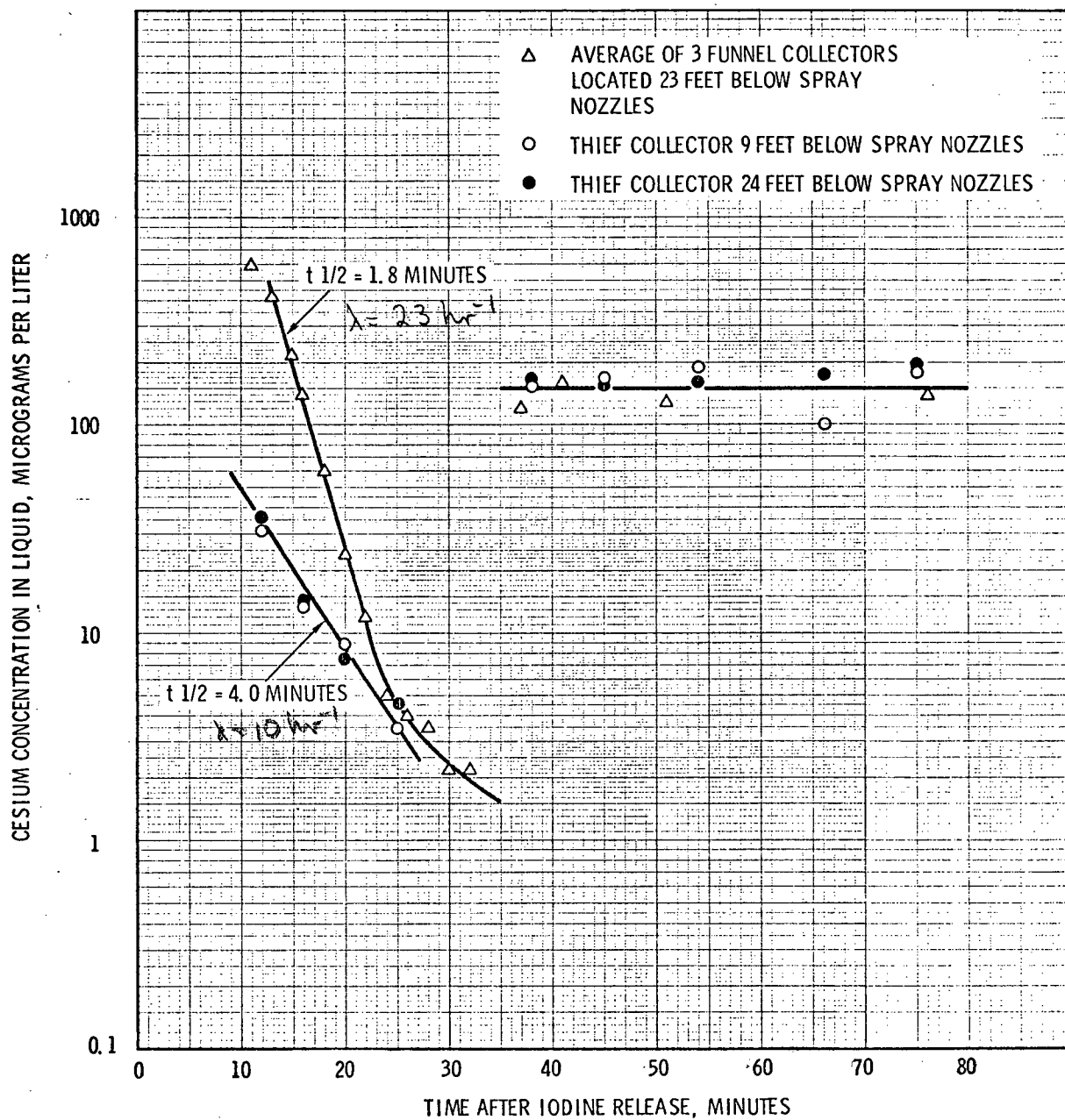


FIGURE 25. CESIUM CONCENTRATION IN SPRAY DROPS IN RUN C-1

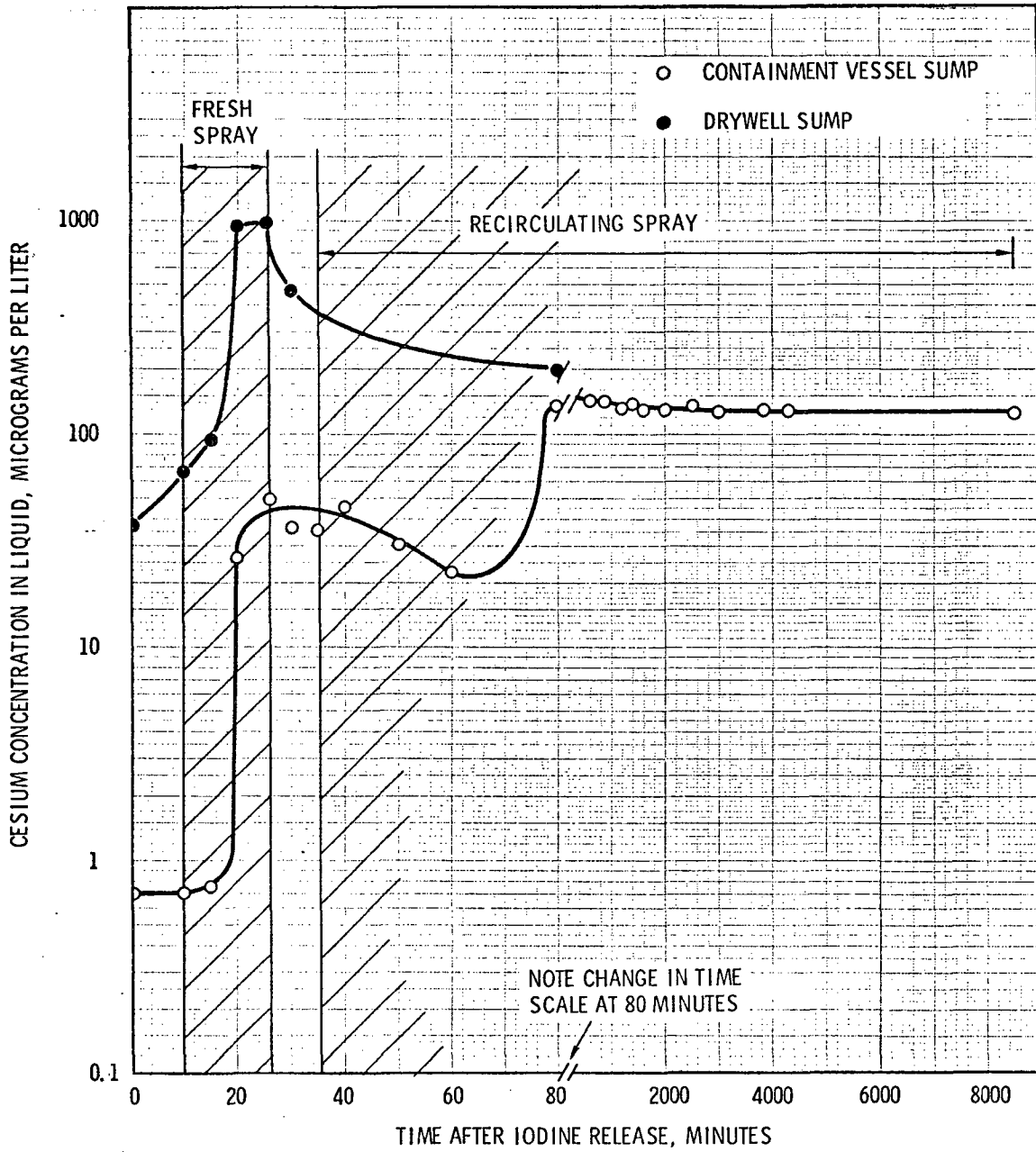


FIGURE 26. CESIUM CONCENTRATION IN LIQUID POOLS

of cesium by drops falling the greater distance into the drywell. At 80 minutes (45 min of recirculation) the two sumps are well mixed.

4. Comparison of Iodine Washout with CSE Run A-7

a. Comparison of Spray Conditions for Runs A-7 and C-1

1. Temperature of Atmosphere and Spray Liquid

The temperatures of the vessel atmosphere and spray liquid were very similar for these two runs. A small difference was caused in Run C-1 where steam flow was increased subsequent to spray initiation in order to re-attain thermal equilibrium at 250 °F more quickly. The spray flow rate in C-1 was 3 times greater than in A-7, hence the temperature decrease, during fresh spray, was 3 times greater on an absolute time scale basis. When compared on the basis of volume of liquid sprayed, the temperature history for the two runs is similar. The temperatures in these two runs are compared in Table 12.

TABLE 12

COMPARISON OF CONTAINMENT TEMPERATURES

FOR TWO BORIC ACID SPRAY TESTS

<u>Time Period</u>	<u>Location</u>	<u>Temperature, °F</u>	
		<u>Run C-1</u>	<u>Run A-7</u>
Prior to Spray Initiation	Vapor, main room	249	249
Prior to Spray Initiation	Spray Solution	92	80
End of Fresh Spray	Vapor, main room	192	203
After 1 hr recirculation	Vapor, main room	235	230

2. Iodine Concentration

The partition coefficient of elemental iodine may be dependent on the solution concentration. Hence the iodine concentration in both the gas and liquid phases is potentially important. The iodine concentrations for the two boric acid spray tests are compared in Table 13.

TABLE 13
COMPARISON OF IODINE CONCENTRATION
IN TWO BORIC ACID SPRAY TESTS

<u>Item</u>	<u>Run C-1</u>	<u>Run A-7</u>
Mass of Iodine Injected Into Cont. Vessel, g	100.4	97.6
Gas phase elemental iodine conc. at start of fresh spray, mg/m ³	75	25
Gas Phase Conc. at end of Fresh Spray	2.5	0.19
Liquid Phase Conc. During Recirculation, mg/l	5.0	3.5

The major difference in these two tests is that in Run A-7, initiation of spray was 30 minutes after start of iodine release, while in Run C-1 it was only 10 minutes. Natural deposition on walls and other surfaces decreased the iodine concentration to a greater extent in Run A-7 than in Run C-1, as shown in Table 13. In Run C-1 the airborne concentration at the beginning of the fresh spray was 3 times greater than in Run A-7.

3. Cesium Concentration

It is conceivable that cesium ions may play a role in the chemistry of iodine dissolution. Hence, it is interesting to compare the cesium concentration in the vapor and liquid phases for the two boric acid runs. In Table 14, the concentration of cesium in the two phases is compared at important time periods. The cesium concentrations were not significantly different in the two runs.

TABLE 14
COMPARISON OF CESIUM IN TWO

BORIC ACID SPRAY TESTS

<u>Quantity, Time and Location</u>	<u>Run C-1</u>	<u>Run A-7</u>
Mass of Cs injected into containment vessel, g	3.24	2.13
Gas phase conc. at start of fresh spray, mg/m ³	1.3	1.0
Gas phase conc. at end of fresh spray, mg/m ³	0.045	0.028
Liquid conc. during recirculation, mg/l	0.15	0.13

4. Spray Flow Rate and Drop Size

The total spray flow rate in Run C-1 was 160 gal/min, which is 3.2 times higher than used in Run A-7. Thus, on the basis of other CSE tests and theory, washout of elemental iodine should have been approximately 3 times faster in Run C-1.

Drop size is a variable to which washout may be highly sensitive. Drop size was not measured in CSE tests, and the comparison must be made on the basis of data obtained by the manufacturer of the nozzles. Drop size data for the two Runs are compared in Table 15.

5. Spray Solution Composition

The spray solutions used in both Run C-1 and A-7 were made up in the same equipment. The only difference was that Technical grade boric acid was used in Run A-7, whereas Special Quality grade was used in Run C-1. Both materials were obtained from the same supplier, the U. S. Borax and Chemical Company. Chemical analyses were not performed on either type of the granular material. The manufacturer's specifications for the Special Quality grade were shown in Table 6.

TABLE 15
COMPARISON OF SPRAY CHARACTERISTICS FOR
RUNS C-1 AND A-7

<u>Items</u>	<u>Units</u>	<u>Run C-1</u>	<u>Run A-7</u>
Total spray flow rate	GPM	160	49
Average spray flux	GPM/ft ²	0.32	0.10
Wall flow rate*	GPM	2.1	1.0
Drop mass median diameter	microns	1100	1210
Geometric Std. Dev. of drop distribution	None	1.5	1.5
Method for drop size analysis		Flash Photography single nozzle in air	Flash Photography single nozzle in air

*Corrected to account for drops falling into wall trough.

Spectrochemical analysis of the solutions in the makeup tank for the two tests gave identical results, with iron being the only significant impurity. The permanganate demand for the solution used in Run A-7 was 8.6 ppm. This is larger than the $KMnO_4$ demand of 1.3 ppm measured for Run C-1.

The resistivity of the demineralized water used in Run C-1 averaged 0.25 megohm-cm, while that used in Run A-7 was about 0.05 megohm-cm.

b. Comparison of Spray Effectiveness for Runs A-7 and C-1

1. Elemental Iodine

Elemental iodine was the major component of iodine initially present in the gas phase. For a given spray drop the effectiveness is judged by its enrichment compared to the gas phase concentration at the end of the fall height. This ratio of liquid concentration to gas concentration was calculated from the spray flow rate and the observed washout rate, using

$$\left(\frac{C_l}{C_g} \right) = \frac{V}{F} \lambda_s \quad (24)$$

where λ_s = measured washout coefficient for spray alone.

The drop enrichment calculated from Equation (24) is compared to absorption theory in Figure 27 for the fresh spray periods. It is obvious that the solution used in Run A-7 was initially much more effective than that used in Run C-1, but during the second period it was less effective than that used in Run C-1.

For longer time periods, the spray is nearly at equilibrium with the gas phase. Thus for long times, the ratio of liquid concentration to gas phase concentration is a good measure of spray effectiveness. The observed partition coefficient for recirculated spray is shown for Run C-1 in Figure 28. Also shown is the observed partition coefficient for an experiment (CSE Run A-10) using sodium hydroxide spray with pH = 9.5.

The data presented in this section show that the boric acid solution used in Run A-7 was more effective initially for elemental iodine than that used in Run C-1. After 10 minutes of spraying, the solution used in Run C-1 proved more effective than that used in A-7. For recirculated sprays it is interesting to note that the iodine absorption capacity of the boric acid solution compared favorably to that observed in an earlier CSE test which used caustic.

2. Methyl Iodide

Methyl iodide is absorbed slowly by sprays which do not contain a reactive additive such as sodium thiosulfate. The absorption rate is controlled by liquid phase mass transfer resistance. One would not expect boric acid solutions to differ greatly from caustic spray regarding CH_3I washout rate. The methyl iodide concentration observed in Runs A-10 and C-1 are shown in Figure 29.

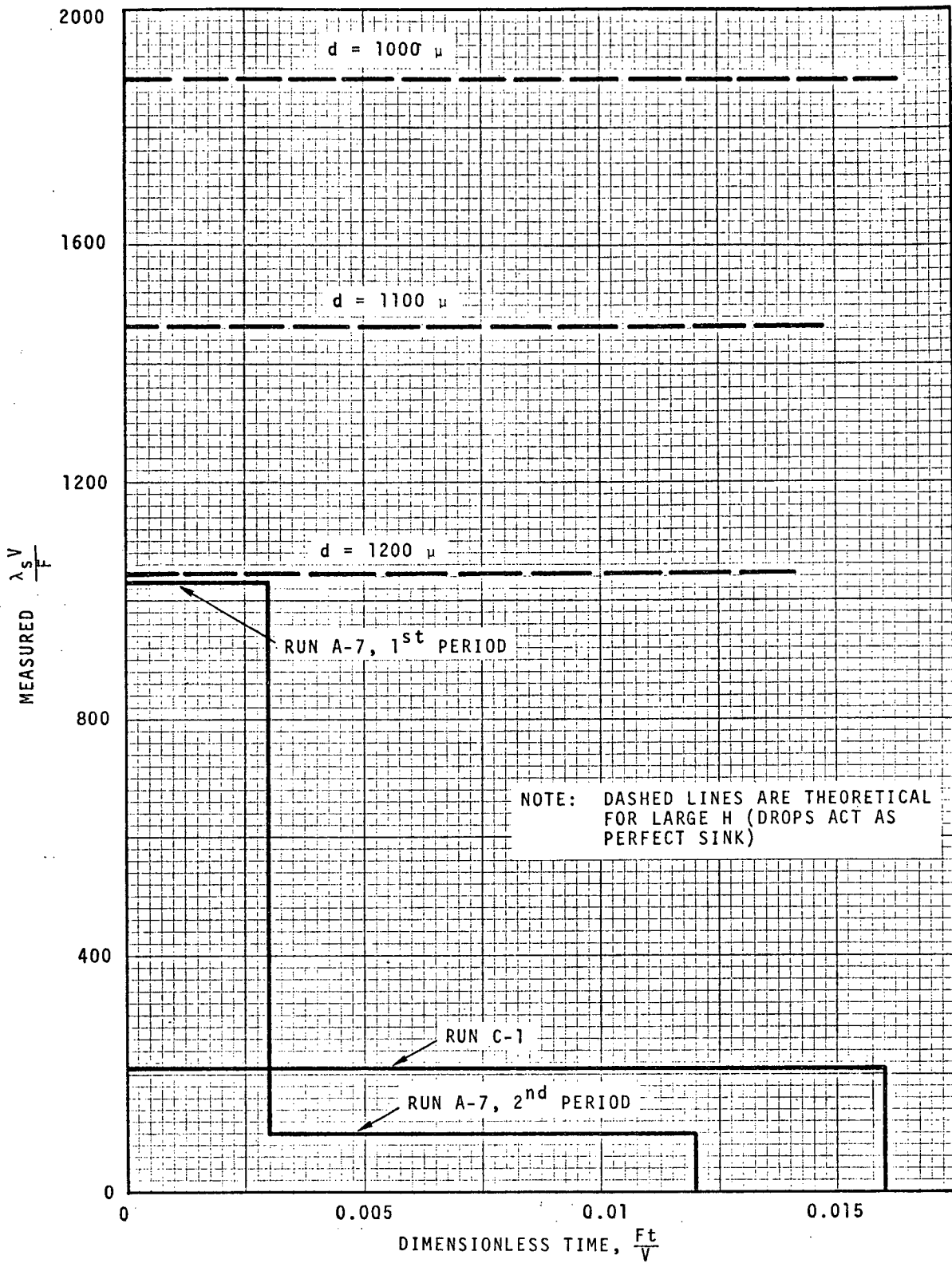


FIGURE 27. COMPARISON OF SPRAY DROP EFFECTIVENESS FOR TWO BORIC ACID SPRAY TESTS

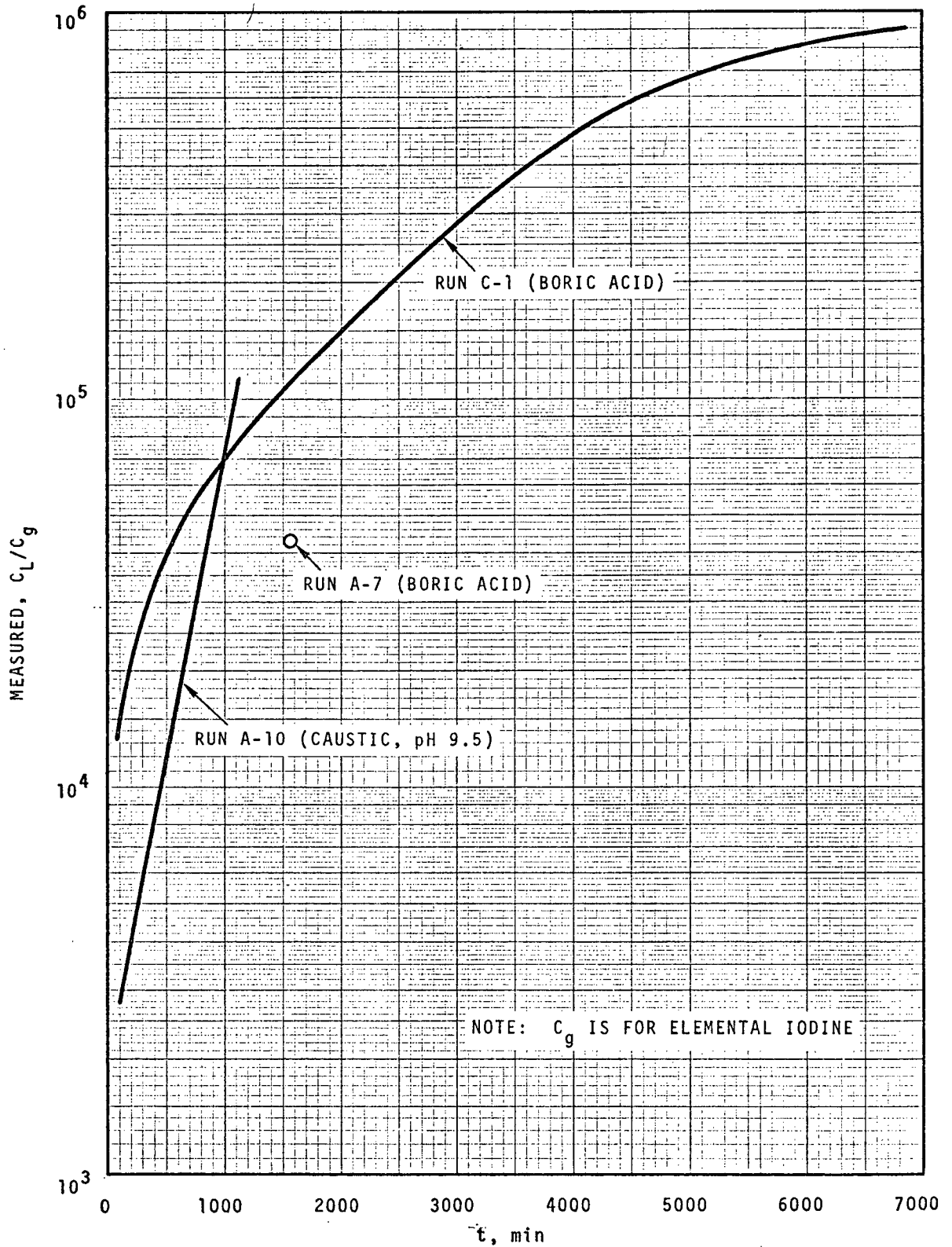


FIGURE 28. PARTITIONING OF ELEMENTAL IODINE BY RECIRCULATED SPRAYS

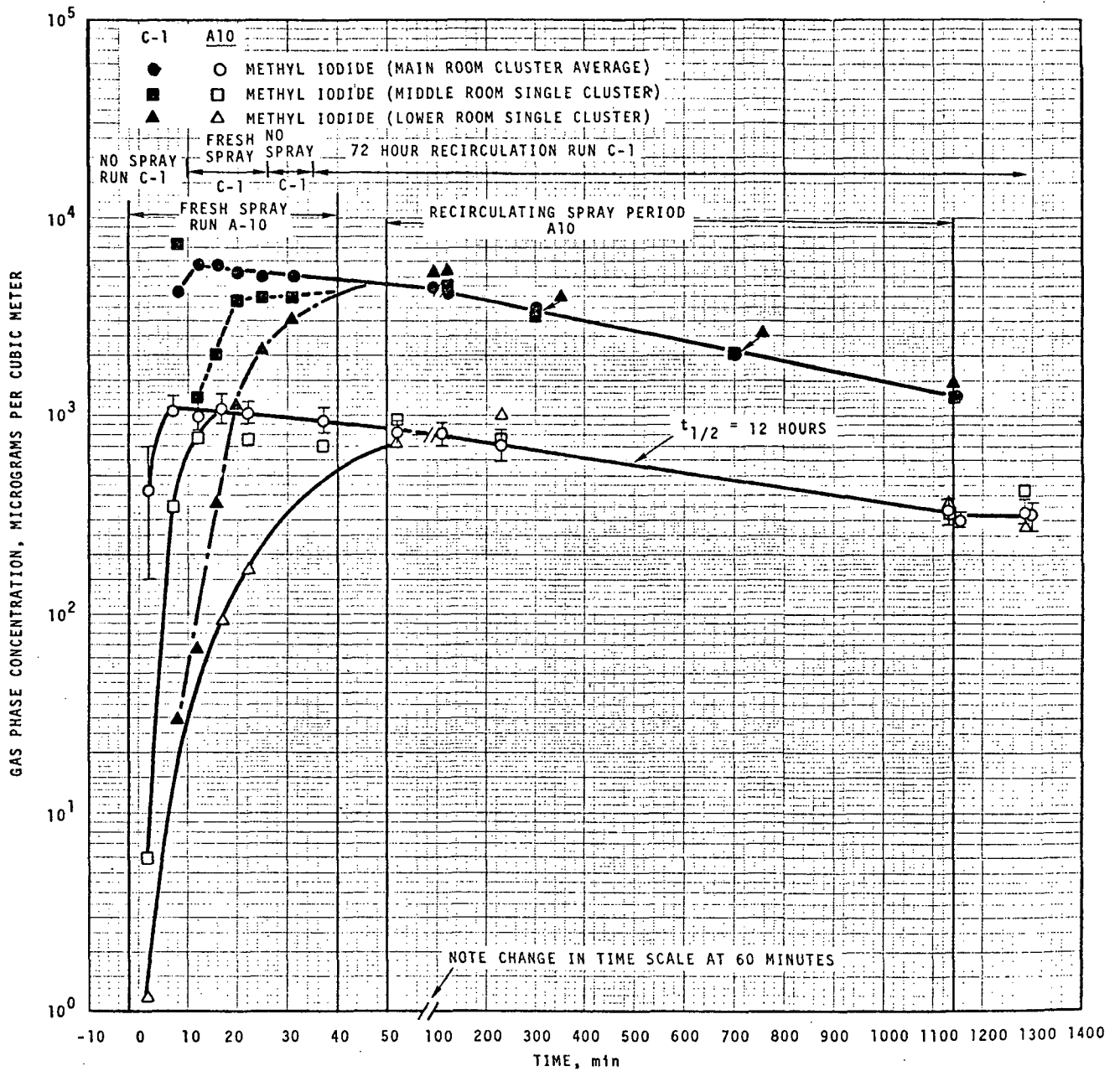


FIGURE 29. METHYL IODIDE REMOVAL BY CAUSTIC AND BORIC ACID SPRAYS

It is obvious that neither of these solutions is effective in giving appreciable 2 hr dose reduction factors for CH_3I . For long time periods, however, methyl iodide removal by both acidic and basic sprays is significant.

c. Conclusions Regarding Comparisons of Spray Effectiveness in Runs C-1 and A-7

Elemental iodine was removed from the containment atmosphere at an appreciably higher rate during the first few minutes of Run A-7 than in Run C-1. At longer times the two runs were very similar. The superior initial performance during Run A-7 is attributed to differences in two important experimental conditions. First, the airborne iodine concentration in Run A-7 was a factor of 3 lower than in Run C-1 at the time fresh spray was started. A lower iodine concentration favors a higher partition coefficient, leading to the higher washout rate observed in Run A-7. This effect is discussed more fully in Section VII and Figure 31.

A second cause of the superior initial removal in Run A-7 was the presence of impurities. Although the impurity content in Run A-7 was very low, the spray solution used in Run C-1 was purer as judged by boric acid purity, resistivity of the demineralized water, and permanganate demand of the spray solutions. Inasmuch as effective iodine removal by all water spray systems depends on rapid chemical reaction in solution, it is not surprising that impurities in solution can have an important effect on absorption of iodine at the low aqueous concentrations encountered in PWR accident situations.

Methyl iodide removal was substantially the same for the two boric acid runs. The removal of airborne particles was also equally effective

for both runs. These results are expected since rapid solution reactions play a negligible role in absorption of methyl iodide and particles.

It is concluded that the two large-scale experiments are in satisfactory agreement, if differences in iodine concentration and impurity levels are considered.

VI. COMPARISON OF LARGE-SCALE TEST RESULTS WITH PREDICTIONS BASED ON SMALL-SCALE PARTITION COEFFICIENT MEASUREMENTS

A. Initial Washout Rate for Elemental Iodine

The removal rate due to spray drops during the fresh spray period is given by Equation (4a)

$$\text{spray absorption rate} = FHE C_g \quad (4a)$$

If the removal at the vessel surfaces is assumed to be negligible, a mass balance for elemental iodine in the containment gas volume gives, for the initial conditions of $C_g = C_{g0}$ at $t = 0$:

$$\frac{C_g}{C_{g0}} = e^{-\frac{FHEt}{V}} = e^{-\lambda_s t} \quad (25)$$

or, for the washout coefficient, λ_s ,

$$\lambda_s = \frac{FHE}{V} \quad (26)$$

As discussed in Section III, E can be evaluated by assuming either that the drops are stagnant during their entire fall, Equation (6), or are well mixed, Equation (5). It was shown in Section III that differences between predictions using these two assumptions are < 30% for conditions pertinent to containment systems. Since the assumption that the drops are

well mixed gives an equation which is easily evaluated, and introduces only a small error, it will be used here.

$$E = 1 - \exp \left(-\frac{6k_g t_e}{Hd} \right) \quad (5)$$

The drop exposure time, t_e , can be approximated by

$$t_e = \frac{h}{U_t} \quad (27)$$

where h = drop fall distance,

U_t = drop terminal settling velocity.

For reactive solutions where H is very large (> 5000), Equation (5) can be approximated by

$$E = \frac{6 k_g h}{HU_t d} \quad (28)$$

and Equation (26) becomes

$$\lambda_s = \frac{6k_g Fh}{V U_t d}, H = \text{large} \quad (29)$$

which applies for cases where the drops act as perfect sinks for absorption of elemental iodine. For systems where H is expected to be small, e.g., boric acid - iodine, Equation (5) should be used.

In Run C-1, the concentration of elemental iodine in the main room gas space at the time that fresh sprays were initiated was 75 mg/m^3 . The instantaneous partition coefficient for inorganic iodine associated with this concentration, as measured in the small-scale experiments (shown in Figure 9) is 80. Curve B of Figure 9 is chosen because the solution used in Run C-1 had a value of H_0 which fell on Curve B (see experiment CRJ and Figure 8).

The concentration of inorganic iodine in the containment atmosphere was predicted for Run C-1 by using Equations (5) and (25) and the values

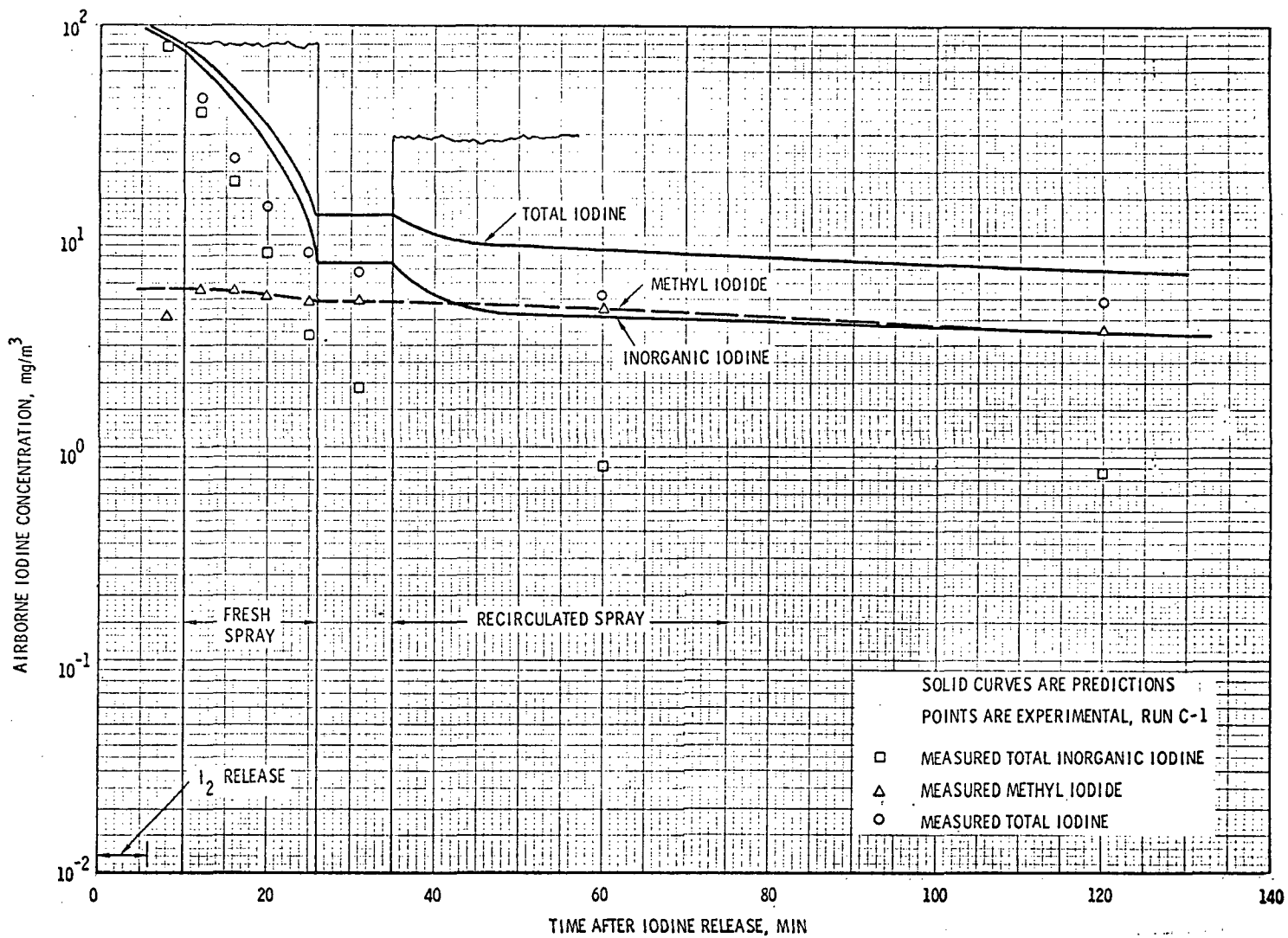
of H_0 shown in Figure 9, Curve B. Since H_0 is a function of iodine concentration, which changes with time during sprays, the calculations were made by dividing the fresh spray period into 2-minute time steps. Figure 30 shows the predicted concentration as a function of time. The washout rate is predicted to start rather slowly but increase with time as the concentration is lowered. Also shown in Figure 30 is the predicted total iodine concentration. This curve was obtained by adding the observed methyl iodide concentration (dashed line) to the concentration predicted for inorganic iodine.

The experimentally measured concentrations are plotted in Figure 30 for comparison with the predicted values. The inorganic iodine concentration decreased faster than predicted and at the end of the fresh spray period was a factor of 3 lower than predicted. The higher washout rate observed was probably caused by unavoidable contamination in the large-scale experiment by iron and other impurities. Also, some removal at vessel surfaces probably occurred and this was not accounted for in the prediction.

B. Recirculation Period

The small-scale partition coefficient tests and all previous experiments in the CSE have shown that H is not constant but increases with time. Curve CRJ of Figure 7 shows that for the same solution used in Run C-1 the magnitude of H doubled every 8 minutes until it reached a value of about 1000, after which it doubled every 230 minutes. The relatively slow reaction responsible for the 8-minute doubling, converted a large fraction of the absorbed iodine in the liquid in the vessel sumps to a non-volatile form. When recirculation was started the liquid pumped

FIGURE 30. COMPARISON OF IODINE WASHOUT IN RUN C-1 WITH WASHOUT PREDICTED FROM PARTITION COEFFICIENT MEASUREMENTS



from the sump to the spray manifold acted nearly as a fresh spray. A pseudo-equilibrium was quickly attained, as expressed by Equation (30)

$$\left(\frac{C_g}{C_{go}}\right)_{\text{equilib.}} = \frac{1}{1 + \frac{LH_t}{V}} \quad (30)$$

where H_t = time dependent value of H,
L = total liquid volume contained,
V = total gas volume,
 C_{go} = gas concentration at time zero.

The predicted concentration during the recirculation period is plotted in Figure 30, using Equation (30), curve CRJ of Figure 7, and liquid volumes from Figure 22. As for the fresh spray period, the experimentally measured concentrations were lower than predicted for inorganic iodine. An improved theory which would account for wall effects and added impurities from the containment system would probably give better agreement with experiment.

VII. APPLICATION OF RESULTS TO A LARGE PWR

A. Scope

Predictions of iodine washout by boric acid spray in large PWR containment vessels will be briefly considered to show the order of magnitude of the removal which may be expected. It must be recognized that the iodine absorption rate depends on geometry and flow parameters, hence will vary from one plant to another. The calculations presented in this chapter apply to one hypothetical plant for which the flow parameters are believed typical of PWR's.

The scope of the present work did not permit extensive study of mathematical models which permit application of test results to containment vessels. Thus the washout calculations presented here are tentative. Better methods for applying the present test results to containment vessels may be developed in the future.

B. Physical Parameters and Assumptions

Physical parameters assumed for the PWR are listed in Table 16.

TABLE 16

PHYSICAL PARAMETERS ASSUMED FOR A LARGE PWR

<u>Parameter</u>	<u>Units</u>	<u>Numerical Value</u>
Contained gas volume	ft ³	1.5 x 10 ⁶
Average drop fall distance	ft	100
Average temperature for initial 2 hr	°F	250
Average pressure for initial 2 hr	psia	48
Mean drop diameter	microns	1000
Spray flow rate	gpm	2600
Total water volume added	ft ³	3 x 10 ⁴
Fraction of total iodine released as methyl iodide	None	0.1
Duration of fresh spray	Min	43.2

Assumptions made to simplify the calculations included the following:

- Iodine release occurs as a puff at time zero.
- Sprays operate continuously following the iodine release
- Recirculation begins as soon as fresh spray solution has been injected into the containment vessel.

C. Predicted 2 hr Dose Reduction Factor

1. Direct Application of Large Scale Test Results

A straightforward estimate of the iodine absorption rate in a PWR may be made by assuming that the drops in the large containment vessel are enriched to the same extent as was measured in Run C-1. The drop effectiveness early in Run C-1 may be obtained from Figures 18 and 20. From the data shown, one calculates $HE = 190$, where H is the partition coefficient, and E is the fractional saturation.

After prolonged circulation, a pseudo-equilibrium between gas and liquid is achieved. The gas concentration during this equilibrium period is

$$\left(\frac{C_g}{C_{go}} \right)_{\text{equil}} = \frac{1}{1 + \frac{LH_t}{V}} \quad (30)$$

For the large scale test, the value of H_t was calculated from the data shown in Figures 18 through 21.

The gas phase concentration early during recirculation was estimated from the concentration predicted by fresh spray washout, and the equilibrium concentration given by Equation (30).

The dose reduction factor (DRF) was calculated as the ratio of mass which would leak if the concentration were invariant with time, to the actual mass leaked:

$$DRF = \frac{C_{To} t}{\int_0^t C_T dt} \quad (31)$$

where C_{T_0} = total iodine concentration at $t = 0$,
 C_T = total iodine concentration at $t = t$.

Application of C-1 data to the assumed PWR containment vessel gives a 120 minute DRF of 3.65. This calculation is an underestimate of the DRF as it neglects wall deposition and improved iodine absorption due to greater fall height in the PWR.

2. Application of Small Scale Test Data

Spray washout in a PWR vessel was also predicted on the basis of the small scale partition coefficient experiments described in this report. The instantaneous partition coefficient applicable to spray absorption was taken as curve B of Figure 9. Iodine washout was predicted using Equations (5) and (25) for the fresh spray. For prolonged recirculation, the gas phase concentration was estimated on the basis of Equation (30), using H_t data from Figure 7. Early during recirculation, the spray was considered "fresh" with the dissolved iodine being present as a non-volatile reacted form. The calculations were performed numerically, using either 2 minute or 4 minute time intervals.

The airborne concentrations of inorganic iodine predicted from the small scale tests are shown in Figure (31) for three initial gas phase concentrations. The dependency of washout rate on concentration is a point of difference between the large scale and small scale test results.

The dose reduction factors obtained by numerically integrating the concentration histories presented in Figure (31) are summarized in Table 17.

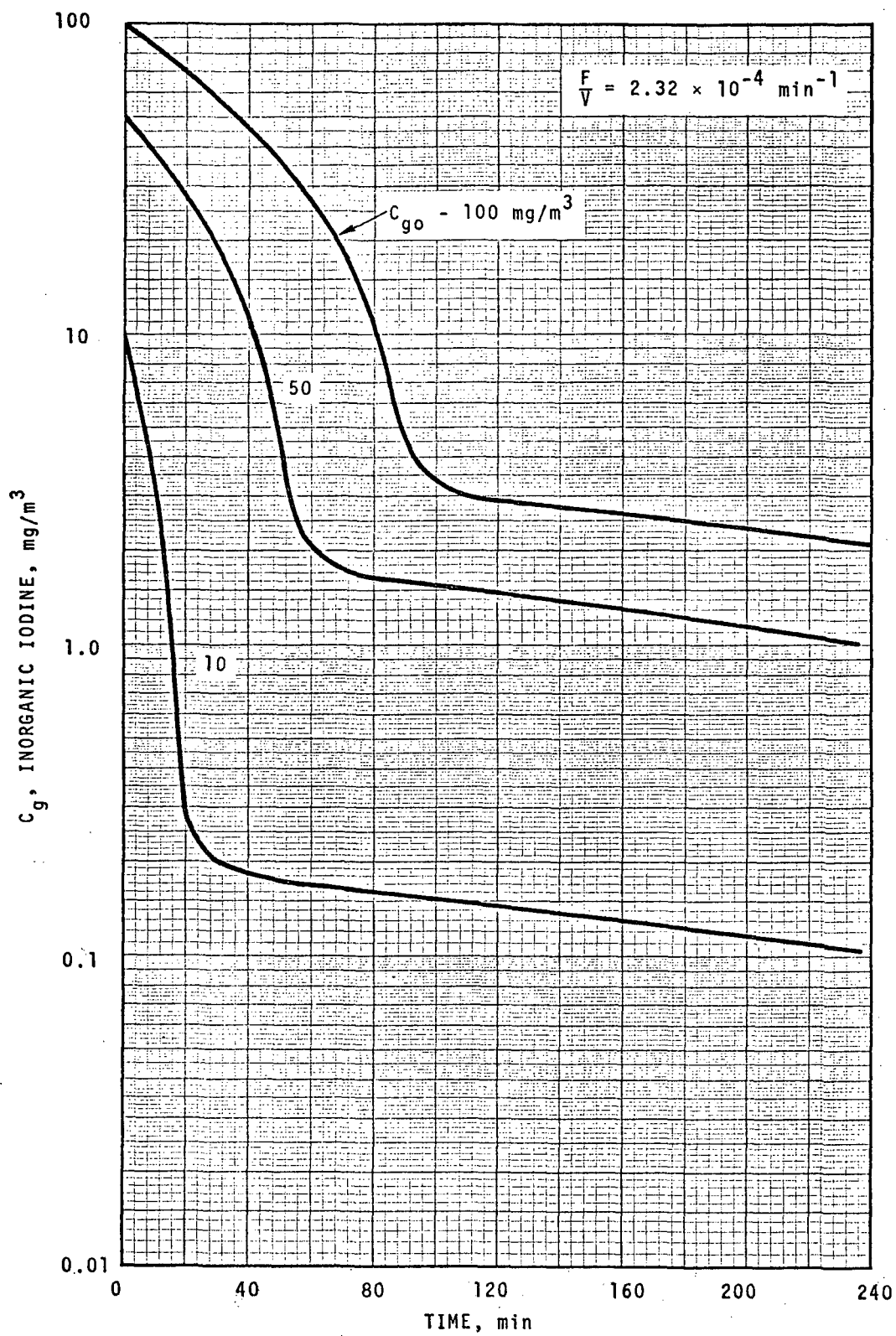


FIGURE 31. PREDICTED CONCENTRATION OF INORGANIC IODINE IN THE GAS SPACE OF A PWR DURING BORIC ACID SPRAY

TABLE 17

2 HR DRF IN A PWR PREDICTED

FROM PARTITION COEFFICIENT EXPERIMENTS

<u>Parameter</u>	<u>Case A</u>	<u>Case B</u>	<u>Case C</u>
C_o , in organic iodine, mg/m^3	10	50	100
C_o , methyl iodide, mg/m^3	1.1	5.5	11
C_{To} , total iodine, mg/m^3	11.1	55.5	111
C_{2-hr} avg., inorganic, mg/m^3	0.81	11.5	34.2
C_{2-hr} avg., methyl iodide, mg/m^3	1.1	5.5	11
C_{2-hr} avg., total iodine	1.91	17.0	45.2
DRF_{2-hr} , total iodine	5.80	3.26	2.46

The dose reduction factors predicted from the small scale tests (Table 17) bracket the dose reduction factor predicted by direct use of the results of the large scale test. For the large test, Run C-1, the initial iodine concentration was about $80 mg/m^3$. For this concentration, a 2 hr DRF of 2.8 in a PWR is predicted from the small scale test. This is appreciably lower than the value of 3.65 predicted from the large test, C-1.

3. Comparison with Caustic

A calculation based on small scale tests for caustic has been made.⁽¹⁹⁾ In this calculation, an iodine partition coefficient of 5000 was assumed for the 120 minute calculational period. For 10% of the iodine present as methyl iodide (assumed constant in concentration) the 2 hr DRF was predicted to be 8.62. Thus, caustic spray is expected to provide superior iodine removal for early times. After a few hours the two spray solutions are about equivalent in iodine removal capability.

VIII. REFERENCES

1. J. L. Gallagher, et al. "Design of Spray Additive Systems", paper presented at American Nuclear Society Annual Meeting, Los Angeles, California, June 29, 1970.
2. W. E. Joyce, "Sodium Thiosulfate Spray System for Radioiodine Removal", paper presented at American Nuclear Society Meeting, Los Angeles, California, June 29, 1970.
3. T. H. Row, "The Reactor Containment Spray System Research Program", paper presented at the American Nuclear Society Annual Meeting, Los Angeles, California, June 29, 1970.
4. R. K. Hilliard, et al., "Removal of Iodine and Particles from Containment Atmospheres by Sprays -- Containment Systems Interim Report", BNWL-1244. Battelle-Northwest Richland, Washington, February, 1970.
5. W. B. Cottrell. "ORNL Nuclear Safety Research and Development Program Bimonthly Report for Jan.-Feb. 1970", ORNL-TM-2919, Oak Ridge National Lab., May 1970, pp 65-75.
6. P. V. Danckwerts. "Absorption by Simultaneous Diffusion and Chemical Reaction into Particles of Various Shapes and Into Falling Drops", Trans. Faraday Soc., Vol. 47, pp 1014-1023. 1951.
7. H. Rosenberg, et al., "Fission Product Deposition and Its Enhancement Under Reactor Accident Conditions: Development of Reactive Coatings". BMI-1874. Battelle Memorial Institute, Columbus, Ohio, November, 1969.
8. A. K. Postma, "Absorption of Methyl Iodide by Aqueous Hydrazine Solutions Within Spray Chambers" PhD Thesis, Oregon State University, Corvallis, Oregon, 1970.

9. L. F. Coleman. "Preparation Generation, and Analysis of Gases and Aerosols For The Containment Systems Experiment", BNWL-1001, Battelle-Northwest, Richland, Washington, April 1969.
10. J. D. McCormack. "Maypack Behavior in the Containment Systems Experiment -- A Penetrating Analysis", BNWL-1145, Battelle-Northwest, Richland, Washington, August 1969.
11. D. E. Byrnes. "Some Physico-Chemical Studies of Boric Acid Solutions at High Temperatures", WCAP-3713, Westinghouse Electric Corporation September, 1962.
12. M. E. Meek. "The Calculated pH of Aqueous Boric Acid Solutions As a Function of Temperature and Added Base Content", WCAP-3269-51, Westinghouse Electric Corporation, March 1965.
13. A.E.J. Eggleton. "A Theoretical Examination of Iodine-Water Partition Coefficients", AERE-R-4887. Harwell, England, February, 1967.
14. L. C. Watson, et al. "Iodine Containment by Dousing in NPD-II", CRCE-979 Chalk River, Ontario, Canada, October 1960.
15. Yukinori Nishizawa, et al. "Vapor-Water Partition Coefficient of Iodine and Organic Iodides. ORNL-Tr-2255 Oak Ridge National Laboratory, Oak Ridge, Tennessee (date unknown).
16. C. E. Linderoth. "Containment Systems Experiment, Part I. Description of Experimental Facilities", BNWL-456. Battelle-Northwest, Richland, Washington, March 1970.
17. R. K. Hilliard, et al. "Comparisons of The Containment Behavior of a Simulant with Fission Products Released From Irradiated UO₂", BNWL-581. Battelle-Northwest, Richland, Washington, March 1968.

18. B. F. Roberts, et al. "Evaluation of Various Methods of Fission Product Aerosol Simulation", ORNL-TM-2628, Oak Ridge National Laboratory, Oak Ridge, Tennessee, September 1969.
19. R. K. Hilliard, et al. "Removal of Iodine and Particles By Sprays In The Containment Systems Experiment", BNWL-SA-3175, Battelle-Northwest, Richland, Washington, June 1970.

IX. ACKNOWLEDGEMENTS

The work outlined in this report was financially supported by a consortium of private utilities and reactor manufacturers. This support is gratefully acknowledged. Special thanks are due G. B. Mantheyney, Consumers Power Company, who served as a coordinator between Battelle Northwest and the supporting companies.

Corporations which provided financial support included the following:

The Babcock & Wilcox Company
P. O. Box 1260
Lynchburg, Virginia 24505

Southern California Edison Co.
P. O. Box 351
Los Angeles, California 90053

Duke Power Company
422 South Church Street
Charlotte, North Carolina 28201

Commonwealth Edison Company
P. O. Box 767
Chicago, Illinois 60690

Virginia Electric and Power Co.
Richmond, Virginia 23209

Westinghouse Electric Corporation
715 West Michigan Avenue
Jackson, Michigan 49201

Yankee Atomic Electric Company
Turnpike Road
Westboro, Massachusetts 01581

Nuclear Power Department
Combustion Engineering, Inc.
Windsor, Connecticut 06095

Electric Engineering and
Construction Division
Baltimore Gas and Electric Co.
Baltimore, Maryland 21203

Jersey Central Power & Light Co.
Interpace Building
260 Cherry Hill Road
Parsippany, New Jersey 07054

Portland General Electric Co.
621 S. W. Alder Street
Portland, Oregon 97205

Consumers Power Company
212 West Michigan Avenue
Jackson, Michigan 49201

APPENDIX A

FIGURES OF IODINE CONCENTRATION -
TIME RELATION FOR PARTITION EXPERIMENTS

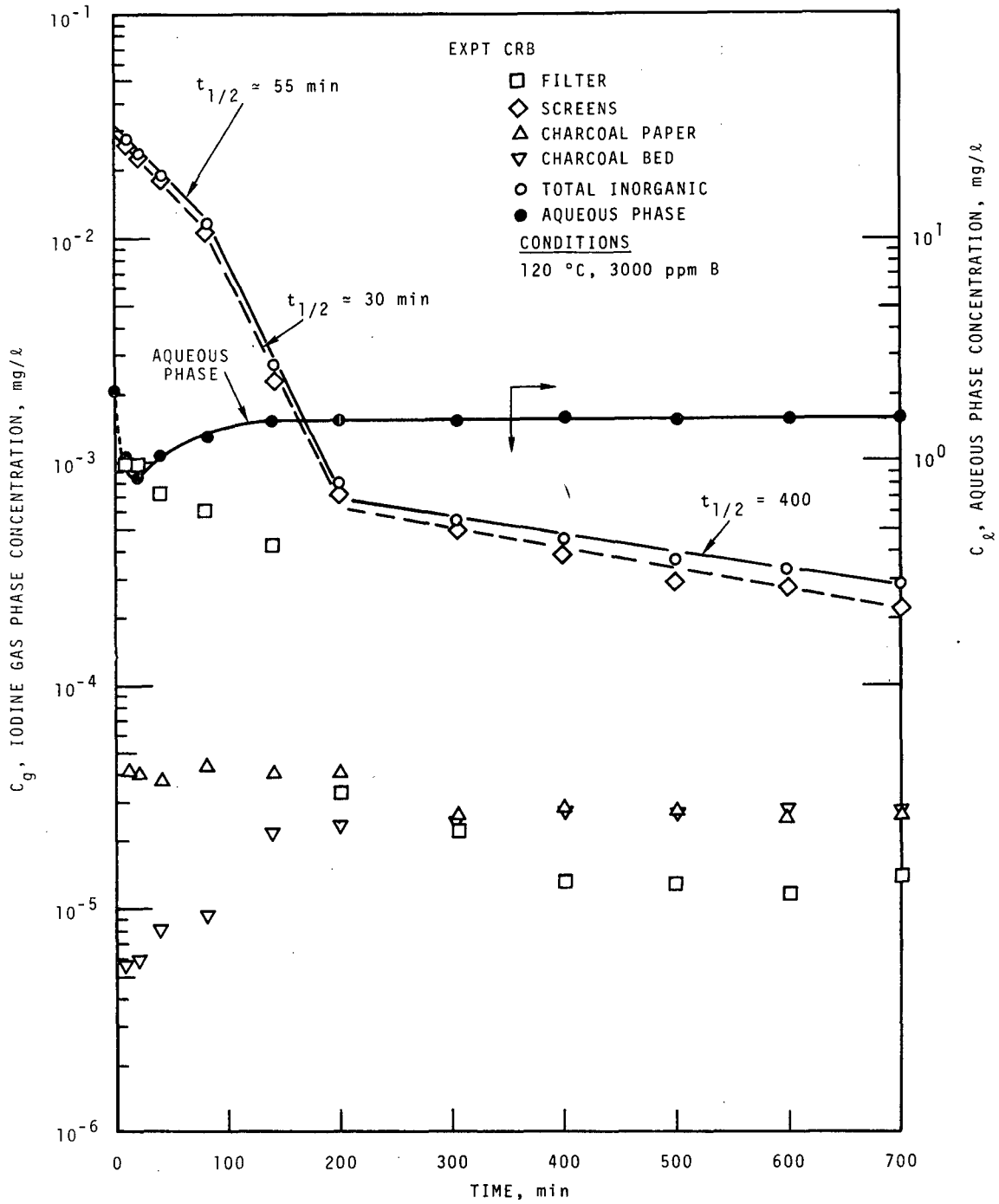


FIGURE A-1. IODINE BEHAVIOR -- EXPT CRB

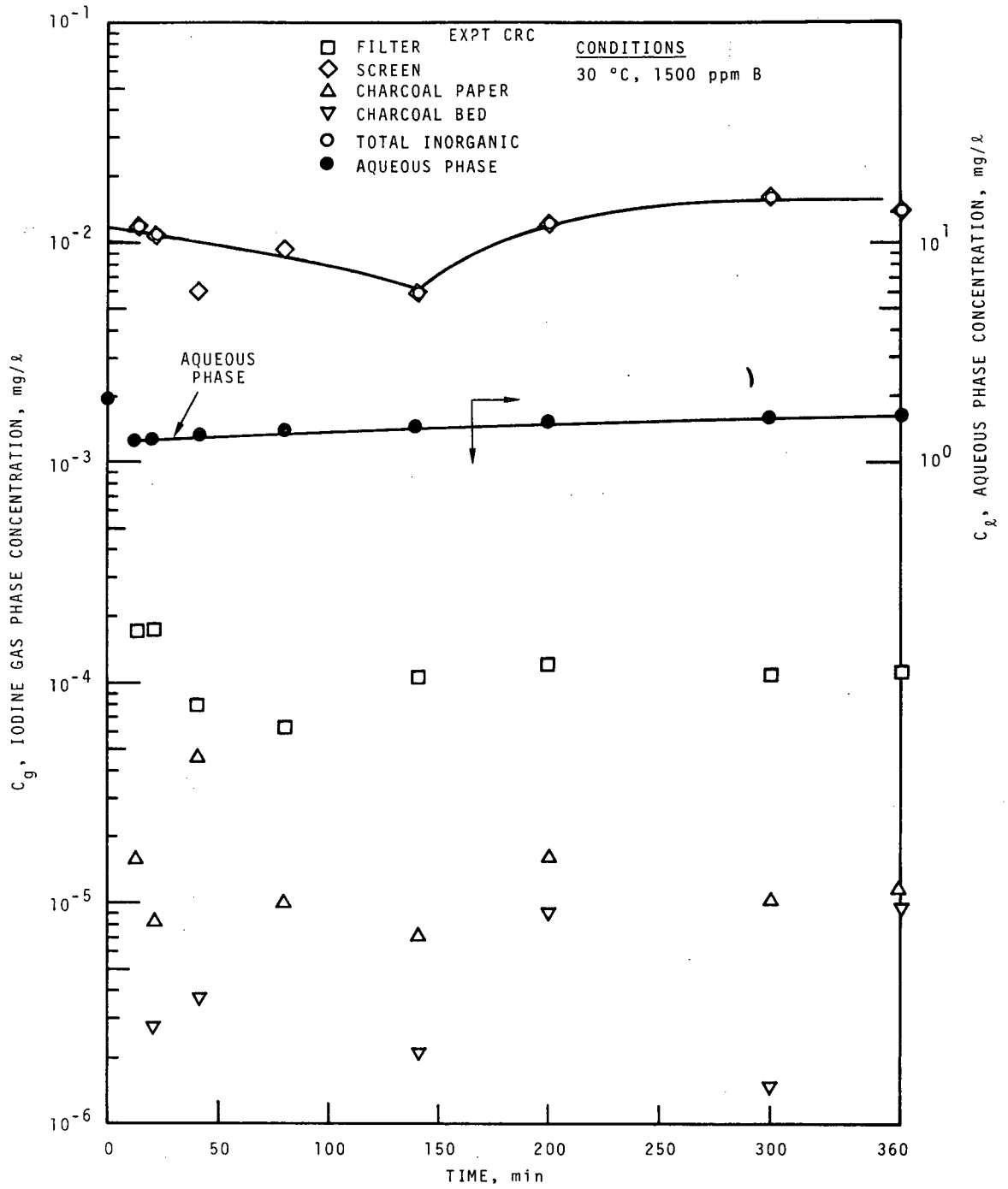


FIGURE A-2. IODINE BEHAVIOR EXPT CRC

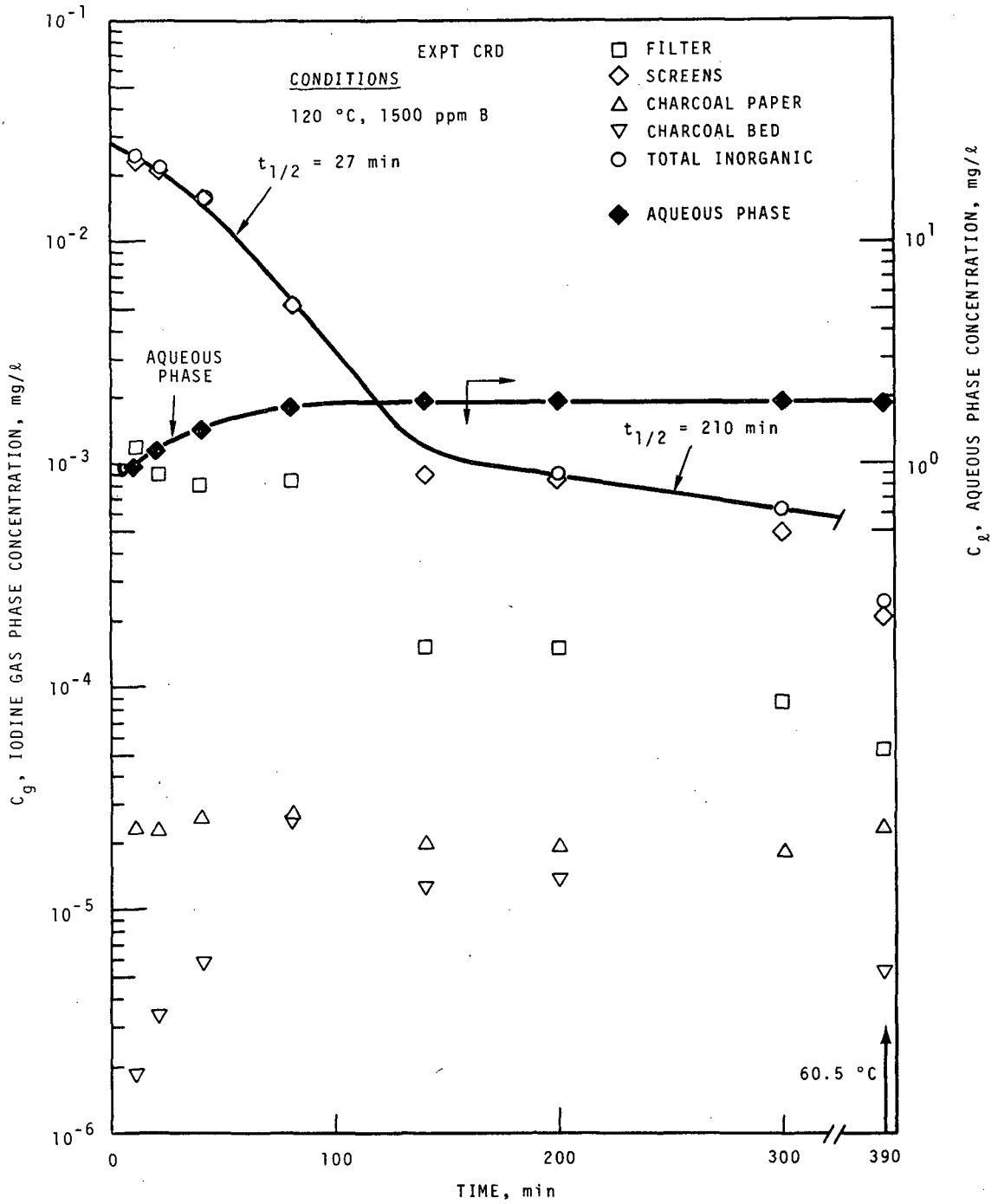


FIGURE A-3. IODINE BEHAVIOR -- EXPT CRD

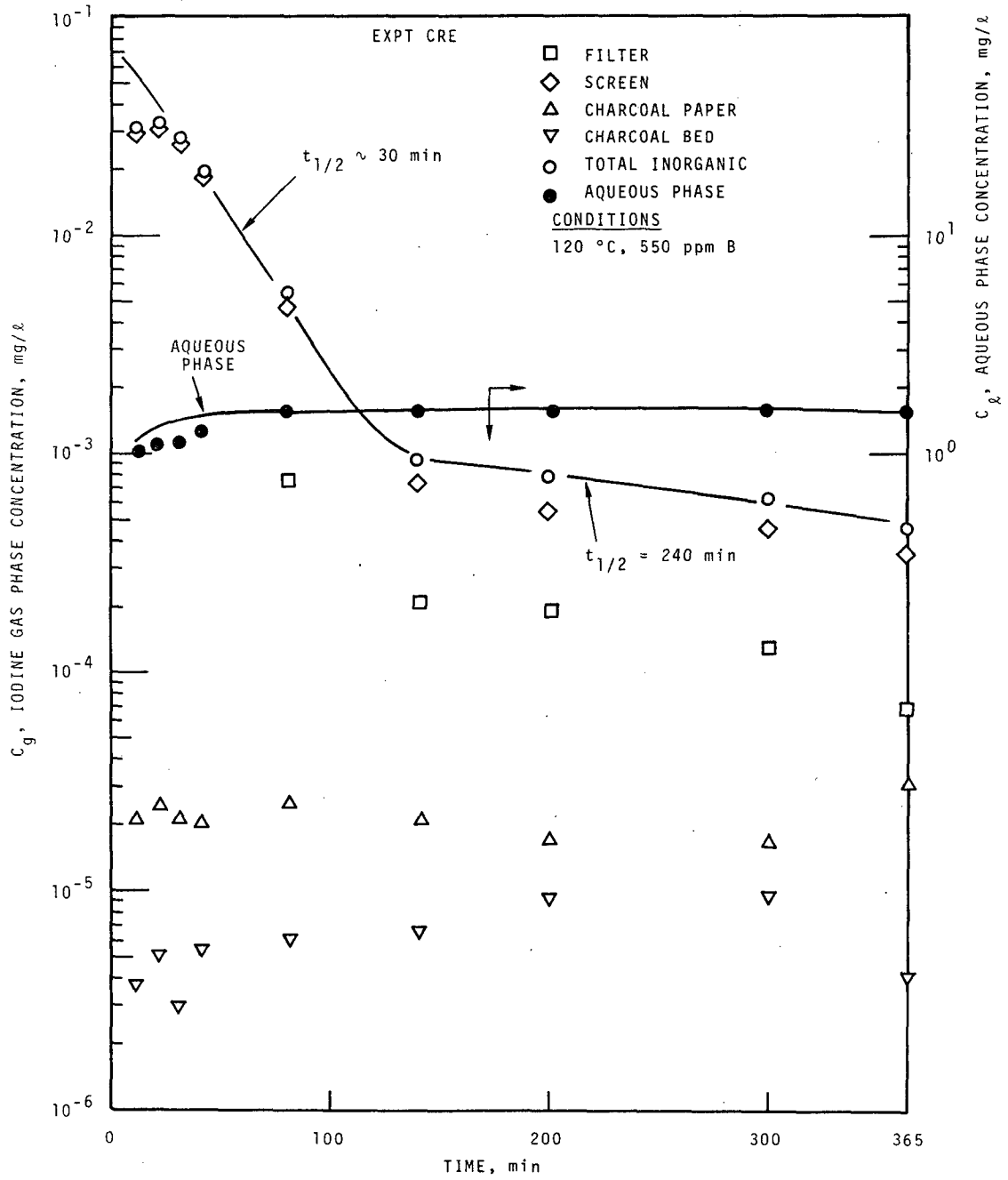


FIGURE A-4. IODINE BEHAVIOR -- EXPT CRE

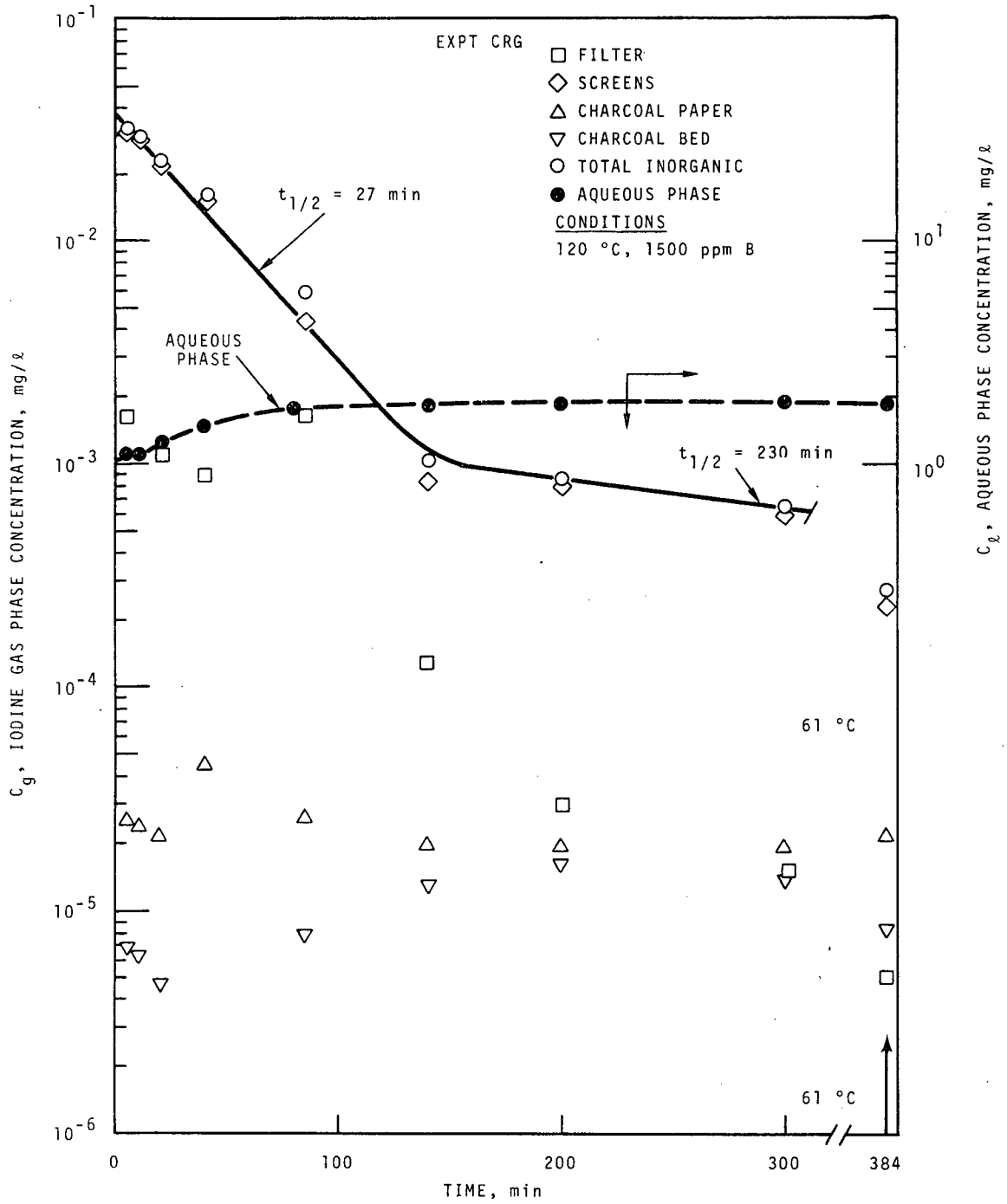


FIGURE A-5. IODINE BEHAVIOR -- EXPT CRG

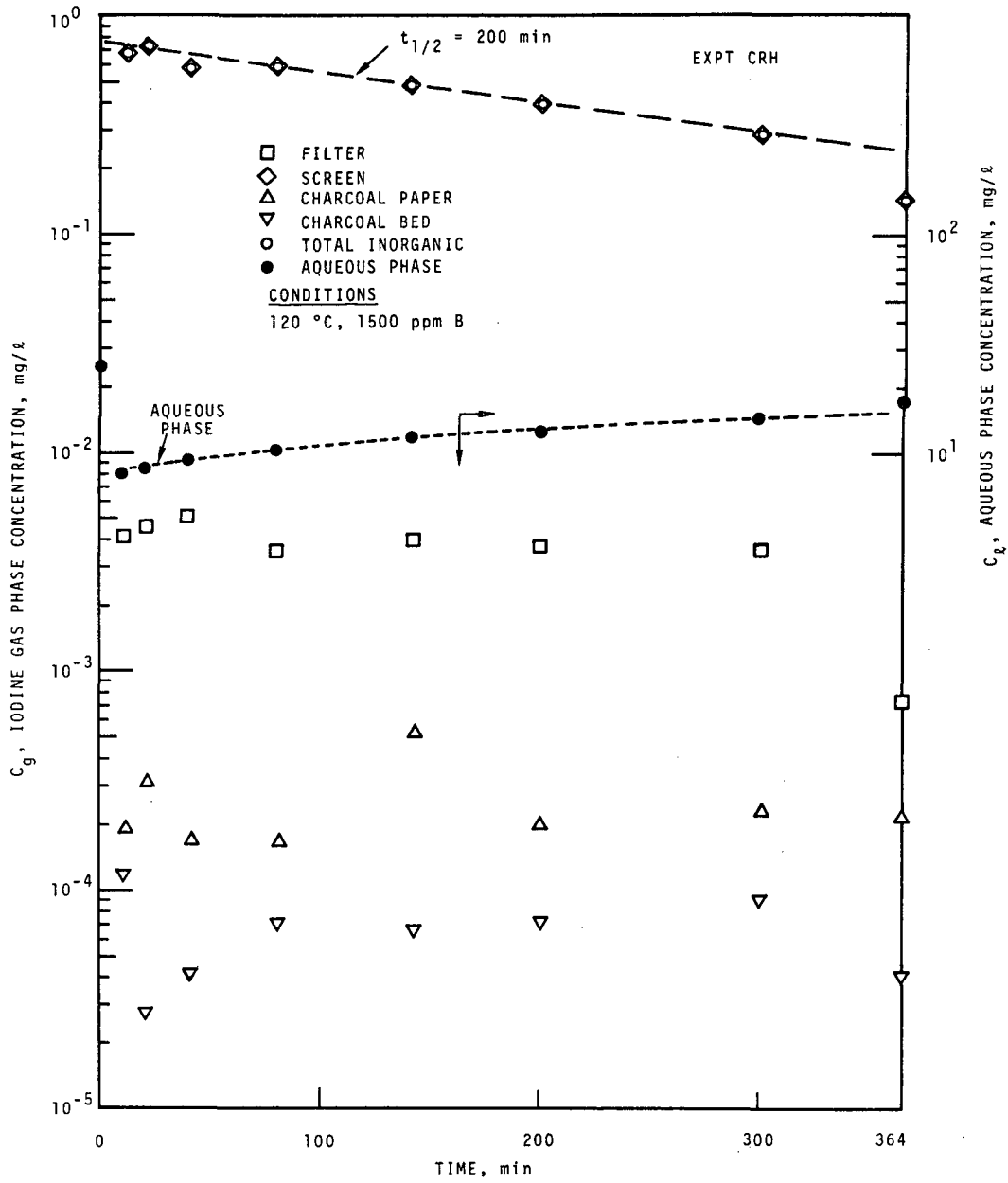
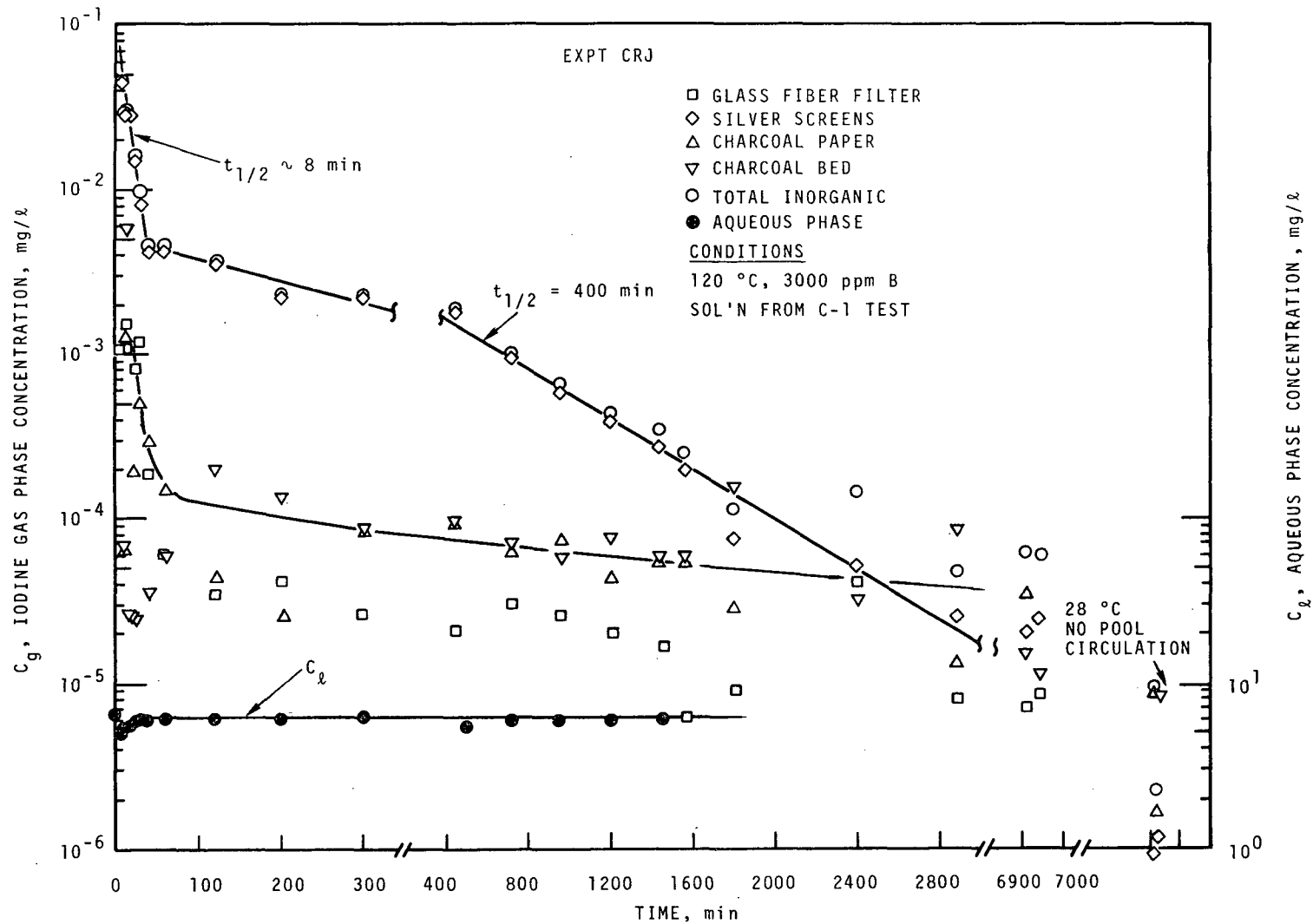


FIGURE A-6. IODINE BEHAVIOR -- EXPT CRH

FIGURE A-7. IODINE BEHAVIOR -- EXPT CRJ



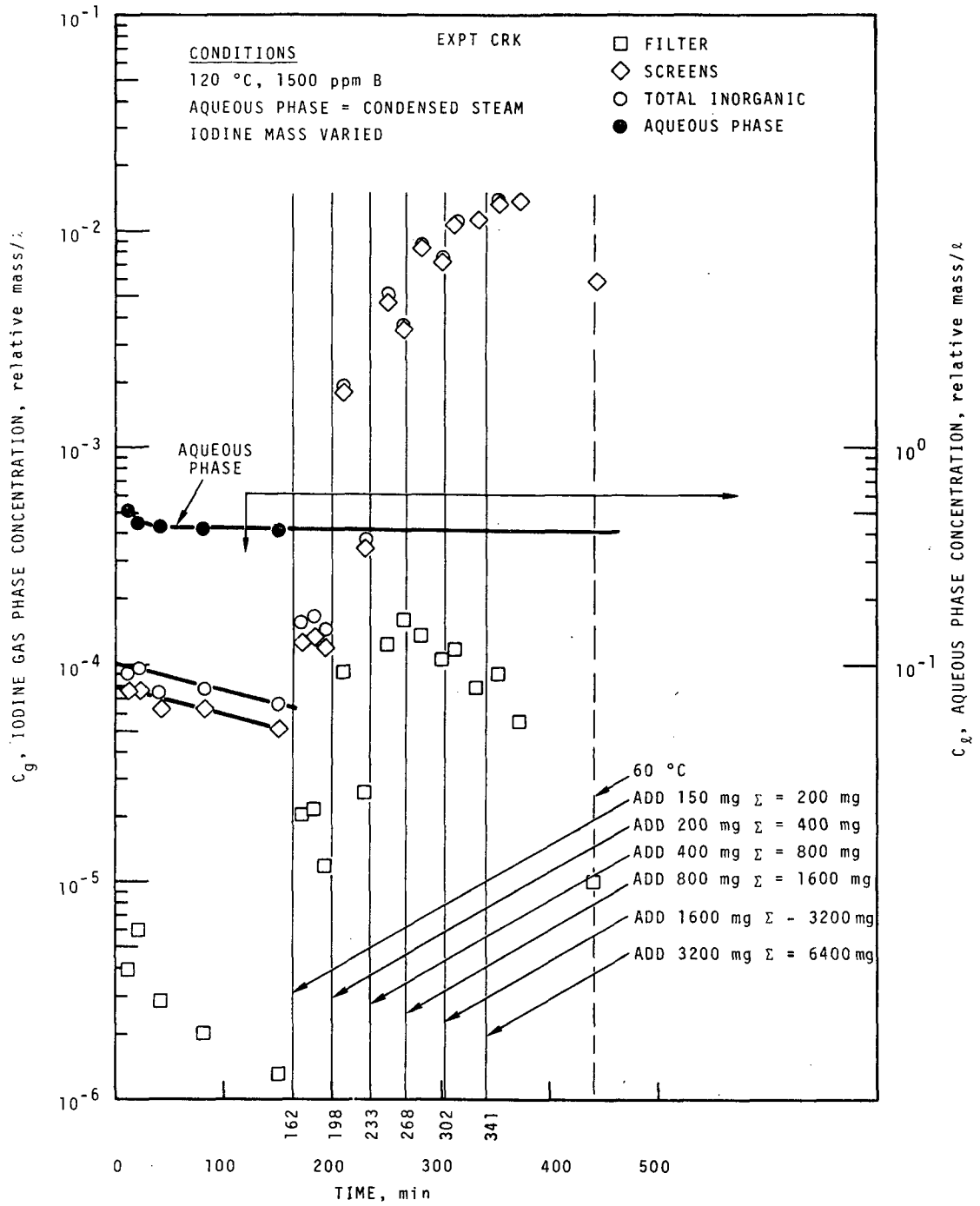


FIGURE A-8. IODINE BEHAVIOR -- EXPT CRK

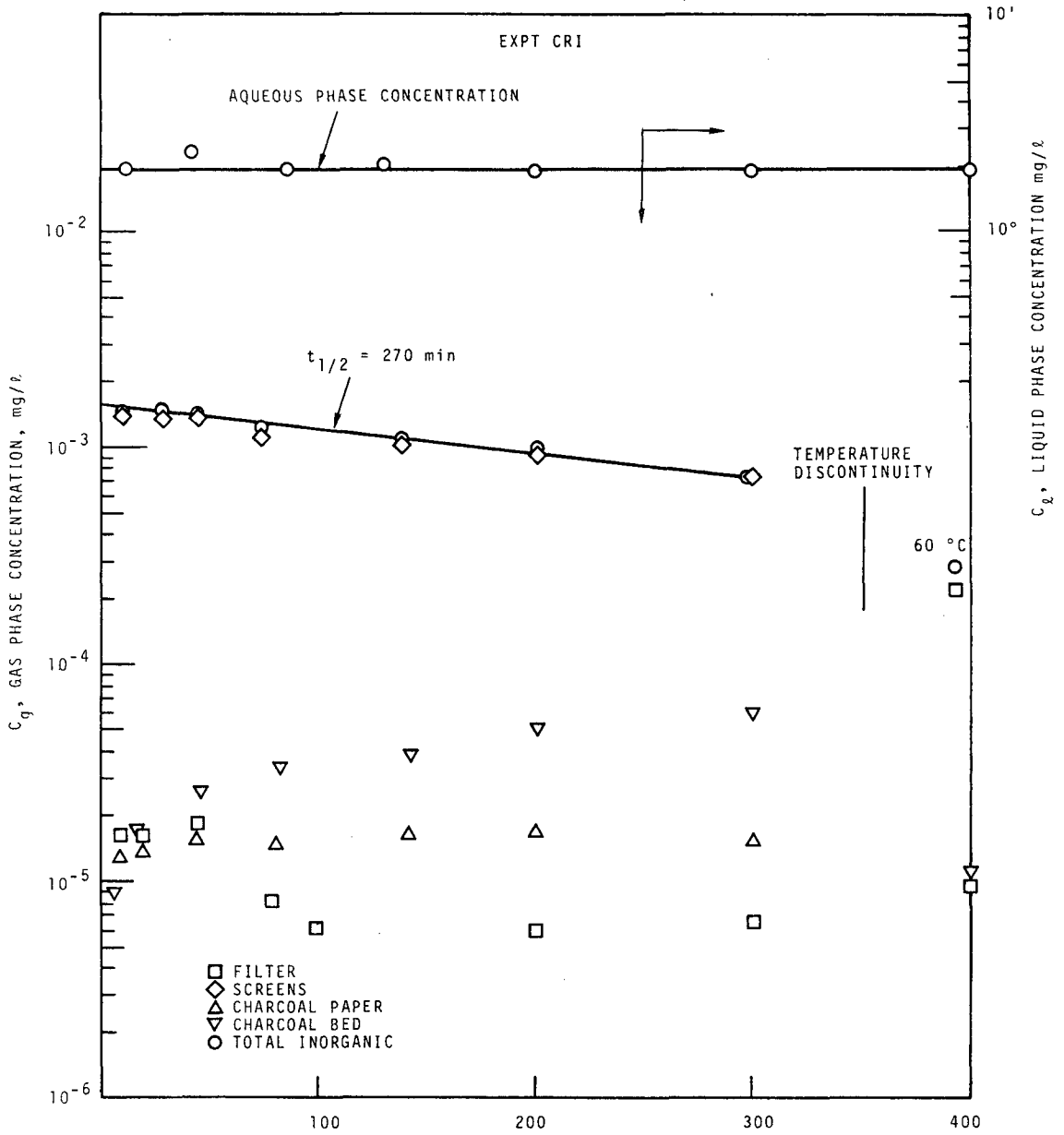


FIGURE A-9. IODINE GAS PHASE BEHAVIOR -- EXPT CRI

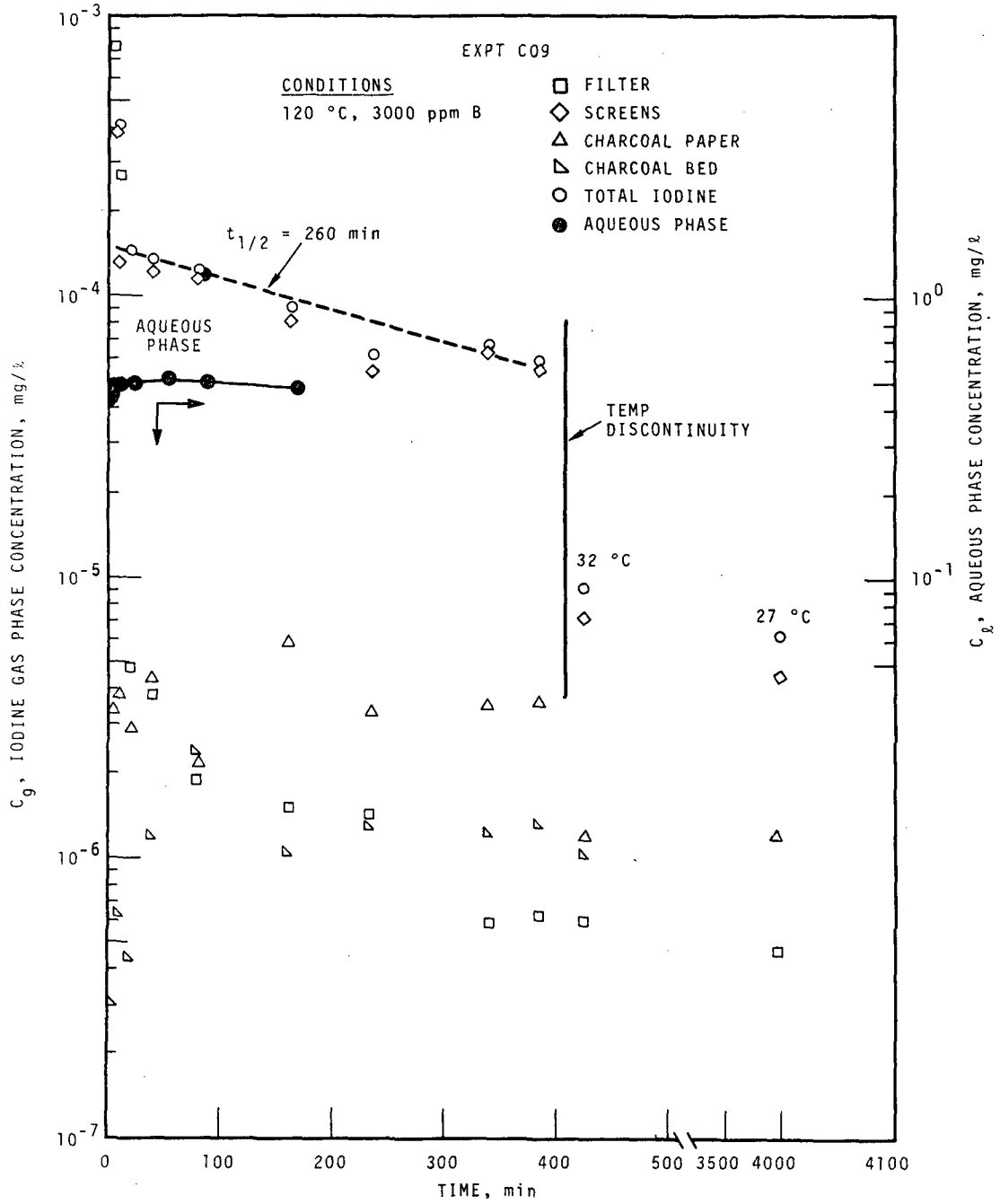


FIGURE A-10. IODINE BEHAVIOR -- EXPT C09

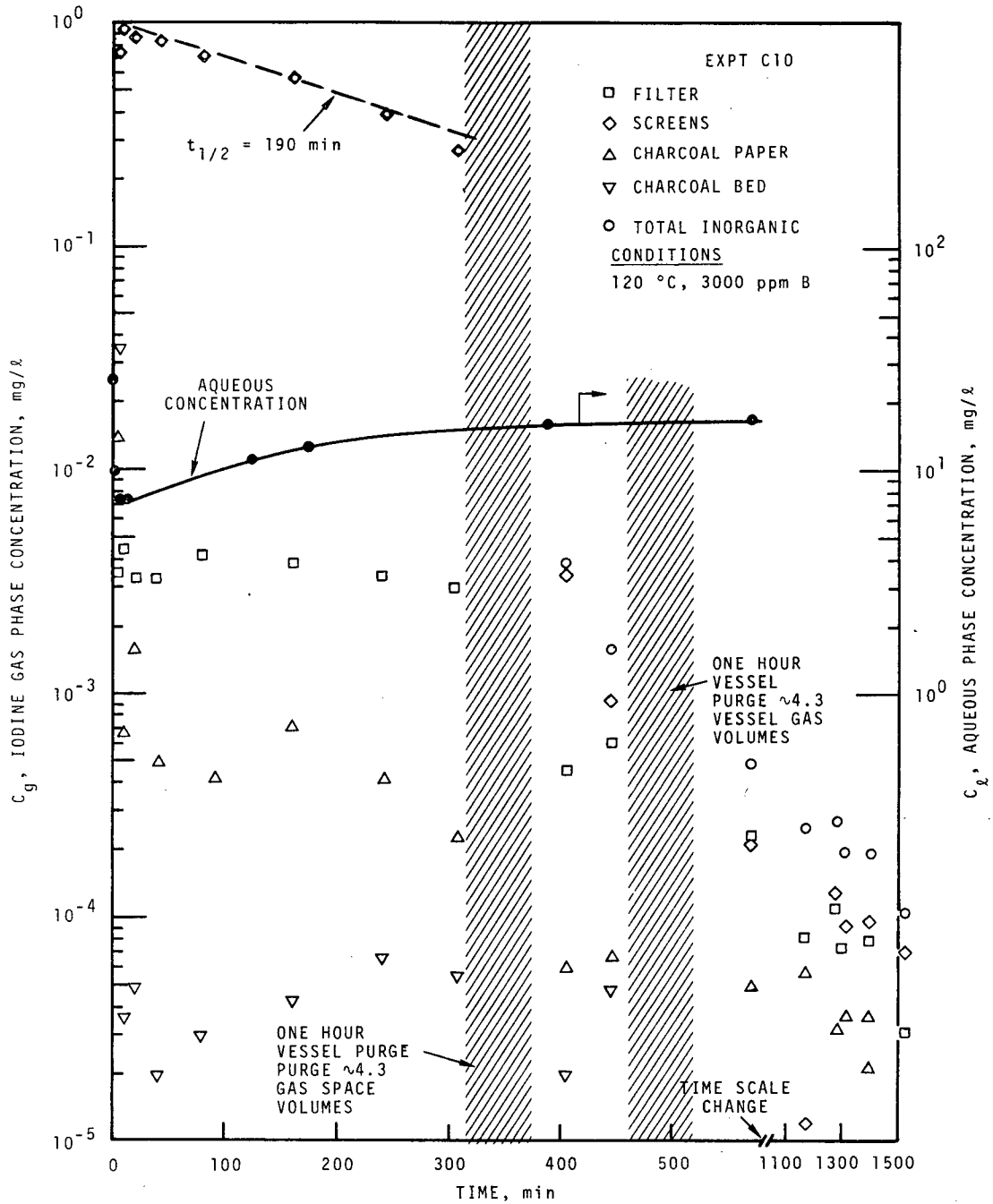


FIGURE A-11. IODINE BEHAVIOR -- EXPT C10

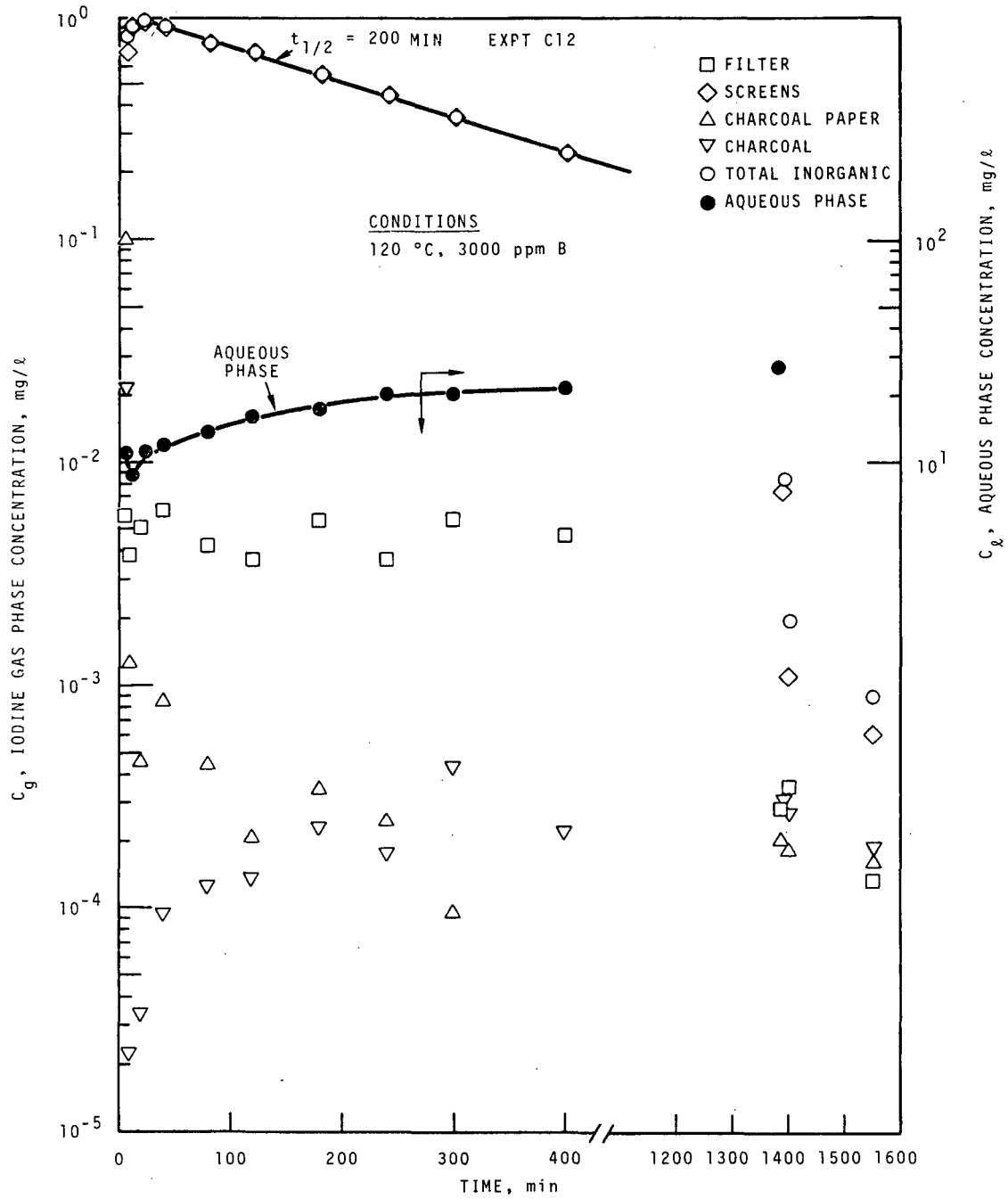


FIGURE A-12. IODINE BEHAVIOR -- EXPT C12

APPENDIX B

TABLES OF MAYPACK SAMPLE DATA

TABLE B -1 TABLE B-1 CONCENTRATIONS IN MAIN VAPOR SPACE
FROM CLUSTER SAMPLES - RUN C-1

Time, min	Concentration, ^(a) $\mu\text{g}/\text{m}^3$										
	8	12	16	20	25	31	60	121	301	721	1141
Elemental Iodine	77,840 (3)	36,940 (8)	16,830 (12)	7,850 (7)	2,820 (9)	1,463 (11)	378 (18)	308 (20)	203 (38)	80.2 (19)	67.1 (64)
Particulate Iodine	56.5 (19)	0	0	0	0	0	0	0	0	0	0
Iodine Associated with Charcoal Paper	898 (31)	1,867 (44)	976 (23)	560 (23)	545 (30)	373 (35)	418 (50)	436 (34)	375 (45)	298 (37)	219 (50)
Iodine on Maypack Inlet	890 (86)	159 (87)	78.2 (35)	64.5 (53)	37.1 (38)	44.6 (33)	10.5 (36)	12.9 (58)	7.37 (51)	9.65 (59)	10.0 (47)
Total Inorganic Iodine	79,700 (3)	39,020 (8)	17,900 (12)	8,479 (7)	3,409 (16)	1,886 (20)	813 (31)	763 (30)	592 (43)	394 (34)	302 (53)
Methyl Iodide	4,188 (11)	5,633 (12)	5,606 (8)	5,222 (9)	4,951 (8)	4,891 (8)	4,357 (8)	4,110 (10)	3,498 (8)	2,014 (6)	1,237 (12)
Total Iodine (All Forms)	83,890 (5)	44,650 (7)	23,510 (9)	13,700 (5)	8,360 (6)	6,777 (6)	5,170 (8)	4,873 (9)	4,090 (8)	2,409 (7)	1,539 (12)
Cesium	1270 (17)	193 (11)	104 (13)	69.6 (6)	48.0 (8)	43.4 (5)	24.2 (5)	7.03 (10)	0.651 (36)	0.255 (85)	0.324 (87)
Uranium											

(a) Mean concentration of 12 sampling locations in main vapor space.

() Numbers in parentheses are standard deviation from the mean - in percent.

TABLE B-2 CONCENTRATIONS IN MAIN VAPOR SPACE
FROM "THIEF" SAMPLES - RUN C-1

Time, min	Concentration, $\mu\text{g}/\text{m}^3$										
	-51	-31	-11	7	13	18	25	32	40	60	121
Elemental Iodine	2.18 (26)	2.53 (21)	2.95 (22)	109,400 (21)	26,140 (a)	10,650 (a)	2,476 (a)	1,547 (22)	356 (a)	293 (10)	246 (13)
Particulate Iodine	0	0	0	766 (16)	0	0	0	0	0	0	0
Iodine Associated with Charcoal Paper	59.9 (48)	99.4 (26)	139 (24)	832 (5)	2,251 (a)	647 (a)	616 (a)	523 (44)	549 (a)	565 (33)	219 (70)
Iodine on Maypack Inlet	0.338 (54)	0.276 (110)	0.875 (64)	416 (145)	237 (a)	34.1 (a)	17.1 (a)	7.09 (78)	1.34 (a)	2.22 (83)	7.77 (134)
Total Inorganic Iodine	62.4 (47)	102 (26)	143 (24)	111,400 (21)	28,630 (a)	11,330 (a)	3,109 (a)	3,016 (19)	907 (a)	860 (25)	473 (41)
Methyl Iodide	1,497 (42)	2,227 (36)	2,325 (66)	4,117 (23)	5,895 (a)	4,925 (a)	4,780 (a)	3,429 (27)	4,389 (a)	2,672 (3)	2,736 (47)
Total Iodine (All Forms)	1,559 (42)	2,329 (36)	2,468 (64)	118,117 (21)	34,525 (a)	16,255 (a)	7,889 (a)	6,445 (23)	5,296 (a)	3,532 (8)	3,209 (46)
Cesium	0.024 (23)	0.032 (46)	0.054 (46)	1,750 (21)	155 (a)	83.3 (a)	42.3 (a)	33.0 (50)	19.8 (a)	23.4 (13)	7.06 (20)
Uranium	2.13 (a)	3.28	0.69	553.46	82.02 (a)	56.32 (a)	64.93 (a)	27.46	11.30 (a)	12.12	6.92

(a) Single value

() Number in parentheses are standard deviation from the mean - in percent.

TABLE B-3 CONCENTRATIONS IN MAIN VAPOR SPACE
FROM "THIEF" SAMPLES - RUN C-1

Time, min	Mean Concentration, $\mu\text{g}/\text{m}^3$										
	202	301	457	735	985	1214	1441	1561	1805	2410	2885
Elemental Iodine	170 (7)	138 (38)	79.8 (13)	59.4 (28)	46.9 (2)	37.2 (20)	30.5 (38)	29.1 (11)	15.3 (11)	12.6 (48)	9.16 (46)
Particulate Iodine	0	0	0	0	0	0	0	0	0	0	0
Iodine Associated with Charcoal Paper	544 (29)	434 (1)	276 (51)	287 (43)	203 (60)	219 (37)	262 (3)	173 (77)	144 (64)	123 (42)	88.1 (37)
Iodine on Maypack Inlet	2.46 (48)	2.53 (96)	2.08 (125)	0.305 (6)	1.11 (80)	0.339 (13)	0.307 (44)	0.506 (110)	0.176 (25)	2.36 (121)	0.144 (13)
Total Inorganic Iodine	716 (24)	575 (10)	351 (44)	347 (40)	251 (49)	253 (35)	289 (7)	203 (67)	159 (59)	138 (44)	97.4 (38)
Methyl Iodide	3,132 (23)	2,536 (14)	1,915 (41)	1,504 (36)	1,404 (57)	1,017 (25)	766 (16)	493 (47)	595 (4)	380 (5)	349 (34)
Total Iodine (All Forms)	3,848 (23)	3,111 (13)	2,260 (42)	1,851 (37)	1,655 (56)	1,270 (27)	1,055 (14)	696 (53)	754 (16)	518 (15)	446 (35)
Cesium	1.67 (66)	0.553 (36)	0.201 (58)	0.049 (14)	0.141 (83)	0.045 (52)	0.055 (52)	0.172 (144)	0.023 (40)	0.021 (79)	0.034 (57)
Uranium	2.60	2.52 (a)	2.54 (a)	0	0.70 (a)	0	0	0	0	0	0

-123-

(a) Single value

() Numbers in parentheses are standard deviation from the mean - in percent.

TABLE B-4 CONCENTRATIONS IN MAIN VAPOR SPACE
FROM "THIEF" SAMPLES - RUN C-1

Time, min	Mean Concentration, $\mu\text{g}/\text{m}^3$								
	3303	3802	4326	4601	8548	8578	8649	8708	8768
Elemental Iodine	4.61 (15)	4.65 (14)	3.36 (20)	3.54 (4)	2.08 (29)	1.66 (50)	0.344 (61)	0.239 (95)	0.313 (81)
Particulate Iodine	0	0	0	0	0	0.016 (327)	0.112 (40)	0.371 (103)	0.131 (33)
Iodine Associated with Charcoal Paper	99.2 (21)	96.9 (10)	87.2 (15)	72.9 (8)	18.1 (37)	16.5 (59)	1.50 (59)	0.780 (21)	0.546 (95)
Iodine on Maypack Inlet	0.290 (67)	0.241 (40)	0.257 (13)	0.166 (59)	0.102 (45)	0.162 (75)	0.083 (69)	0.102 (43)	0.104 (4)
Total Inorganic Iodine	104 (21)	100 (10)	90.8 (15)	76.6 (8)	20.3 (36)	18.3 (59)	2.04 (59)	1.49 (55)	1.09 (75)
Methyl Iodide	245 (25)	249 (28)	235 (9)	194 (28)	121 (32)	93.7 (3)	2.14 (42)	0.790 (33)	0.253 (16)
Total Iodine (All Forms)	349 (24)	349 (24)	326 (11)	271 (22)	141 (33)	112 (12)	4.18 (50)	2.28 (47)	1.34 (64)
Cesium	0.014 (44)	0.016 (41)	0.021 (68)	0.024 (24)	0.018 (a)	0.014 (80)	0.014 (32)	0.016 (60)	0.012 (108)

(a) *Single value*

() *Numbers in parentheses are standard deviation from the mean - in percent*

TABLE B-5 CONCENTRATIONS IN MIDDLE
VAPOR SPACE - RUN C-1

Time, min	Concentration, (a) $\mu\text{g}/\text{m}^3$										
	8	12	16	20	25	31	60	121	301	721	1141
Elemental Iodine	120	5,964	6,072	3,770	1,620	587	196	271	141	82.8	67.7
Particulate Iodine	72.2	543	357	260	141	110	0	0	0	0	0
Iodine Associated with Charcoal Paper	211	926	1100	592	760	401	259	502	394	364	293
Iodine on Maypack Inlet	24.23	31.87	70.51	34.81	56.10	38.92	1.20	6.53	6.84	7.86	1.78
Total Inorganic Iodine	427	7,465	7,600	4,657	2,577	1,137	456	780	542	455	362
Methyl Iodide	7,253	1,234	1,988	3,514	3,925	3,760	2,619	4,923	3,107	2,023	1,231
Total Iodine (All Forms)	7,680	8,699	9,588	8,171	6,502	4,897	3,075	5,703	3,649	2,478	1,593
Cesium	40.18	58.56	66.89	53.26	41.85	41.66	12.84	8.35	1.11	0.363	0.262
Uranium	54.54	31.80	32.85	37.93	30.26	29.27	8.38	7.10	0.38	0.37	1.09

(a) Single value, one location.

TABLE B-6 CONCENTRATIONS IN LOWER
VAPOR SPACE - RUN - C-1

Time, min	Concentration, ^(a) $\mu\text{g}/\text{m}^3$										
	8	12	16	20	25	31	60	121	301	721	1141
Elemental Iodine	5.60	113	388	755	651	326	297	264	120	68.1	45.8
Particulate Iodine	0	0	86.8	143	100	70.0	15.3	0	0	0	0
Iodine Associated with Charcoal Paper	10.4	130	219	257	176	210	278	368	121	55.9	41.6
Iodine on Maypack Inlet	0	4.01	35.69	7.87	118	21.2	0.991	2.88	0	1.22	2.44
Total Inorganic Iodine	16.0	247	729	1,163	1,045	627	591	635	241	125	89.8
Methyl Iodide	28.6	66.4	354	1,127	2,101	3,058	5,249	5,351	3,319	2,097	1,443
Total Iodine (All Forms)	44.6	313	1,083	2,290	3,146	3,685	5,840	5,986	3,560	2,222	1,533
Cesium	0.042	0.291	4.09	13.2	25.8	26.4	25.3	9.01	0.323	0.082	0.106
Uranium	12.54	2.06	3.79	10.98	16.87	21.27	16.96	5.84	5.33	1.62	0

(a) Single value, one location.